NATURAL GAS FUEL CELL BASED POWER SYSTEM FOR MUN ENGINEERING BUILDING

By

Mahmuda Ahmed Tanni

A thesis submitted to the

School of Graduate Studies

in partial fulfillment of the requirements for the degree of

MASTER OF ENGINEERING

Faculty of Engineering and Applied Science

Memorial University of Newfoundland

May, 2014

St. John's **Newfoundland**

ABSTRACT

This research presents analysis and design of a natural gas fuel cell based power system for the engineering building of Memorial University of Newfoundland (MUN). Introduction and literature review provide background on energy consumptions in buildings and modeling techniques of fuel cells. The main objective of this research is to develop a fuel cell based power system for MUN engineering building. In chapter three, energy consumption analysis for MUN engineering building is presented. Modeling of the building in BEopt (Building Energy Optimization) and HOT-2000 software is presented with a short description of MUN engineering building. These BEopt and HOT models show the actual energy consumption of the building. Then an improved model of this building is developed in BEopt software with a list of recommendations. This model shows less energy consumption than the actual building and also suggests a list of recommendations about how to reduce the energy consumption. The successful simulation of the improved model also shows the limitations of the existing design. A 440 kW natural gas fuel cell based power system is proposed for the improved model in chapter three. A 440 kW natural gas fuel cell based power system is developed in Matlab/Simulink software with its Power System Blocksets (PSB) from chapter four to six. In chapter four, modeling of fuel cell system is presented in Matlab/Simulink software. Three models are developed and the best model is chosen for further research. In chapter five, the best chosen Simulink model from chapter four is connected to the power electronics part with the help of Matlab/Simulink blocks and Power System Blocksets (PSB). In chapter six, the fuel cell system with its power electronics part is

connected to the grid. A simple control mechanism is also developed to deliver the required power. Basically the required power indicates the power needed to meet the energy demand of MUN engineering building as indicated in the chapter three. Finally, this thesis ends with the successful modeling of natural gas fuel cell based power system for MUN engineering building.

ACKNOWLEDGEMENTS

The author would like to convey her earnest gratitude and respect to her supervisor Dr. Tariq Iqbal for his great supervision and helpful support to this research. The author is grateful and thankful to him for encouraging her and sharing his valuable knowledge throughout her research work in M.Eng at Memorial University of Newfoundland. It won't be possible to successfully complete this thesis work without his help.

The author would like to thank UTC Power for the financial support to this research in the first year of her M.Eng study. She also would like to thank Dr. Md Arifujjaman, the company representative of UTC Power, who gave helpful directions to this research.

The author would like to thank Memorial University of Newfoundland for all kind of support to this research.

The author would like to thank her family members, especially her husband and parents for their unconditional love and mental supports.

Table of Contents

List of Tables

List of Figures

List of Symbols

E_{nernst} - Nernst Potential

V_{act} - Activation Loss

V_{ohmic} - Ohmic Loss

V_{conc} - Concentration Loss

V_{cell} - Cell Output Voltage

E^0 - Reference Potential at Unity Cavity

p'_{H2} - Partial Pressure of Hydrogen

p'_{O2} - Partial Pressure of Oxygen

p'_{H20} - Partial Pressure of Vapor

R - Gas Constant

T - Temperature

F - Faraday Constant

A - Cell Area

n - Numbers of Electrons Participating in the Reaction

α - Electron Transfer Coefficient

i_0 - Exchange Current Density

i_L - Limiting current density

i - Current Density

I - Electrical Current

R_{int} - Internal Resistance

V_{stack} - Stack Voltage

N - Number of Fuel Cell in a Stack

V_{system} - System Output DC Voltage

List of Abbreviations

MUN - Memorial University of Newfoundland

BEopt - Building Energy Optimization

PAFC - Phosphoric Acid Fuel Cell

MMBTU - Million British Thermal Unit

ZNE - Zero Net Energy

RH - Relative Humidity

BR - Bedroom

FFA - Finished Floor Area

CMU - Concrete Masonry Unit

SIP - Structural Insulated Panel

ICF - Insulating Concrete Form

IECC - International Energy Conservation Code

ACH - Air Changes Per Hour

ERV - Energy Recovery Ventilation

HRV - Heat Recovery Ventilation

AFUE - Annual Fuel Utilization Efficiency

SWH - Solar Water Heating

BTU - British Thermal Unit

DG - Distributed Generation

RES - Renewable Energy Source

IGBT - Insulated Gate Bipolar Transistor

PWM - Pulse Width Modulation

PCU - Power Conditioning Unit

CHAPTER 1

Introduction

1.1 Background

Energy is very important for the technical, industrial, economic and social development of a nation [1]. The demand of energy is increasing from the middle of the last century mainly because of industrial development and population growth [2]. It is possible to reduce the demand if the classification and sectors of global energy consumption are investigated.

The global total energy consumption (GTEC) indicates the economy and environment of a country. Figure 1.1 shows the broadly categorized GTEC [1].

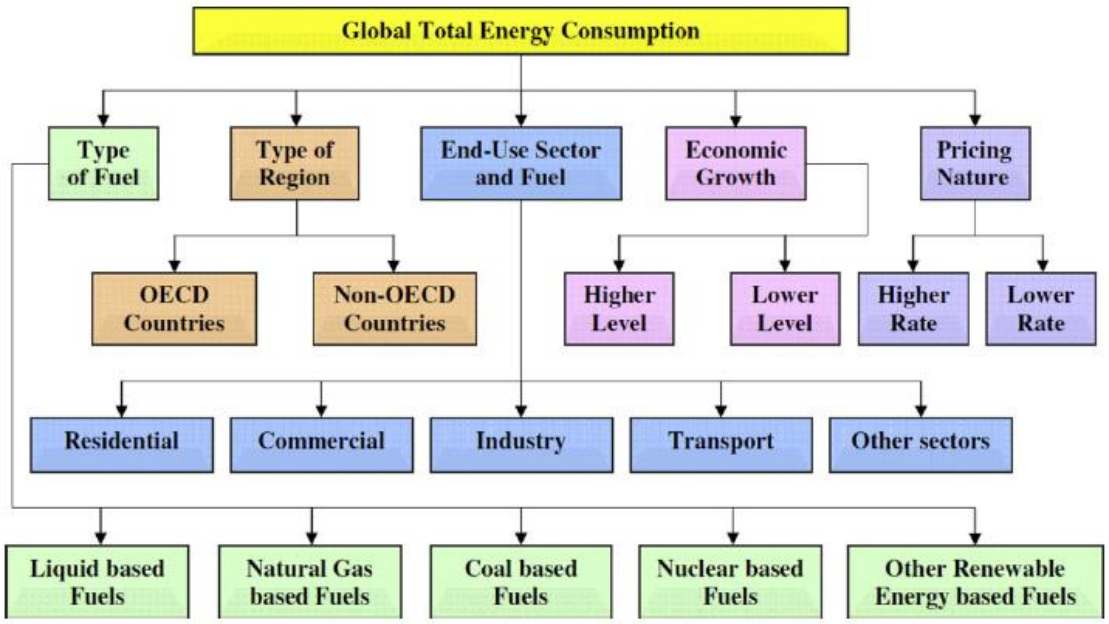

Figure 1.1: Classification of global total energy consumption (GTEC) [1]

From the classification, energy used by the end user is the most important category since it deals with the generation, distribution and conservation of the overall energy. These sectors have great significance to improve the economical status. According to International Energy Agency (IEA), the break-up structure of energy consumption for these sectors is given below [1].

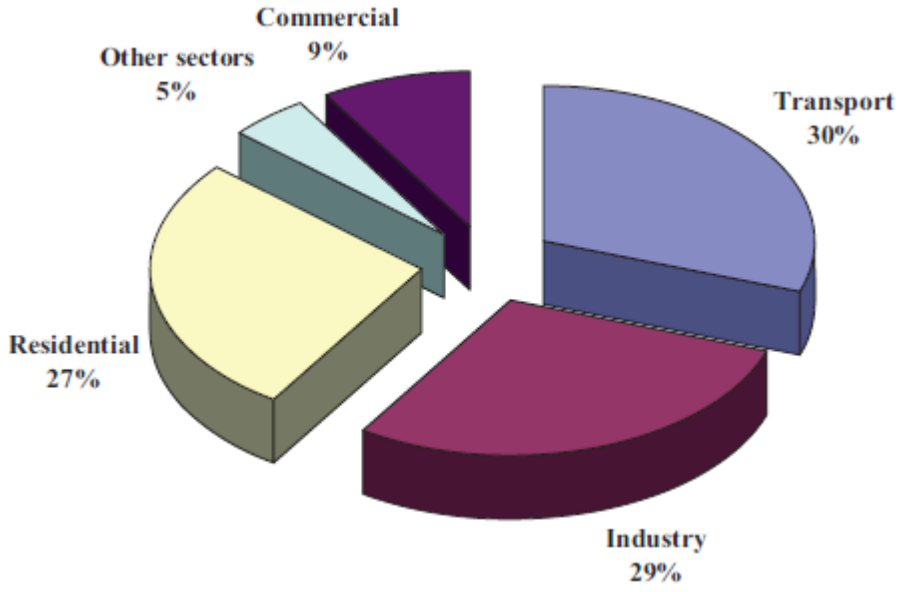

Figure 1.2: Sector wise energy consumption break-up [1]

The consequent result of this high energy consumption points to a development of new and renewable energy sources in worldwide [2]. This situation also indicates the alarming limit for usage of conventional fossil fuel based energy sources [1].

The sun, the wind, water, the Earth's heat, and plants are renewable energy sources that are continually replenished by nature. These fuels can be turned into usable forms of energy such as electricity, heat, chemicals or mechanical power. Moreover, hydrogen is used as a fuel and it produces water as the only emission. Now-a-days, hydrogen fuel cells produce electrical power for distributed energy systems and some vehicles. On the

other hand, the sun is a renewable energy source but it can't provide energy all the time. Renewable energy is becoming popular since it can be stored in hydrogen form until it is required [3].

Recently, it is determined that buildings use 40% of global energy [1] [4]. Some literature is reviewed below to investigate how buildings consume such high rate of energy.

1.2 Energy Use in Buildings

The building sector consumes the largest amount of energy [4]. The following figure shows the average energy break-up in buildings [1].

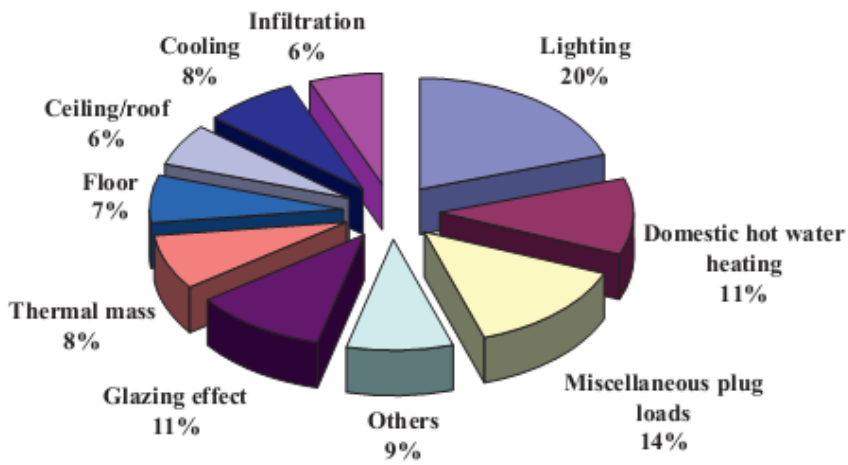

Figure 1.3: Relative average break-up of end-energy usage in buildings [1]

Residential and commercial buildings consume different amount of energy in different countries. The following table shows the percentage of buildings energy consumption.

Table 1.1: Percentage of buildings energy consumption [5]

Final energy consumption (%)	Commercial	Residential	Total
USA	18	22	40
UK	11	28	39
EU	11	26	37
Spain	8	15	23
World	7	16	24

Since commercial building includes schools, universities, hospitals, restaurants etc., total energy consumption is very high for commercial buildings. Moreover, sometimes these commercial buildings need to be scaled for calculating energy consumption due to their large floor area. Since this research includes a scaled version of MUN engineering building, scaling factor is very important here.

1.3 Scaling Factor

Two important steps are necessary to calculate the energy consumption of a building. The first step is to estimate the total floor areas and the second step is to estimate energy use intensity [28]. In the first step, scaling factor is an important factor to calculate the total floor area.

In this research, MUN engineering building is scaled to calculate actual energy consumption. Since this building has a large floor area, it is difficult to fit the whole area in one simulation. So this building is divided into some parts and simulations are done for each part. Then results of all parts are added to calculate the total energy consumption of this building. In this case, scaling factor is introduced to calculate the actual energy consumption from scaled to actual building. Details of this design and scaling factor can be found in the manuscript of the third chapter of this thesis.

1.4 Natural Gas Resources around NL

In Newfoundland and Labrador (NL), there are many commercial buildings where energy consumption is too high because of the harsh environment. Moreover, winter is long and summer is short here in St. John's, NL. So some natural and renewable energy resources should be used to meet the high energy demand. If these resources are in and around NL, it will be easier and beneficial to use. The transportation cost, maintenance cost and energy cost will be reduced. Besides, system reliability will increase.

Among different energy resources in NL, natural gas is very important and is of our interest.

In Newfoundland and Labrador (NL), there exist abundance of oil, natural gas, hydroelectricity and wind resources. Moreover, there is a potential to supply energy from other sources such as uranium, biomass, hydrogen, wave and tidal [6].

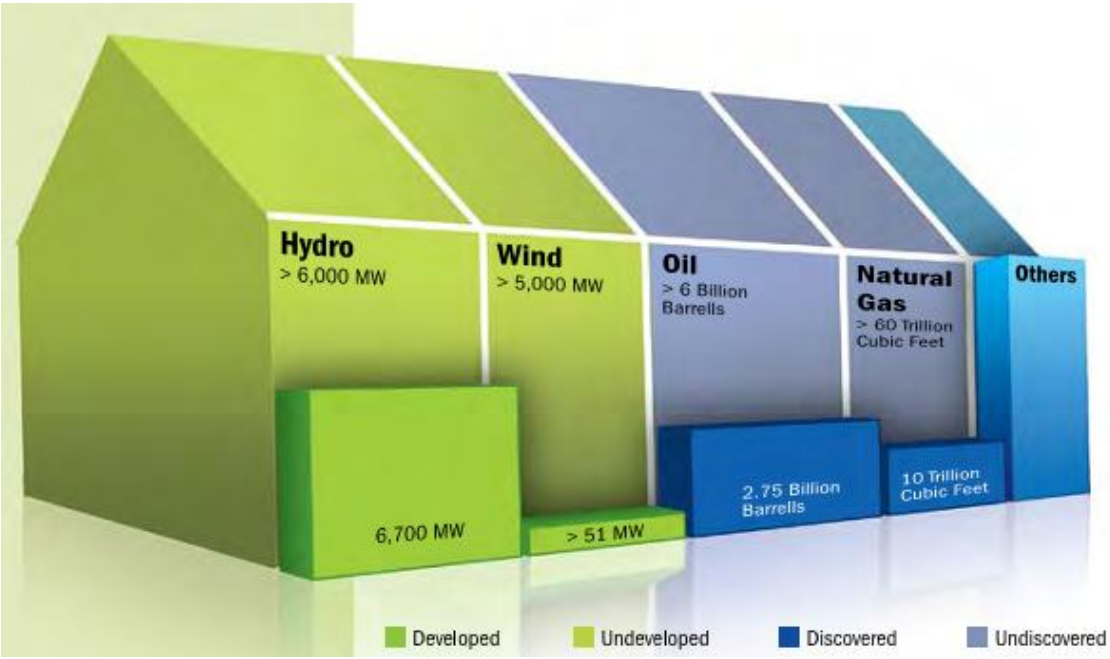

Figure 1.4: Newfoundland and Labrador's Energy Warehouse [6]

In NL, the amount of oil and gas resources in total is over eight billion barrels of oil and 70 trillion cubic feet (tcf) of natural gas [6]. The discovered and undiscovered amount of oil and natural gas in NL can be observed in the following figure.

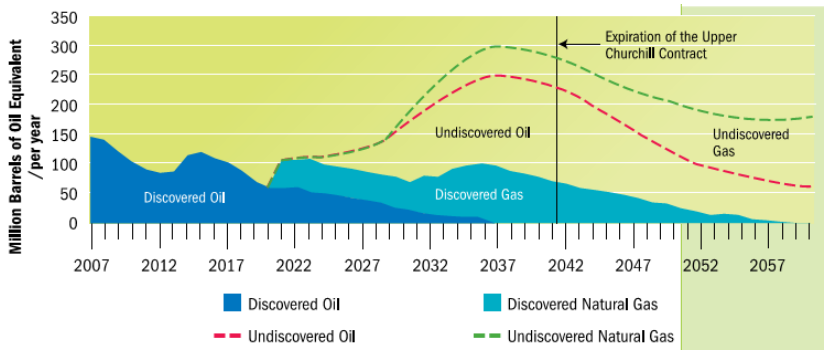

Figure 1.5: Potential Opportunity for Petroleum Production, 2007-2060 [6]

Since the energy demand is increasing, the value of natural gas is also increasing. The following figure shows the increasing value of natural gas.

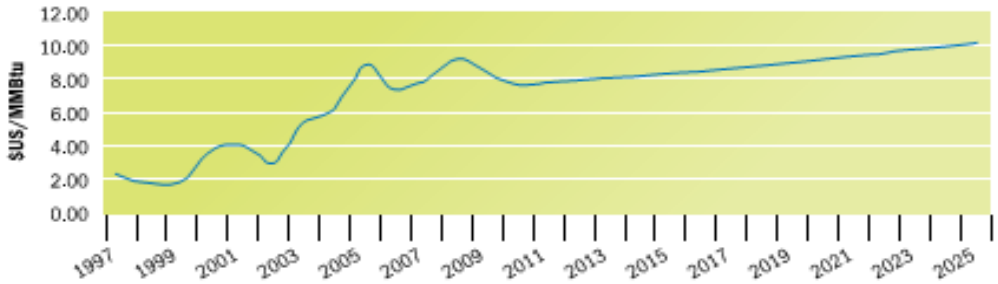

Figure 1.6: Natural Gas Price Forecast (Nominal $US) [6]

It is observed that there is great resource of natural gas in NL. This natural gas can be used in fuel cells to produce electricity and power large buildings.

1.5 Fuel Cell Systems

Fuel cells are electrochemical devices which directly convert chemical energy in fuels into electrical energy. It produces power generation with high efficiency and causes low

environmental impact. According to the type of electrolyte used in the cells, the most common classification of fuel cell includes (a) polymer electrolyte fuel cell (PEFC), (b) alkaline fuel cell (AFC), (c) phosphoric acid fuel cell (PAFC), (d) molten carbonate fuel cell (MCFC) and (e) solid oxide fuel cell (SOFC) [7].

1.5.1 Phosphoric Acid Fuel Cell (PAFC)

The first commercialized fuel cell technology was phosphoric acid fuel cell (PAFC). Most of the plants of PAFC are in the capacity range of 50 to 200 kW but large plants also have been built like 1 MW and 5 MW. The largest plant operated to date produced 11 MW of grid quality ac power. Improvement of PAFCs for stationary, dispersed power plants and on-site cogeneration power plants is an important concern for U.S. In this case, the most important industrial participants are UTC Fuel Cells in the U.S. and Fuji Electric Corporation, Toshiba Corporation, and Mitsubishi Electric Corporation in Japan [7].

1.5.2 Working Principle of PAFC

Phosphoric acid which is concentrated to 100 percent can be used as the electrolyte in PAFC fuel cell. It generally operates from 150 to 220 ^{0}C. Phosphoric acid is a poor ionic conductor at lower temperatures and so the poisoning of CO of the Pt (Platinum) electro-catalyst in the anode becomes severe with use. But the relative stability of concentrated phosphoric acid is higher than other common acids. Consequently, the PAFC can operate at the high end of the acid temperature range i.e. from 100 to 220 ^{0}C. Moreover, it is possible to minimize the water vapor pressure by using concentrated acid (100 percent). For this reason, water management in the cell is not difficult. Silicon carbide is the most

commonly used matrix to retain the acid. The electro-catalyst in both the anode and cathode is Pt [7].

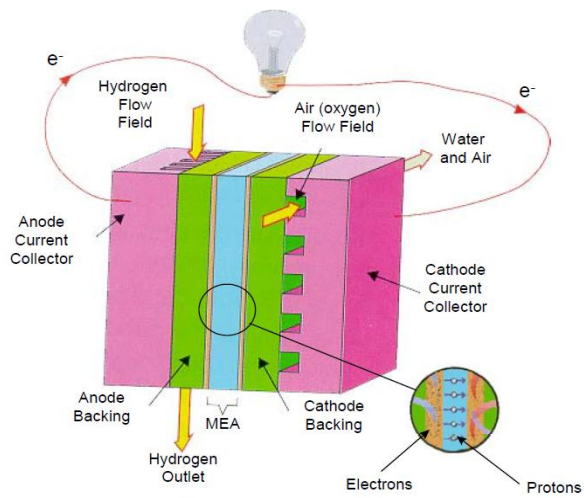

Figure 1.7: Principles of Operation of Phosphoric Acid Fuel Cell (Courtesy of UTC Fuel Cells) [7]

Figure 1.7 shows the operating configuration of the phosphoric acid fuel cell. The electrochemical reactions occurring in PAFCs are given as below [7].

Anode Reaction: $H_2 \rightarrow 2H^+ + 2e^-$ (1)

Cathode Reaction: $\frac{1}{2}O_2 + 2H^+ + 2e^- \rightarrow H_2O$ (2)

Overall Cell Reaction: $\frac{1}{2}O_2 + H_2 \rightarrow H_2O$ (3)

1.5.3 Natural Gas Fuel Cells

For the clean and efficient generation of electricity, natural gas fuel cells are very popular. The natural gas fuel cells have many benefits such as [8]:

a) Clean Electricity**:** It is known that fuel cells provide the cleanest method of producing electricity from fossil fuels. Usually a pure hydrogen and pure oxygen fuel cell produces only water, electricity and heat. But in practice fuel cells produce small amounts of sulfur compounds and very low levels of carbon dioxide. Besides, the produced carbon dioxide can be concentrated and readily recaptured, as opposed to being emitted into the atmosphere [8].

b) Distributed Generation**:** This type of fuel cells are in extremely compact sizes. Moreover, they allow placement wherever electricity is needed. This placement includes residential, commercial, industrial, and even transportation settings [8].

c) Dependability**:** There are completely enclosed units in fuel cells. They have no moving parts or complicated machinery. This indicates that fuel cell is a dependable source of electricity, capable of operating for thousands of hours. Moreover, they are very quiet and safe sources of electricity. They also don't have electricity surges. This means they can be used where a constant, dependable source of electricity is needed [8]. Fuel cell could be installed in or close the building and heat coming out of fuel cell can also be used for heating the building.

d) Efficiency**:** Fuel cells are much more efficient than traditional generation of electricity using combustion, since they convert the energy stored within fossil fuels into electricity. This indicates that less fuel is required to produce the same amount of electricity [8].

Since the traditional generation of electricity is a very polluting and inefficient process, the future of electricity generation is expected to change dramatically in the next ten to

twenty years with the new fuel cell technology. Moreover, research and development into fuel cell technology ensures that the technology is cost-effective for all varieties of electric generation requirements [8].

Based on the above discussion, it can be proposed that natural gas based fuel cell is very useful. So it can be used to power the engineering building of Memorial University of Newfoundland (MUN) which is a commercial/institutional building. This will be discussed later in the next chapters of this thesis.

1.6 Thesis Organization

By observing the significance of fuel cells, it can be said that fuel cells can be used to meet the energy demand of buildings. The use of Phosphoric Acid Fuel Cell (PAFC) for MUN engineering building is one of our research objectives. Research work is described through the four manuscripts from chapter 3 to 6.

In chapter two, a literature review is given to support the background and manuscripts. Since the main objectives of this thesis includes building energy consumption and fuel cell, some literatures are reviewed related to building energy consumption. These literatures will help to understand the modeling of MUN engineering building. After that, some literatures are reviewed based on PAFC modeling. These literatures will help to understand the modeling of natural gas fuel cell based power system.

In chapter three, MUN engineering building energy consumption and models in BEopt (Building Energy Optimization) software and NRCan (Natural Resources Canada) HOT-2000 software is presented. The BEopt and HOT-2000 models show almost actual energy

consumption of this building. The results of this BEopt and HOT-2000 models are validated with the provided data by MUN Facilities Management Department. Then the limitations of the existing design of the engineering building are figured out and a list of recommendations is provided. An improved model of the engineering building is proposed in BEopt software which shows less energy consumption. Improved MUN engineering building could be powered by a natural gas based fuel cell system. This chapter has been published and presented in the *22nd IEEE Newfoundland Electrical and Computer Engineering Conference (NECEC), 2013, St. John's, Newfoundland and Labrador, Canada*.

In chapter four, three simulink models of a PAFC system are developed. Here the steady state modeling of a PAFC system is developed in three ways. All of these models are simulated in Matlab/Simulink environment. The detailed of each model is described. The results of each model are compared and the best model is chosen. Moreover, the advantages of these models are also presented. This chapter has been published and presented in the *21st IEEE Newfoundland Electrical and Computer Engineering Conference (NECEC), 2012, St. John's, Newfoundland and Labrador, Canada*.

In chapter five, the dynamics of a phosphoric acid fuel cell (PAFC) system and its associated power electronics part are described. The best chosen model of the PAFC system from chapter 4 is elaborated here with the power electronics part. This dynamic model is based on empirical equations. This model is simulated in Matlab/Simulink environment with its Power System Blockset (PSB). Basically, the dc power of the chosen PAFC system is converted into ac power through an inverter to observe the dynamics of the model. Simulation results are discussed at different stages of this model.

This chapter has been published and presented in the *International Conference on Future Environment and Energy (ICFEE), Rome, Italy, February 2013*. Moreover, this paper has also been published in the *Journal of Clean Energy Technologies (JOCET), vol 1, no. 3, pp. 178-183, ISSN: 1793-821X, July 2013.*

In chapter six, the modeling and control of a grid connected PAFC system is developed. Basically, the output of the previous model i.e. ac power is supplied to the grid. A closed-loop control mechanism of a 440kW fuel cell system including power electronics and grid side filters is described in this chapter. This model is also based on empirical equations and the simulation is done in Matlab/Simulink software with its Power System Blocksets (PSB). The advantages of this model are discussed here. A simple control mechanism to control the PWM inverter is developed. This chapter has been accepted for publication in the *International Journal of Energy Science (IJES), Paper ID: IJES10380.*

In chapter seven, conclusions are discussed. The summary of works, research contributions and achievements are also presented in this chapter. Moreover, some recommendations are listed for future works.

CHAPTER 2

Literature Review

2.1 Energy Consumption in Canadian Buildings

Since the objective of this thesis is to propose natural gas fuel cell based power system for MUN engineering building, it is necessary to know the energy consumption of Canadian buildings. At first, energy use in residential buildings is investigated and then energy use in commercial buildings is investigated.

In [9], total energy consumption of Canada is 7000 Petajoules and about 20% of this total energy is used for residential buildings. They studied the effect of appliance efficiency and fuel substitution for space and domestic hot water heating in residential buildings of Canada. This study is done to identify the potential savings of energy consumption that can be improved through efficiency and fuel substitution. Moreover, this study is based on simulation which is conducted on the Expanded STAR database. This consists of detailed descriptions of 937 houses from different regions of Canada. This study uses an hour-by-hour building energy simulation program. The following table shows the energy consumption of household appliances used in this study for simulation purpose.

Table 2.1: Appliance energy consumption values used in simulations [9]

Appliance	Annual electricity consumption (kWh)			
	Baseline	Efficiency Level 1	Efficiency Level 2	Efficiency Level 3
Refrigerator	1440	890	700	420
Freezer	1530	570	470	285
Dishwasher (excl. hot water)	280	230	230	230
Clothes washer	90	same; savings in hot water consumption included below		
Clothes dryer	1050	830	620	520
TV	410	165	135	135
Hot water heater	4490	3090	2080	1850
Lights and conv.	4700	4075	3535	3100
All other appliances		5% improvement	10% improvement	15% improvement

In results, this study shows that improving appliance efficiency reduces overall end-use energy consumption in the residential sector.

In [10], correlations are studied between building characteristics and energy use. This paper studies these correlations based on the data of Toronto. These correlations are important to identify the largest contributing factors to energy intensity properly. This identification of contributing factors help to prioritize retrofit measures and new building code measures. The identification of more uniform and complete building characteristic and energy use data are also done in this study. This study uses the meta-analysis data set and the refined data set. The meta-analysis data set is the combination of energy use data and basic building characteristics from three different data sources. The refined data set is composed of 40 buildings to address the data limitations of the meta-analysis data set. The following table shows the weather-normalized minimum, maximum and average total annual energy intensity, the associated GHG emission intensity and the average energy source mix of each data set.

Table 2.2: Summary of building energy-use statistics [10]

Data set	Energy intensity (ekWh/m^2)			GHG emission intensity (ekgCO_2/m^2)			Energy mix	
	Min	Max	Avg	Min	Max	Avg	Electricity	Natural gas
Meta-analysis	88	520	295	16.6	96.6	55.3	38%	62%
Refined	90	510	292	14.8	90.9	50.2	33%	67%

The results of this study are normalized to the CWEC (Canadian Weather for Energy Calculations) for the future work of researchers. This study also recommends procedures to improve the quantity and quality of MURB (Multi Unit Residential Buildings) energy-use data and building characteristics to help researchers.

In [11], the bottom-up CHREM (Canadian Hybrid Residential End-Use Energy and Greenhouse Gas Emissions Model) statistical method is used to estimate the national residential energy consumption. The climatic conditions and the house thermal envelope affect the space heating and space cooling end-use energy consumption. This model is done for AL i.e. space heating, space cooling, appliances, lighting and for DHW i.e. (domestic hot water) energy consumption of single-detached (SD) and double/row (DR) houses. Both AL and DHW energy consumption primarily consists of occupant behaviour, appliance ownership, demographic conditions, and occupancy rate. The results of this model are scaled as representative of the Canadian housing stock. The results are observed with respect to different regions of Canada such as Atlantic provinces consisting of Newfoundland and Labrador, Nova Scotia, Prince Edward Island, and New Brunswick (AT), Quebec (QC), Ontario (ON), Prairies consisting of provinces Manitoba, Saskatchewan, and Alberta (PR), British Columbia (BC) for Single-detached (SD) houses and Double/row (DR) houses.

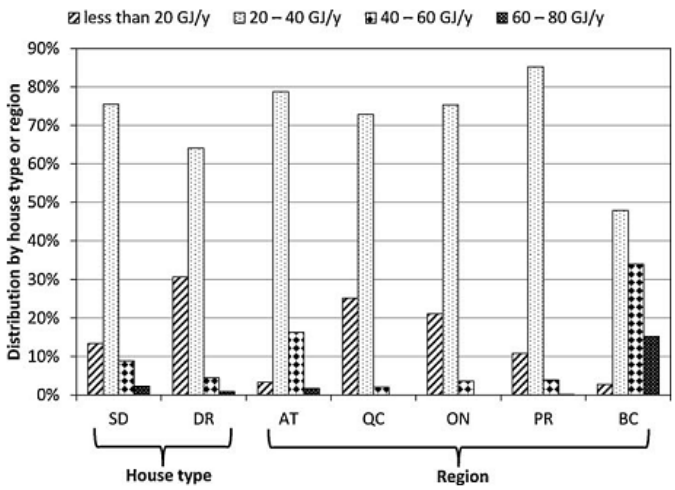

Figure 2.1: Annual AL energy consumption estimates (GJ/year) obtained using the NN model – summarized by house type and region [11]

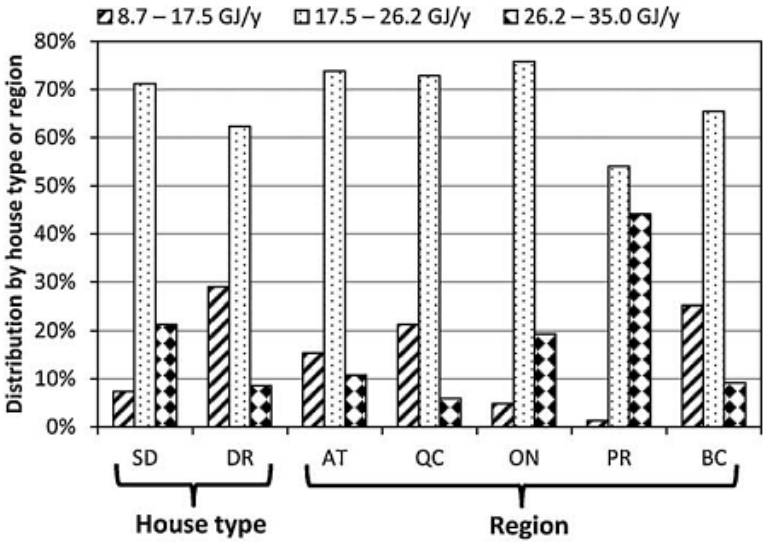

Figure 2.2: DHW consumption estimates by house type and region, obtained using the NN model for annual energy consumption (GJ/year) [11]

The following table shows the total view in case of regional and national demand.

Table 2.3: Regional and national AL and DHW annual energy consumption estimates by end-use and energy source for SD and DR house types [11]

House type or region	By end-use		By energy source			Combined (PJ)
	AL (PJ)	DHW (PJ)	Electricity (PJ)	Natural gas (PJ)	Heating oil (PJ)	
SD	205.4	166.1	273.6	93.6	4.3	371.5
DR	42.5	34.7	54.3	22.3	0.6	77.2
AT	24.2	16.1	35.4	0.0	4.9	40.3
QC	47.1	40.4	87.5	0.0	0.0	87.5
ON	86.0	79.7	102.0	63.7	0.0	165.7
PR	43.7	41.9	48.8	36.7	0.0	85.5
BC	46.9	22.6	54.2	15.4	0.0	69.6
Canada	247.9	200.7	327.9	115.9	4.9	448.7
Canada percentage	55%	45%	73%	26%	1%	-

The annual total AL and DHW energy consumption is found to be 448.7PJ which is within 6% of a top-down model estimate. This is an acceptable level of agreement. Moreover, the CHREM investigates that there is larger energy consumption of AL than DHW energy consumption. This is opposite of the top-down model. The differentiation of the AL and DHW energy consumption is undertaken as a key strength of the CHREM bottom-up modeling methodology since it independently estimates each end-use. For this reason, the CHREM energy consumption estimates proposes a new relationship between the occupancy influenced AL and DHW end-uses.

In [12], a methodology is developed to screen office buildings for their current level of energy consumption and potential for retrofit application. Climate, occupancy, heating and cooling systems, envelope properties and building geometry have a great influence on the selection of an optimal set of ERMs (Energy Retrofit Measures). This selection is accomplished by characterizing office building stock into a manageable set of archetypes and simulating building operations using energy simulation software. A model is developed here for estimating the energy consumption using regression analyses. This

model uses three categories of buildings of Vancouver, Edmonton and Ottawa. These categories are Building Type LV – Large (12 storey; 24,000 m^2) with a brick Veneer/concrete block backup exterior wall, Building Type LC – Large (12 storey; 24,000 m^2) with an exterior Curtain wall, and Building Type S – Small (2 storey; 4200 m^2) with a brick Veneer/concrete block backup exterior wall. The results of this model can be observed in the following table. It shows the breakdown of energy consumption for those types of buildings in terms of percentage.

Table 2.4: Energy consumption break-down for building types LV, LC and S built post-1975 and current standards [12]

		Energy consumption (%)								
		Building Type LV			Building Type LC			Building Type S		
	Location	Vancouver	Edmonton	Ottawa	Vancouver	Edmonton	Ottawa	Vancouver	Edmonton	Ottawa
Post-1975	Lights	20.3	16.7	16.7	18.4	15.0	15.2	19.1	16.6	16.3
	Process	5.7	4.7	4.7	5.1	4.2	4.2	7.7	6.7	6.6
	Computers	28.5	23.5	23.4	25.9	21.1	21.3	32.2	27.9	27.5
	Pumps	1.5	1.3	1.5	1.5	1.4	1.5	1.6	1.4	1.6
	Fans	21.4	20.1	20.5	25.1	23.7	23.6	11.8	11.7	12.0
	DHW	1.3	1.1	1.1	1.2	1.0	1.0	1.5	1.3	1.2
	Chiller	5.5	4.5	5.4	6.6	5.1	5.9	11.1	8.9	10.7
	Boiler	15.4	28.1	26.9	16.1	28.6	27.4	15.1	25.6	24.1
Current Standards	Lights	11.5	9.2	9.4	8.9	6.9	6.9	7.2	5.9	5.8
	Process	8.5	7.5	7.4	8.1	7.0	7.1	7.8	7.1	6.8
	Computers	42.8	37.5	37.3	41.0	35.3	35.5	32.7	29.7	28.4
	Pumps	1.9	1.8	2.0	2.1	1.9	2.1	1.4	1.4	1.9
	Fans	2.4	2.4	2.4	3.0	3.1	3.0	0.8	0.8	0.8
	DHW	2.1	1.9	1.9	2.1	1.8	1.8	1.6	1.5	1.4
	Chiller	5.4	4.2	5.2	6.0	4.7	5.6	3.3	2.7	5.3
	Boiler	25.5	35.6	34.4	28.9	39.3	38.0	45.2	50.8	49.5

So the developed methodology can simply retrofit the ranking of buildings; select and combine ERMs, and plan energy and GHG reduction activities. The model determines the expected payback periods and the overall rate of return on investment.

In [13], a novel approach is studied to use renewable energy options for buildings. This will make the buildings more efficient, more cost effective, more environmentally benign, and more technologically attractive. This study includes four buildings. Different renewable energy options are studied for these buildings to replace the conventional ways

of supplying electricity, heat and cols. Moreover, environmental impacts and cost aspects of these renewable energy options are studied through four case studies. The first case study is a 4+1 bedroom detached house where there are five residents, located in Brampton, Ontario. The second case study is another detached house in Oshawa, Ontario having four bedrooms with five residents. The third case study is a central public library located in Brampton, Ontario. This is a two storey institutional building with a residential area. The fourth case study is a plastic injection company located in Mississauga, Ontario. The electricity consumption of the first case study is 5506 kWh for the entire year and 13,303 kWh for the second case study. Moreover, the measured electricity consumption for this library is 765,765kWh (i.e., 765.8MWh) per annum. Since the fourth case study is an industrial building, the energy consumption pattern is totally different from previous cases. In this case, the measured consumption of electricity is 1320MWh for 12 months period. The following figures show the energy consumption of these four cases in different sectors.

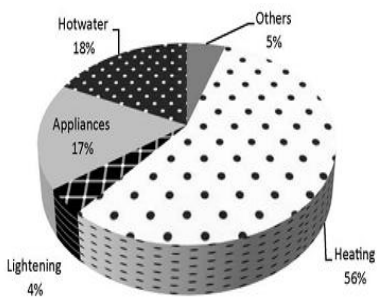

(a)

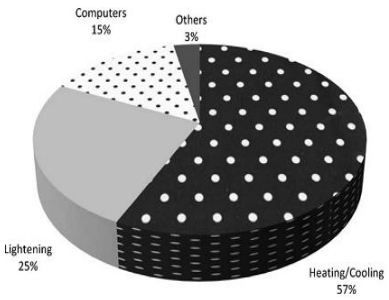

(b)

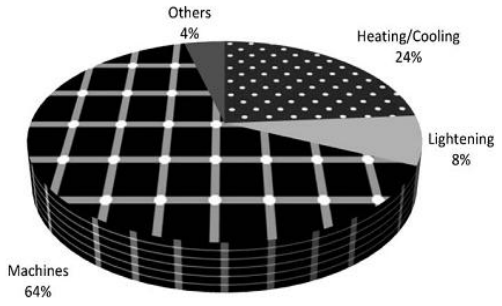

(c)

Figure 2.3: Electricity usage distributions for (a) the first case study, (b) the third case study and (c) the fourth case study [13]

Since the second case study is also a residential building, it will follow almost similar electricity usage like the first case. The results of this study indicate that the hybrid systems are the best choice to reduce the CO_2 emissions. On the other hand, the decision making is based on budget. So the solar water heaters are the first choice and the hybrid systems are the last choice in this case. Here prioritizing the choices based on technology does not depend on the pattern for all three types of building. It is because of the diverse energy consumption and types of buildings. The decision of choice of renewable technologies not only depends on the environmental protection, technology and cost but also depends on reliability, installation, maintenance and the easy use.

Now some important discussions will be done based on the energy efficiency trends in Canada. In these recent trends (published in December 2011), data are available until year 2009. The following figure shows the energy intensity per household and floor space.

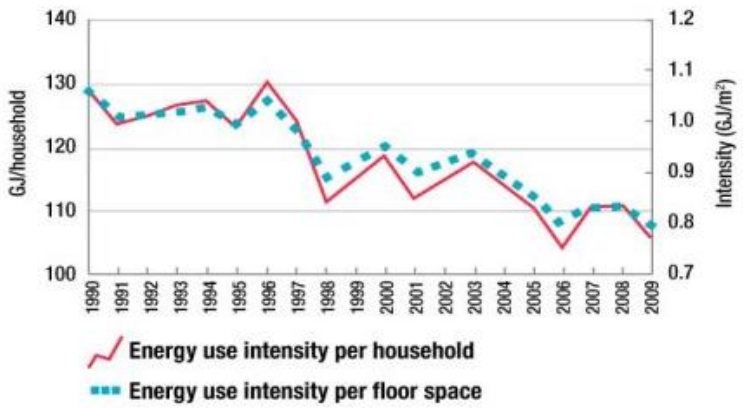

Figure 2.4: Residential energy intensity per household and floor space, 1990–2009 [14]

Since commercial/institutional sector is an important part of the main theme of this thesis, an elaborated study of commercial/institutional sector will be presented.

The floor space of the entire commercial/institutional sector in Canada is equivalent to about 40% of the total residential floor space. This sector was responsible for 14% of the total energy use in Canada in the year 2009. The following figure shows the secondary energy use by sector in 2009 [14].

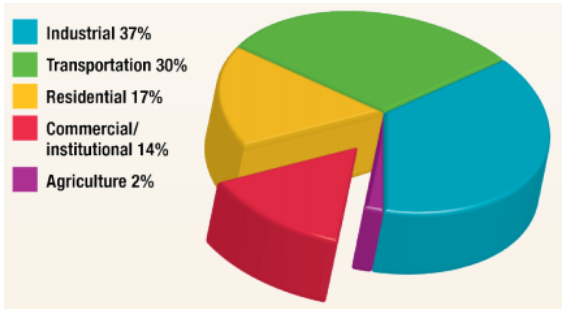

Figure 2.5: Secondary energy use by sector, 2009 [14]

Energy is used for different purposes like space heating, cooling, lighting and water heating in the commercial/institutional sector. Moreover, energy is used for operating auxiliary equipment (such as computers) and motors. The following figure shows the

energy use by end use. This figure indicates that space heating contributes to the largest share of energy use, with about half of the total energy used [14].

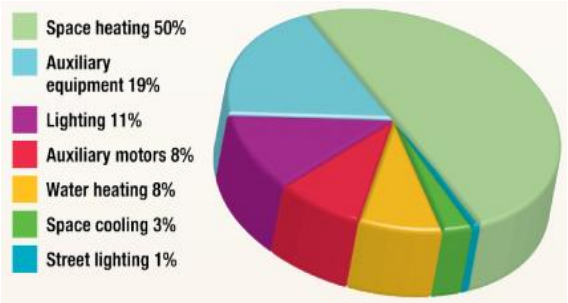

Figure 2.6: Commercial/institutional energy use by end-use, 2009 [14]

The commercial/institutional sector includes 10 subsectors which are related to trade, finance, real estate, public administration, educational and commercial services. Among these activities, offices, retail trade and educational services are responsible for 70% of the total Canadian commercial/institutional floor space which is 709.5 million m^2 according to the year 2009 [14].

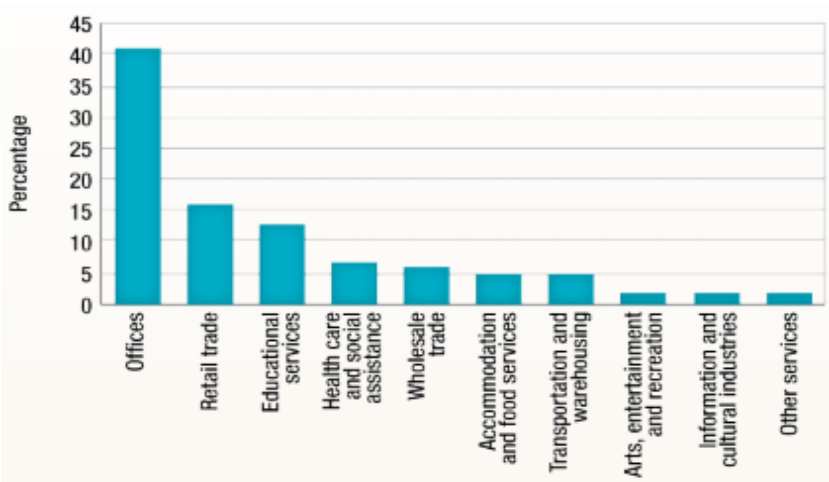

Figure 2.7: Commercial/institutional floor space by activity type, 2009 [14]

Total energy use in the commercial/institutional sector has been increased 37 percent from 867.0 PJ to 1,186.0 PJ during year 1990 to 2009. But natural gas and electricity are

the main energy sources of the commercial/institutional sector. These sources supply 87% of the total energy use. Here electricity is used for lighting, space cooling, auxiliary motors and equipment. And natural gas and the remaining fuels are used for space and water heating. The following figure shows the energy use by fuel type and floor space [14].

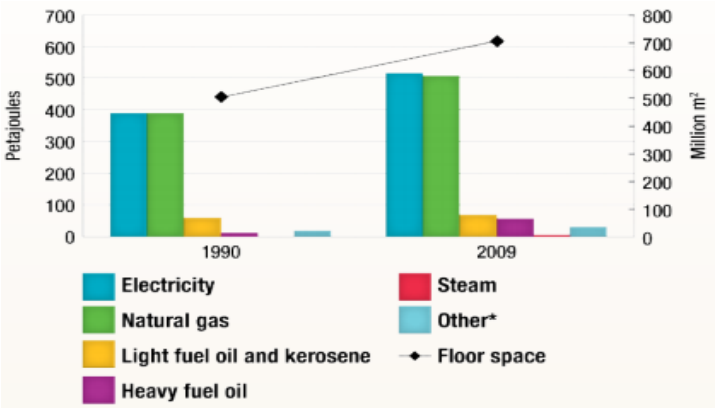

Figure 2.8: Commercial/institutional energy use by fuel type and floor space, 1990 and 2009 [14]

Moreover, energy use for space heating has been increased 26% between 1990 and 2009 which can be seen in the following figure [14].

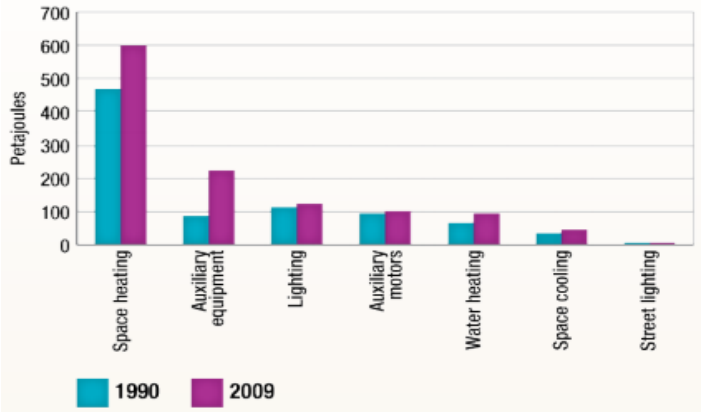

Figure 2.9: Commercial/institutional energy use by end-use, 1990 and 2009 [14]

In the commercial/institutional sector, energy intensity indicates the amount of energy use per unit of floor space (GJ/m^2). Accommodation and food services shows the most energy-intensive behaviour among the commercial/institutional activities. The following figure explains this clearly [14].

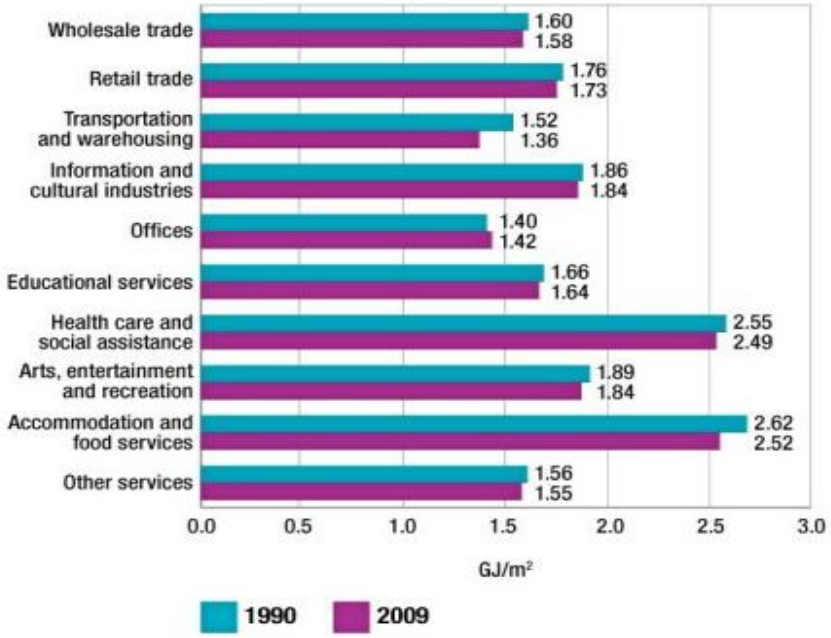

Figure 2.10: Commercial/institutional energy intensity by activity type, 1990 and 2009 [14]

In the commercial/institutional sector, the growth in energy use can be described by several indicators. These indicators include the number of employees, floor space and GDP. The following figure shows that the floor space has increased 39% in 1990 and the number of employees has increased 40% in this sector [14].

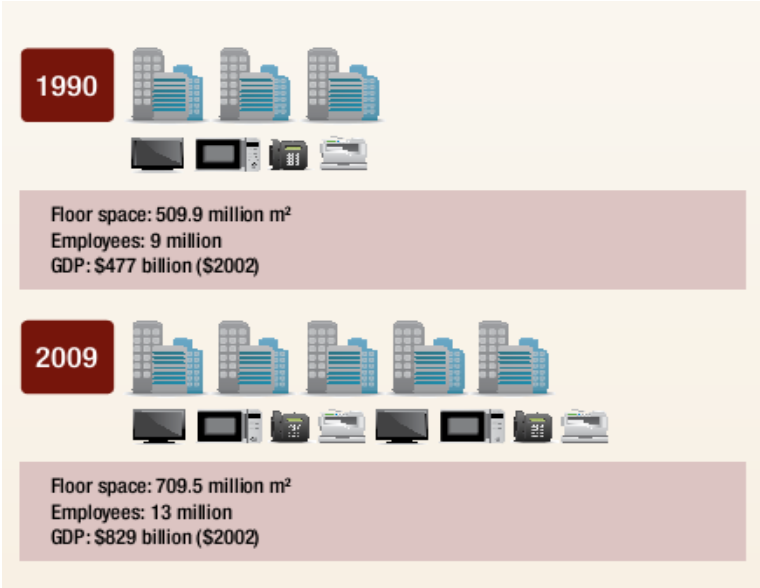

Figure 2.11: Commercial/institutional energy indicators, 1990 and 2009 [14]

Based on the above reviewed literatures, it is determined that the energy consumption in Canadian commercial buildings is high. So one of the main goals of this research is to reduce energy consumption of MUN engineering building which is a kind of commercial building.

2.2 Fuel Cell Modeling

Since the main objective of this thesis is to model natural gas fuel cell based power system for MUN engineering building, it is also important to know about fuel cell systems. Now some literatures will be reviewed based on PAFC (Phosphoric Acid Fuel Cell) modeling.

In [15], a two dimensional steady state model is described for a phosphoric acid fuel cell (PAFC). Here the steady state model is developed to describe the relationship between the

performance of fuel cell and various design options. The open circuit potential of a PAFC is given by the following equation [15].

$$E = -\frac{\Delta G}{nF} = E^0 + (\frac{RT}{nF}) \ln[\frac{a_{hydrogen} a_{oxygen}^{0.5}}{a_{water}}] \quad (1)$$

Where E represents open circuit potential, n represents number of electrons taking part in the reaction, F represents Faraday constant, T represents temperature, R represents gas constant and a represents effective area. Here the modeling requirements are temperature, operating pressure, humidity, electrical load and phosphoric acid management inside PAFC. Pdease2D software is used to numerically solve the model and Macsyma programming language is used to customize and interface.

The proposed model is validated by (a) verification of the basic parameters through a micro setup known as unit cell in one-dimensional mode and (b) evaluation of the two-dimensional model through an experimental setup of a PAFC stack with four cells. The following figure shows the one-dimensional model validation with unit cell data.

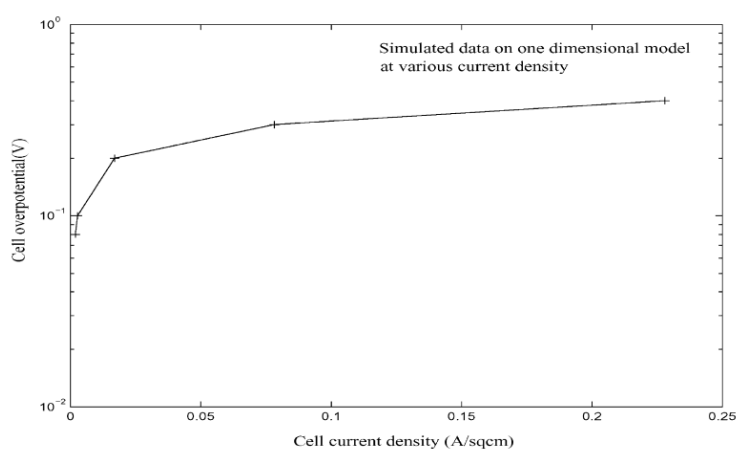

[15]

Figure 2.12: One-dimensional model validation with unit cell data

Different plots are also observed to evaluate the two dimensional model. The advantage of the model is the determination of area of low oxygen concentration and the design of various components of PAFC stack.

In [16], the performance of fuel cell system is optimized with a novel optimization tool in three steps. Firstly, a three-dimensional steady-state detailed model is built based on computational fluid dynamics (CFD) techniques and the simulated results from the CFD model are used for generating a database in a second step. This database contains the fuel and oxidant volumetric rates and utilizations and the corresponding cell voltages. Thirdly, linear regression is used to develop mathematical relationships between the input and output variables by using this database. Finally, by taking into account the constraints and limitations of the system, a multi-objective hierarchical Non-Linear Programming (NLP) problem is formulated and this approach is built upon two steps. The first step is to reduce consumption of the expensive fuel and the second step is to optimize the performance with respect to the oxidant volumetric rate. Now the following equations can be observed which are used to obtain the final cell voltage considering the losses [16].

$$V_C = E - \Delta V_{act} - \Delta V_{ohmic} - \Delta V_{conc}$$

$$\Rightarrow V_C = E - A\ln[\frac{I}{I_0}] - Ir - m\exp(n_C I) \tag{2}$$

where A is the "Tafel constant", I is the current density, I_0 is the exchange current density, r is the area specific resistance, and m, n_c are constants. The following figure can be observed to optimize the performance.

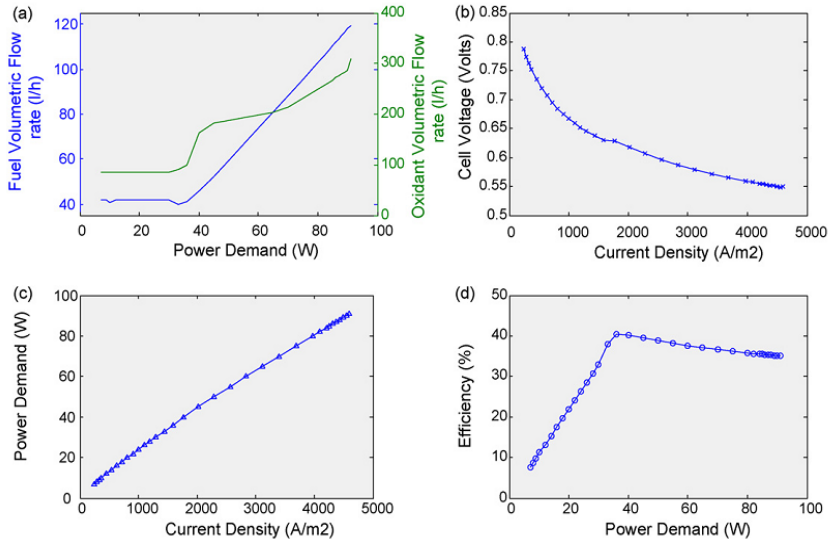

Figure 2.13: (a) Optimal values of fuel and oxidant inlet volumetric rates as a function of power demand, (b) optimal values of cell voltage as a function of current density, (c) optimal values of power demand as a function of current density and (d) optimal values of FC efficiency as a function of power demand [16]

The advantage of this model is that it can reach the process of optimal decision making regarding the operation of the system.

In [17], the impact of various parameters such as Tafel slope, diffusivity etc on the step response of the fuel cell is discussed. In case of large sized PAFC cathode, the effect of partial pressure variation in bulk gas is also analyzed here. Experimental verification for trend analysis based on the model output is done using a small unit cell setup. Two modes of operations are considered here to solve the unsteady state simulation. The following equation is used to express the unsteady state model [17].

$$\left(\frac{D_d}{RT}\right)\left(\frac{\partial^2 p_i}{\partial x^2}\right)+\left(\frac{D_d}{RT}\right)\left(\frac{\partial^2 p_i}{\partial y^2}\right)=\left(\frac{\lambda_d}{RT}\right)\left(\frac{\partial p_i}{\partial t}\right) \qquad [i=1,2]$$

Where D_d represents the diffusivity in diffusion layer for oxygen-water, P_i represents the partial pressure of the ith species, λ_d represents porosity of diffusion layer and R, T are constants.

Pdease2D software is used for solving the unsteady state model which is generally used for solving steady state model. Different experimental and simulated results are plotted here to test the effect of variations in the model parameters on step response. The comparison of experimental step response with simulated data is observed in the following figure.

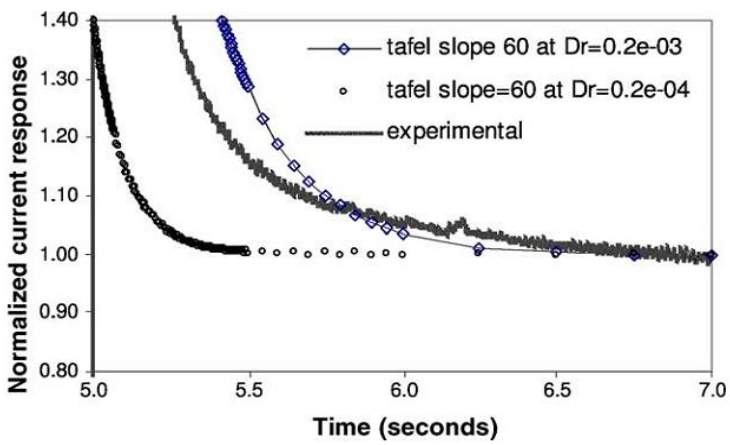

Figure 2.14: Experimental step response with simulated data [17]

The advantage of this model is that the effect of various parameters on the settling time of the cathode suggests for the development of a diagnostic tool employing such transient model. But the wettability of the electrode increases with the increase of age of a cell. The positive side of the effect is the increase of the active area of the electrode and the negative side is the decrease of the reaction layer diffusivity.

In [18], a three-dimensional model of a phosphoric acid fuel cell (PAFC) is described and this model is used to investigate the effects of process parameters on the fuel cell performance. In this case, empirical equations are used considering all irreversibilities as below [18].

$$V_p = E - \Delta V_{ohmic} - \Delta V_{act} - \Delta V_{conc}$$

$$\Rightarrow V_p = E - ir - A\ln[\frac{i}{i_0}] - m\exp(ni) \quad (3)$$

Where E represents the reversible open circuit voltage, ΔV_{ohmic} represents ohmic losses, ΔV_{act} represents activation losses, ΔV_{conc} represents concentration losses, i represents current density, r represents area-specific resistance, i_0 represents exchange current density and A, m, n are constants. Other model equations are derived from these equations. Two basic cases are studied here. They are (a) constant current density (1250 Am^{-2}) and various inlet feed rates and (b) constant inlet feed rates and various current densities. From the following figure, the average cell voltage can be represented as a function of current density.

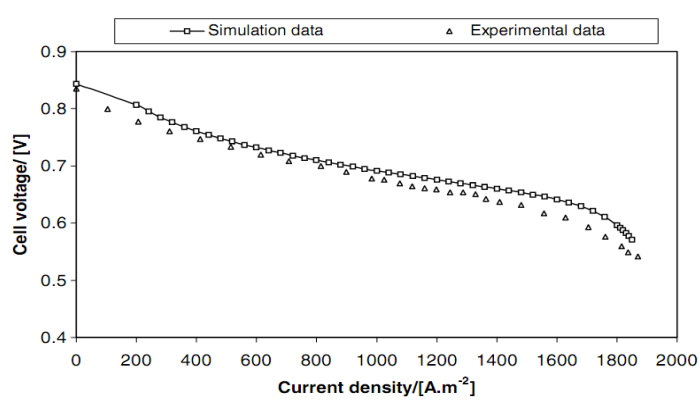

Figure 2.15: Simulated and experimental data concerning the average cell voltage as a function of current density [18]

It can be seen that there is satisfactory accuracy between the numerical and the experimental results. The cell voltage can be determined at a given a constant current density with the developed model. The power and power density both can be predicted for a single cell and a stack of cells, as well as and the overall fuel cell efficiency. Moreover, the working point of a realistic fuel cell can be estimated with the numerical model.

In [19], PAFC cathodes are characterized with a tool called electrochemical impedance spectroscopy (EIS). Here EIS analysis is done with the inducement of potential and measurement of the current response. The failure mechanisms in PAFC cathodes are analyzed and so information related to peak phase angle position is used. Determination of the position of the peak phase angle at various overpotentials at different experimental conditions is explained with a simple mathematical model. Moreover, the study for the effect of various electrode parameters on a newly proposed diagnostic marker is included here. In this case, variation of the output, i.e., the phase lag of the total current when excited with a sinusoidal potential input is analyzed while the system is polarized with a steady overpotential for various parameters. For this analysis the equation of overpotential is given as follow [19].

$$\eta(t) = \eta_{dc} + A\sin(2\pi ft)$$

where η represents local overpotential, η_{dc} represents steady dc polarization, f represents the frequency of the induced sinusoidal potential, t represents time and A is a constant. To

analyze the model and to validate the basic approach, a study of the agglomerate model is included here. From different plots, one simulated plot is given below. (useless could be deleted)

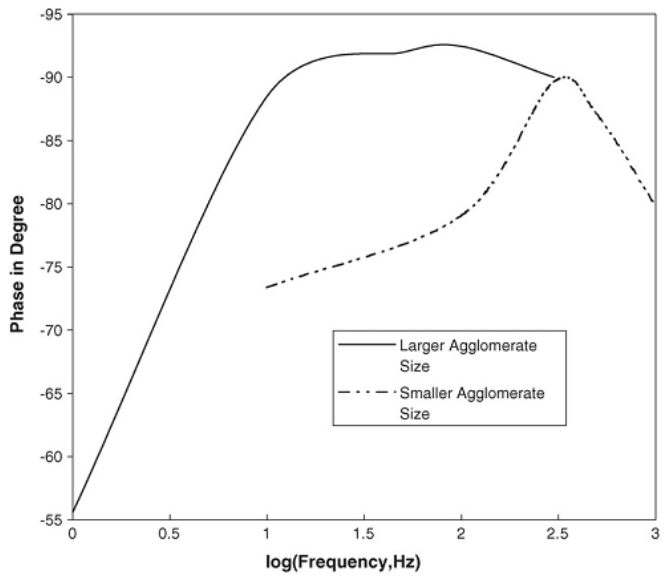

ε	R_{agg}	a_a	κ_{el}	κ_{agg}	η
20e-06	5e-03& 5e-04	35000	1e-06	0.4	-0.1

Figure 2.16: Simulated phase angle plot for different agglomerate sizes [19]

The advantage is the direct analysis of physical parameters like active catalyst area, diffusion resistance and so on. For PAFC cathode diagnostics, the position and relative value of the phase angle is used with respect to frequency as a diagnostic marker.

Based on the above reviewed literatures, it can be said that Phosphoric Acid Fuel Cell is a very useful and commercialized popular fuel cell. So a natural gas based fuel cell can be used to model the power system for the MUN engineering building. This modeling will be described in the manuscripts of next chapters.

CHAPTER 3

Modeling and Simulation of MUN Engineering Building in BEopt and HOT-2000 software

3.1 MUN Engineering Building

MUN Engineering building is a large commercial building. It is a four-storey building with a gross floor area of 25474.3 m^2 [20]. It is facing at southeast direction. The following figure shows the top view of engineering building from the front side.

Figure 3.1: Engineering building of MUN taken from Bing Maps

According to the provided data by facilities management, this engineering building annually requires about 197.9412 kWh/m^2 oil for heating and hot water purpose and

about 190.7 kWh/m^2 electricity [20]. For this research, only the values of the year 2012 are considered as inputs.

3.2 Data Analysis

3.2.1 Electricity Consumption and Cost Data Analysis

The Facilities Management Department of Memorial University of Newfoundland (MUN) provided the energy summary data of S. J. Carew (Engineering) building. The following table shows the electricity consumption and cost data of this building for the year 2012.

Table 3.1: Electricity consumption and cost data of engineering building [20]

Month	**Electricity Consumption (kWh)**	**Electricity Cost ($)**
January	439,560	44,010.84
February	398,352	40,515.41
March	402,930	41,285.40
April	366,300	33,381.34
May	393,773	36,414.60
June	434,982	39,621.18
July	407,509	40,919.94
August	366,300	37,222.01
September	402,930	40,604.67
October	439,560	43,450.79

November	412,088	40,110.36
December	393,773	39,969.11
Total	4,858,059	477,505.65

Table 3.1 indicates the electricity consumption and cost data.

3.2.2 Heat Consumption and Cost Data Analysis

The following table shows the heat consumption and cost data of the engineering building for the year 2012.

Table 3.2: Heat consumption and cost data of engineering building [20]

Month	**Heat Consumption (MMBTU)**	**Heating Cost ($)**
January	2,389	74,272.01
February	2,051	76,992.41
March	1,939	76,431.28
April	1,646	56,243.36
May	1,318	51,980.16
June	1,164	41,878.37
July	774	38,001.31
August	525	35,038.83
September	391	17,794.51
October	1,438	57,251.61

November	1,659	70,060.54
December	1,915	63,990.67
Total	17,210	659,935.06

Table 3.2 indicates the heat consumption and cost data. Both table 3.1 and 3.2 are made from the provided data by Facilities Management Department which is attached in the appendix. It can be observed from both tables that the total amount of energy consumption is very high. One of the main objectives of this thesis is to reduce the energy consumption which will be explained in the following manuscript.

3.3 Preface

In the literature review of the previous chapter, it is already observed that energy consumption in Canadian commercial buildings is too high. Moreover, after analyzing the data of MUN engineering building, it is also clarified that this building also consumes a large amount of energy. So, the energy consumption of this building should be reduced. Now the following manuscript will indicate the details of energy consumption of MUN engineering building. This manuscript will also show the current energy consumption in BEopt and HOT-2000 software, and also recommend the best options in BEopt software to reduce this consumption. Since this manuscript only shows the results of HOT models, the simulation for a particular zone of MUN engineering building is shown in the appendix.

This manuscript has already been published in the 22nd IEEE Newfoundland Electrical and Computer Engineering Conference (NECEC), 2013, St. John's, Newfoundland and

Labrador, Canada. This paper has also been presented in the conference by the principal author Mahmuda Ahmed Tanni. The co-author Dr. Tariq Iqbal supervised the principal author Mahmuda to develop the models described in the paper and provided her necessary tools for clear concept. She wrote this paper, developed these models in BEopt and HOT-2000 and conducted simulation. Dr. Iqbal reviewed the manuscript, helped her with the simulations, corrected and checked all simulations and provided necessary suggestions for manuscript.

This manuscript will end up with a recommendation of natural gas fuel cell based power system for MUN engineering building. This fuel cell based power system will be explained in details in the next chapter. Datasheet of this fuel cell is attached in the appendix from where calculations are done for the required energy of MUN engineering building.

Modeling and Simulation of MUN Engineering Building in BEopt and HOT-2000 software

[1]Mahmuda Ahmed Tanni, *Student Member IEEE*, [2]M. Tariq Iqbal

[1,2] Faculty of Engineering and Applied Science, Memorial University of Newfoundland,

St. John's, Newfoundland, Canada

Abstract- **This paper presents modeling and energy analysis of the engineering building of Memorial University of Newfoundland. The first building model is developed in BEopt (Building Energy Optimization) software. This model shows expected yearly energy consumption of the building. The results are compared with the measured building energy consumption data provided by the MUN Facilities Management Department. The BEopt model is also validated using NRCan HOT-2000 software. The results of both models are compared in the paper. This paper shows the best fitted model with the actual building data. Moreover, an improved building model is presented using BEopt software which shows less energy consumption than the actual measurement. Based on modeling and simulation results, this paper presents a list of recommendations to improve the existing building to reduce its yearly energy consumption. The selection of scaling factor is also explained in the paper to show how simulated data correlate with the measured data.**

Index Terms-Energy Analysis, Zero Net Energy (ZNE) Building, BEopt Software, HOT-2000 software, Scaling Factor.

I. INTRODUCTION

The building which can produce as much energy as it uses annually, is called Zero Net Energy building (ZNE). A ZNE building uses a grid-tied, net-metered photovoltaic (PV) system and active solar for this purpose. Such building requires minimal energy-related costs [1].

This paper presents the energy analysis of MUN engineering building and its energy related costs. Engineering building is like a big commercial building. It is a four-storey building with a gross floor area of 25474.3 m^2 [2].

This building is facing southeast. According to the provided data by the MUN facilities management, the engineering building annually requires about 197.9412 kWh/m^2 oil for heating and hot water purpose and about 190.7 kWh/m^2 electricity [10]. Only the values of the year 2012 are considered as inputs for this paper.

The following figure shows a top view of engineering building from the front side.

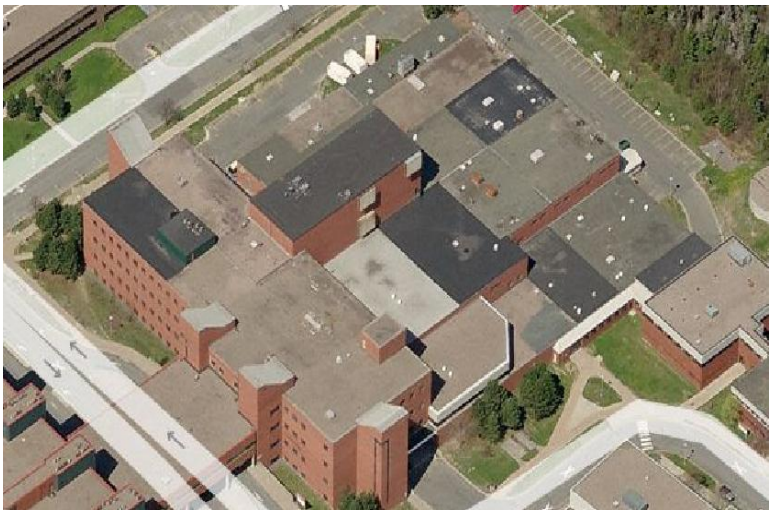

Figure 1. Engineering building of MUN

In this paper, models of engineering building are presented in BEOPT software (Building Energy Optimization) and HOT-2000 software. Basically the actual model of the engineering building in BEopt will indicate the actual energy consumption of the engineering building. The same building is also modeled in HOT-2000 software to validate the BEopt model. Moreover, this paper proposes an improved model of the building which shows lower energy consumption. In this way, this paper indicates the limitations of the existing design and how to improve them. Besides, a list of recommendations is suggested to improve the existing design. The selection of scaling factors is also explained to know how the simulated data correlate with the measured building data.

In this paper, section 2 describes the BEopt model of engineering building, section 3 describes the HOT-2000 model of the engineering building, section 4 shows the proposed improved model of the engineering building in BEopt software, and section 5 concludes the paper.

II. BEOPT MODEL

In BEopt software (http://beopt.nrel.gov/), there are 3 types of inputs which are geometry screen, options screen and site screen. The inputs of this model are explained in the following three sections.

A. Geometry Screen

This screen allows to draw the engineering building. Figure 2 and 3 show the design from front and backside. It is possible to observe the building in a three dimensional

structure from any side in BEopt software. Since BEopt can't design beyond third level, the height of the fourth level is added with the third level. First and second level heights are considered as 13 feet in this simulation. But the third level is considered as 20 feet instead of 26 (13*2) feet because of the limitation of the software. Moreover, BEopt can't design such a large commercial building. So each cell is considered here as 5 feet (scale down). The simulated building looks as shown in figure 2 and 3 with the above mentioned assumptions in BEopt software.

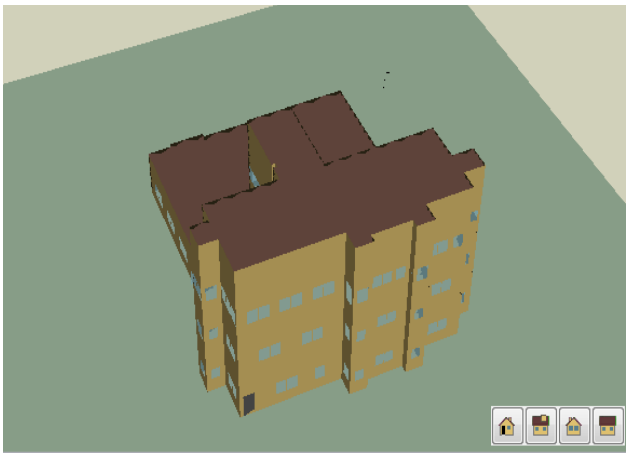

Figure 2. Engineering Building from the front side in BEopt

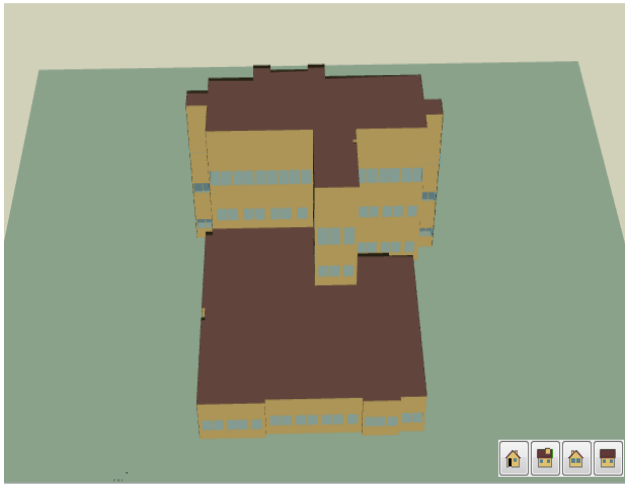

Figure 3. Engineering Building from the back side in BEopt

B. Options Screen

The options screen allows us to choose the specifications of the building. This screen looks as below.

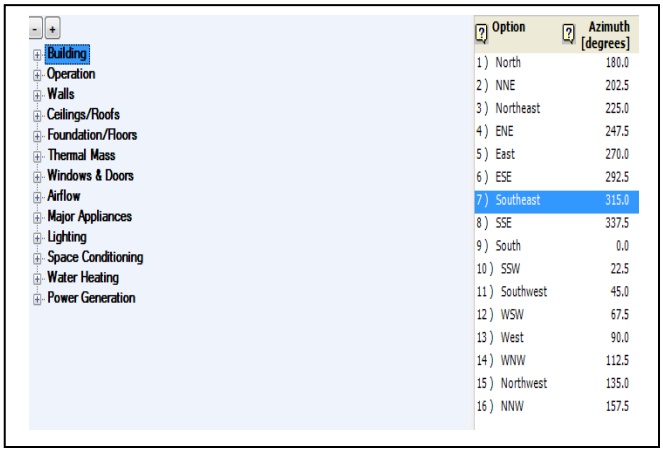

Figure 4. Options Screen in BEopt for engineering building

The options screen consists of 13 options. Each option has some sections. It is important to select the correct option for correct simulation results. If an accurate option is not found, the closest option is selected. Each option is explained below with its sections in a tabular form. Table 1 shows the building option screen.

TABLE 1: BUILDING OPTION SCREEN

Name of the Option	Selected Option
Orientation	Azimuth - Southeast 315^0
Neighbors	None

The top side (arrow) of the geometry screen indicates the north. But the engineering building faces southeast. In this way, the orientation is calculated from the north side. For the second option, it is assumed that there are no neighbors.

TABLE 2: OPERATION OPTION SCREEN

Name of the Option	Selected Option
Heating Set Point	71 F
Cooling Set Point	75 F
Humidity Set Point	45% RH
Miscellaneous Electric Loads	Gas/Electric-24148kWh/yr, All electric-25769kWh/yr
Miscellaneous Gas Loads	0
Miscellaneous Hot Water Loads	0
Natural Ventilation	None
Interior Shading	None

Table 2 shows the operation option screen. Miscellaneous electric loads are calculated with the following two equations.

$$Gas/Electric\,(kWh/yr) = 1595 + 248 \times BR + 0.426 \times FFA$$

$$All\_Electric(kWh/yr) = 1703 + 266 \times BR + 0.454 \times FFA$$

where BR indicates the number of bedrooms and FFA indicates the finished floor area. For these calculations, BR is considered as 76 and FFA is considered as 8681 square feet. If BR is considered more than 76, the calculated value will exceed the highest given value. And the FFA can be observed from the geometry screen. It is calculated by the software with respect to the drawing space.

TABLE 3: WALLS OPTION SCREEN

Name of the Option	Selected Option
Wood Stud	None
Double Wood Stud	None
CMU	12-in Hollow
SIP	None
ICF	None
Other	None
Wall Sheathing	None
Exterior Finish	Brick, Medium/Dark

Table 3 indicates walls option screen. The options are selected by observing the materials used in the building.

TABLE 4: CEILINGS/ROOFS OPTION SCREEN

Name of the Option	Selected Option
Finished Roof	R-47.5 SIPs
Roof Material	Asphalt Shingles, Dark

Table 4 indicates ceilings or roofs option screen. The finished roof option is selected by observing the R-value as 49.8. Since roof R-value value is typically 49 for regions like St. John's according to IECC (International Energy Conservation Code), the closest of this value is chosen. And the roof material is selected as Asphalt Shingles (Dark) by observation of the building.

TABLE 5: FOUNDATION/FLOORS OPTION SCREEN

Name of the Option	Selected Option
Slab	4 feet R10 Perimeter, R5 Gap
Carpet	0% Carpet

Table 5 above indicates the foundation or floors option screen. The slab is selected according to the IECC.

TABLE 6: THERMAL MASS OPTION SCREEN

Name of the Option	Selected Option
Floor Mass	2 inch Gypsum Concrete
Exterior Wall Mass	Concrete
Partition Wall Mass	Concrete
Ceiling Mass	None

Table 6 above indicates thermal mass option screen. The floor mass is selected from the given options by observation. Since no option is accurate for exterior wall mass and partition wall mass, new values are entered for concrete. The ceiling mass option is selected as none.

TABLE 7: WINDOWS AND DOORS OPTION SCREEN

Name of the Option	Selected Option
Window Areas	15% F20 B40 L20 R20
Windows	Double-Pane, Medium-Gain Low E, Metal Frame,

	Air Fill
Eaves	None
Overhangs	None

Table 7 above indicates windows and doors option screen. The window area is selected as a percentage of exterior wall area. The window type is selected by observation of windows used in the building.

TABLE 8: AIRFLOW OPTION SCREEN

Name of the Option	Selected Option
Air Leakage	Constant 0.1 ACH
Mechanical Ventilation	Supply

Table 8 indicates airflow option screen. Air leakage is calculated from the following equation.

$$\frac{Building\_cfm}{Building\_volume} \times 60 = air\_leakage$$

Building cfm of this design can be chosen either 55.9 or 111.8 from mechanical ventilation option. In this way, air leakage for 55.9 cfm is 0.03 and for 111.8 is 0.06. So the air leakage option is chosen the closest one i.e. 0.1 ACH. But the mechanical

ventilation is chosen as supply. Moreover, the actual building mechanical ventilation is neither ERV (Energy Recovery Ventilation) nor HRV (Heat Recovery Ventilation) type.

TABLE 9: MAJOR APPLIANCES OPTION SCREEN

Name of the Option	Selected Option
Refrigerator	None
Cooking Range	None
Dishwasher	None
Clothes Washer	None
Clothes Dryer	None

Table 9 above indicates major appliances option screen. The refrigerator is selected as none, since there is only one freezer in one kitchen of the building. And the energy consumption of this refrigerator is too low to choose.

TABLE 10: LIGHTING OPTION SCREEN

Name of the Option	Selected Option
Lighting	100% Fluorescent, Hardwired & Plugin

Table 10 above indicates lighting option screen. Since there are only fluorescent bulbs in this building, this option is selected as 100% fluorescent.

TABLE 11: SPACE CONDITIONING OPTION SCREEN

Name of the Option	Selected Option
Central Air Conditioner	None
Furnace	None
Boiler	Oil, Hot Water, Forced Draft, 85% AFUE
Electric Baseboard	None
Air Source Heat Pump	None
Ground Source Heat Pump	None
Ducts	None
Ceiling Fan	None
Dehumidifier	None

Table 11 above indicates space conditioning option screen. Since the heating and hot water systems of this building are operated by boiler, this option is chosen. The efficiency of the boiler is given as 85% by the MUN facilities management department.

TABLE 12: WATER HEATING OPTION SCREEN

Name of the Option	Selected Option
Water Heater	Oil standard
Distribution	None
Solar Water Heating	None
SWH Azimuth	Southeast (-45^0)
SWH Tilt	0 degrees

Table 12 above indicates water heating option screen. Since the water heater is oil operated, this option is chosen as oil standard. The SWH (Solar Water Heating) is selected as none and the SWH azimuth is chosen by calculation (building azimuth+90^0=315+90=Southeast-45^0) among given options. Since there is no solar water heater in this building, an option of 0^0 degree is chosen among given options.

TABLE 13: POWER GENERATION OPTION SCREEN

Name of the Option	Selected Option

PV System	None
PV Azimuth	Southeast
PV Tilt	0 degrees

Table 13 above indicates water heating option screen. The PV azimuth and tilt options are selected like the table 12 options. Since there is neither a solar water heater nor a PV system in this building, the selected azimuth and tilt options have no impact on the model.

C. Site Screen

The last input site screen allows to choose the site i.e. location of the building. The following figure shows the site screen.

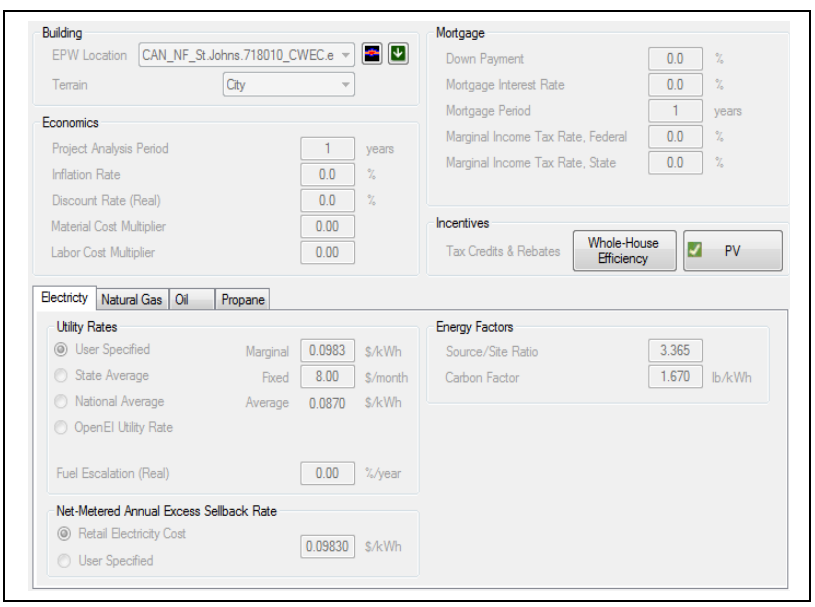

Figure 5. Site Screen in BEOPT for electricity option

Figure 5 above shows that the building is located in St. John's city of Newfoundland, Canada. In this way, BEOPT downloads the weather data of St. John's. Since the economics and mortgage options are not related to this model, these options are considered as zero except two options. For those two options, values greater than zero are required to run, so 1 is entered for each option. In electricity option, only user specified $/kWh (477505.65/4858059 = 0.0983) is entered. This value is calculated from provided data of electricity consumption in kWh and total cost of electricity in dollar ($) for the year 2012.

Since no natural gas and propane are used for engineering building, the user specified options are kept as zero. So their window figures are not shown.

Figure 6 indicates the oil option for this building. It is calculated using the methods described above. Total cost of oil is divided by the amount of oil consumption in gallons (659935.06$/ (17210/0.141)gal = 5.4068$/gal).

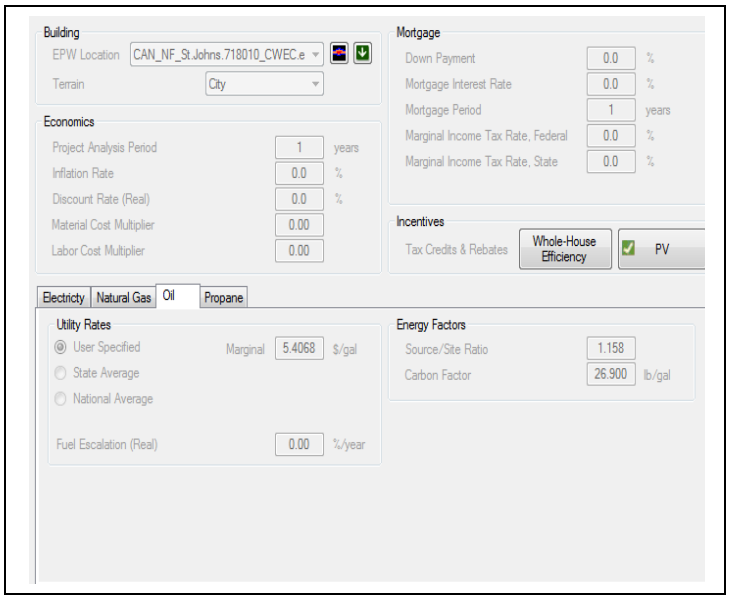

Figure 6. Site Screen in BEOPT for oil option

After running this model in BEOpt, some results are obtained. This model is run with a reference building which is called B10 benchmark. Actually B10 benchmark is a reference case for ideal residential buildings according to IECC. The following figure shows the output screen.

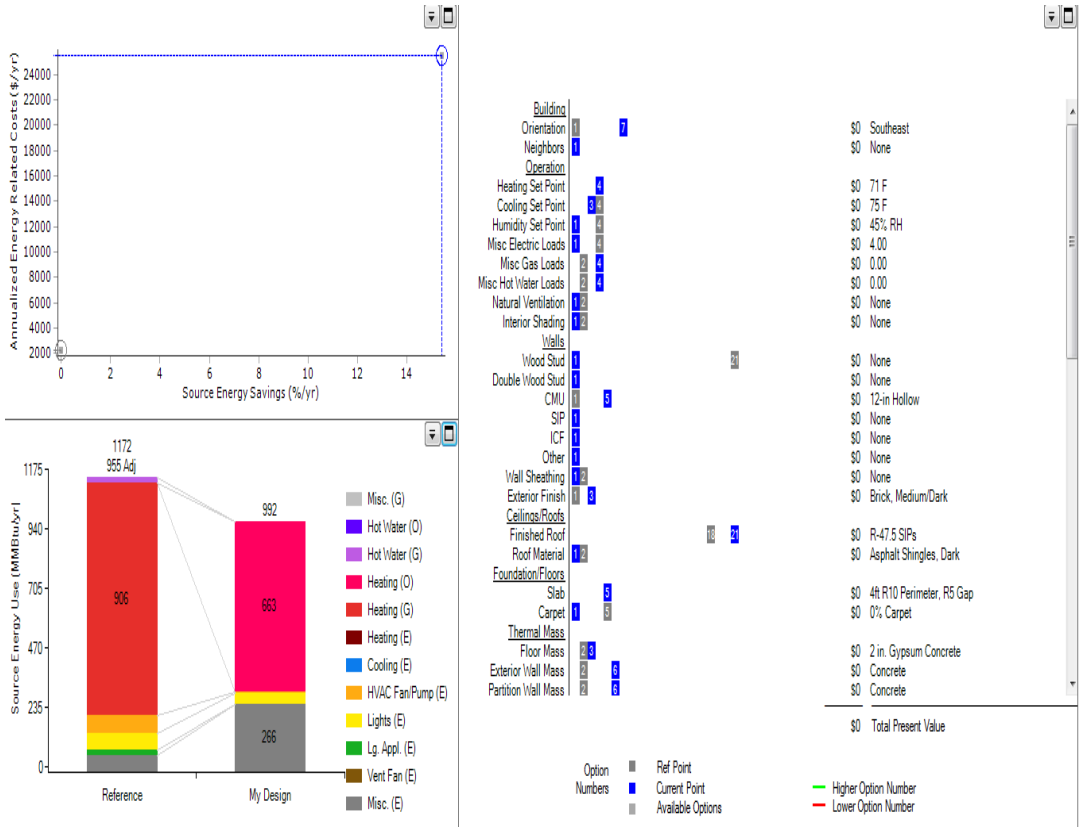

Figure 7. Total Output Screen for the first model

Figure 7 above shows the total output screen. Each figure will be shown separately as below with description.

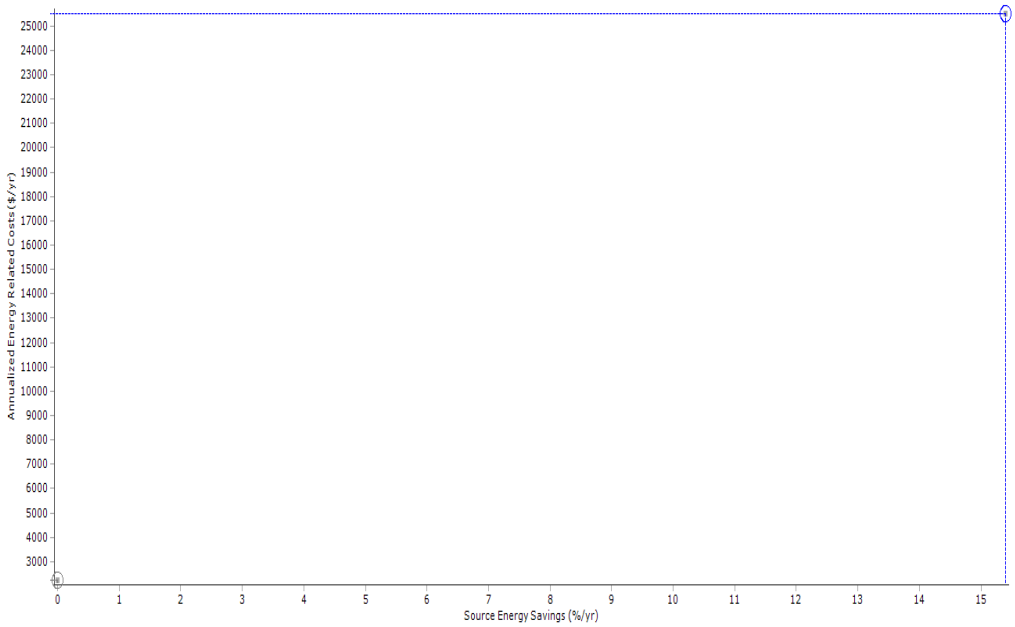

Figure 8. Annualized energy related costs output for the first model

Figure 8 shows that the annualized energy related cost is greater than $25,000. It is 45 times less than the total cost provided by the facilities management department (1137440.17/25000 = 45.5). The scaling factor 28 is obtained by calculation of building volume. Actual volume of the building is 28 times higher than the volume of the building modeled in BEOPT (3191057/118215=27). The scaling factor 33.7 is obtained by calculation of floor area (276044.3/8177=33.7). Actual building gross area and volume are obtained from the facilities management in an excel file [3]. So it can be seen that the volume factor is and the area factor are very close to each other. Moreover, another approximate calculation can be done for surface area. Since it was not possible to obtain surface area of the actual building, it was approximately calculated. In this case, the scaling factor is 8 (290913.6 ft^2/37620 ft^2=7.73). Since it was not possible to draw the

actual building because of the limitation of the software, the outputs have to be scaled for accurate values.

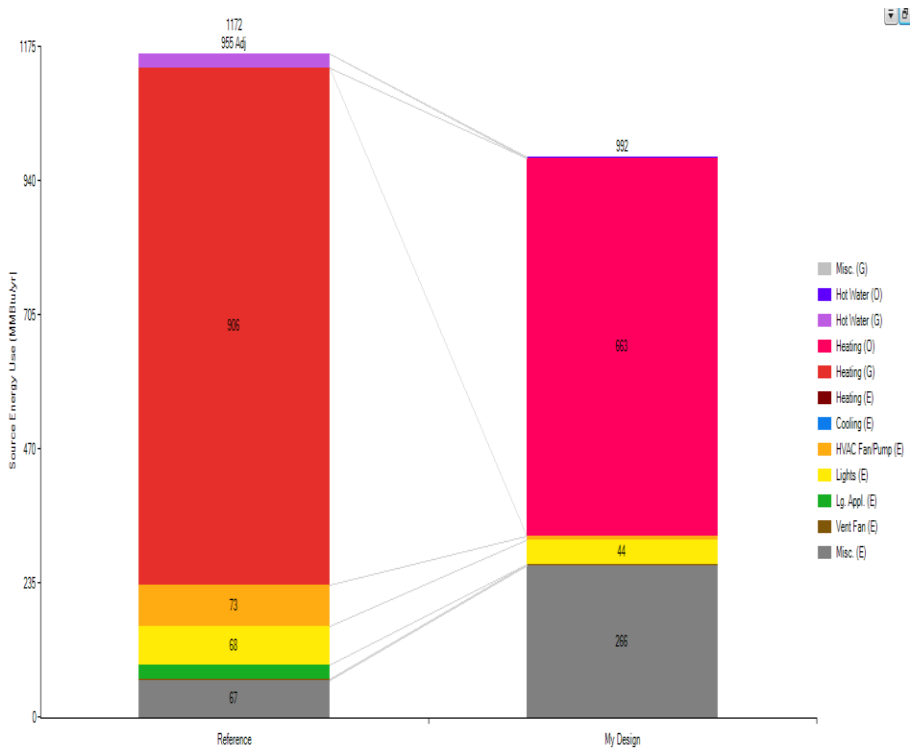

Figure 9. Source Energy Use Output for the first model

Figure 9 above shows the source energy usage in MMBTU per year. This model shows less consumption than the reference building. Because there is no energy consumption for washer-dryer, cooking etc. in this simulated building. But IECC fixes some energy consumption for their reference residential building. The model shows (992-663=329 MMBTU*293.1=) 96429.9 kWh/yr for electricity consumption. This value is approximately (4858059/96429.9) 50.3 times less than the provided data for electricity consumption. This model indicates 663 MMBTU/year for oil consumption. This value is also (17210/663) 26 times less than the provided data for oil consumption.

But the total the cost factor is 45 and not close to the other two area and volume factors. Since this cost factor includes both electricity and oil costs, it is different from them. These results are based on the simulation of the first model in BEOPT. Now the same building will be modeled in HOT-2000 software to verify the and BEopt model.

III. HOT-2000 MODEL

The same engineering building is modeled in HOT-2000 software to validate the previous BEopt model. This section won't show the whole design and modeling. It will only compare the simulated results with the previous results of BEopt model. The following figure will show the top view of the engineering building divided for the design in HOT-2000 software (http://canmetenergy.nrcan.gc.ca/software-tools/hot2000/84).

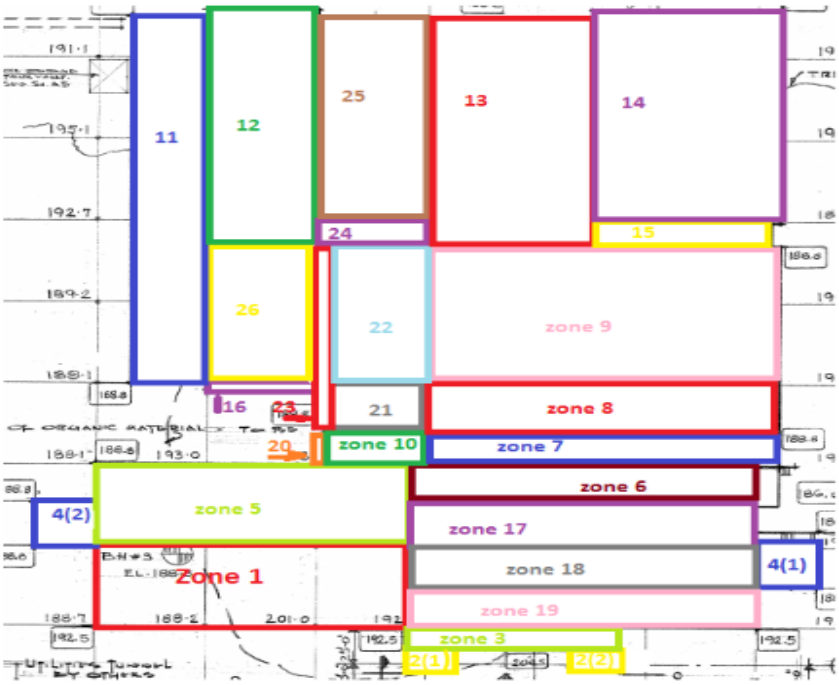

Figure 10. Top view of engineering building with 26 regions

To model the engineering building in HOT-2000, the whole area is divided into 26 zones and almost all inputs are considered same as the BEopt model. Since there are 4 zones where each pair has same floor area but other parameters are different, it can be considered as there are 26 zones. Each region is simulated in HOT software and then the simulated results of all zones are added to calculate the total consumption. The following table shows the electrical and heating consumption of each zone.

TABLE 14: SIMULATION RESULTS OF MODELS IN HOT-2000

Zone No.	Electrical Consumption (kWh)	Heating Consumption (MMBTU)	Zone No.	Electrical Consumption (kWh)	Heating Consumption (MMBTU)
1	188367	1759	13	356039	1586
2(1)	10362	188	14	376261	1361
2(2)	18997	162	15	57158	349
3	55169	769	16	10691	141
4(1)	31547	397	17	170856	1234
4(2)	31547	397	18	170764	1214
5	377361	1424	19	141679	1087
6	146030	1081	20	5057	99

7	109135	763	21	62063	519
8	214933	1132	22	137353	1004
9	390530	1921	23	21667	476
10	37544	353	24	29299	274
11	263580	1268	25	255874	1244
12	243370	1026	26	130411	585
Total				4043644	23813

Table 14 above shows the total electrical and heating consumption in HOT-2000 software which are 4043644 kWh and 23813 MMBTU, respectively. The provided data by the Facilities Management Department are 4858059 kWh for electricity and 17210 MMBTU for heating [2]. It is not possible to adjust the whole building in HOT software due to the large area of this building and limitation of the HOT-2000 software. The simulated data is very close to the provided measured data and to the results of BEopt model. Since all of the inputs of this HOT-2000 model are the same as the BEopt model inputs and they show almost similar results, it can be said that both models are correct.

IV. PROPOSED IMPROVED MODEL

Two building models described above are developed which show almost actual energy consumption of the engineering building. An improved model is developed in BEopt software which shows lower energy consumption than the provided data. This design also

includes the three inputs like the previous BEopt design. For the improved design, only the options screen is changed from the previous design. The other two inputs i.e. geometry screen and site screen are kept as such as the previous design. This means the second model is the improved version of the same building i.e. same geometry with the same site screen. So only the options screen of the improved design is explained below.

Since the building option screen is kept the same for the improved design, it is not given here. Table 15 shows operation options screen of the improved BEopt model.

TABLE 15: OPERATION OPTION SCREEN

Name of the Option	Selected Option
Heating Set Point	68 F
Cooling Set Point	73 F
Humidity Set Point	45% RH
Miscellaneous Electric Loads	Gas/Electric-24148kWh/yr, All electric-25769kWh/yr
Miscellaneous Gas Loads	0
Miscellaneous Hot Water Loads	0
Natural Ventilation	None
Interior Shading	None

From table 15, it can be seen that only heating set point and cooling set point are changed from the previous BEopt design. These points are changed according to the requirements of passive house which is 20^0C as a comfortable temperature [4].

The walls option screen is kept as such. Table 16 shows the ceilings/roofs option screen.

TABLE 16: CEILINGS/ROOFS OPTION SCREEN

Name of the Option	Selected Option
Finished Roof	R-49 Fiberglass, 2×12, R-25 XPS (R-value:73)
Roof Material	Metal, Dark

Finished roof is chosen by calculating the R-value. Suggested R-value for thermal building is less than 0.01 W/m^2. But in BEOPT, the lowest R-value in W/m^2 can be chosen as 0.05 W/m^2 (73h.ft^2 / BTU = 0.05 W/m^2) [4]. And the roof material chosen as metal dark, since it is more energy efficient option.

The foundation/floors and thermal mass options are kept as such. Windows/Doors option screen for the improved design is given in table 17.

TABLE 17: WINDOWS AND DOORS OPTION SCREEN

Name of the Option	Selected Option
Window Areas	12% F25 B25 L25 R25
Windows	Triple-Pane, High-Gain Low E, Insulated Frame, Air Fill
Eaves	None
Overhangs	None

Since the window area is not given in the requirements of passive house design, this option is chosen by simulating and observing the lowest energy consumption. For the windows option, suggested U-value is 0.8 W/m^2 or less [4]. In this improved design, U-value for this type of window is 0.21 BTU/h. ft^2 (0.21 BTU/h. ft^2=0.68 W/m^2).

Table 18 shows the airflow option for the improved design.

TABLE 18: AIRFLOW OPTION SCREEN

Name of the Option	Selected Option
Air Leakage	None
Mechanical Ventilation	HRV, 70%, 50% of ASHRAE 62.2

Suggested ventilation by the requirements of passive house design is the heat recovery ventilation (75% or higher) [4]. In this design, the highest HRV can be chosen as 70%. And for this type of ventilation and building volume of 118215 ft^3 in BEOPT, ACH is ((55.9/118215)*60=) 0.028 So air leakage is chosen as none.

The other option screens are kept as such. In the simulation results of the improved design of the engineering building, the following window can be observed.

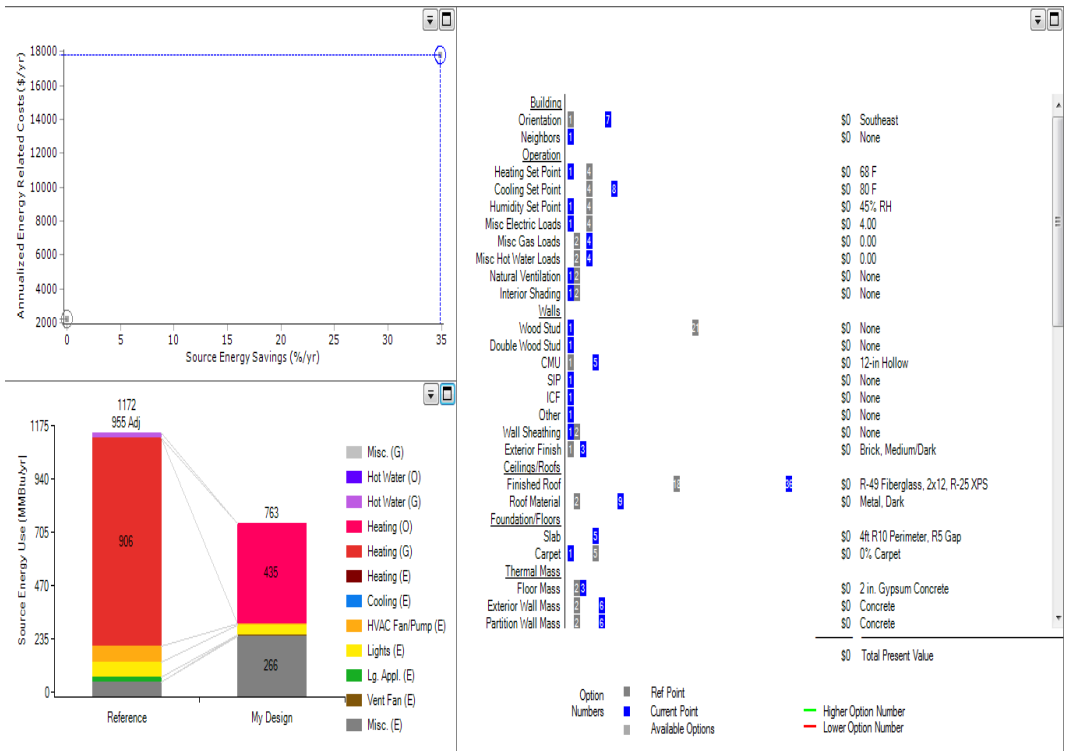

Figure 11. Total Output Screen for the second model

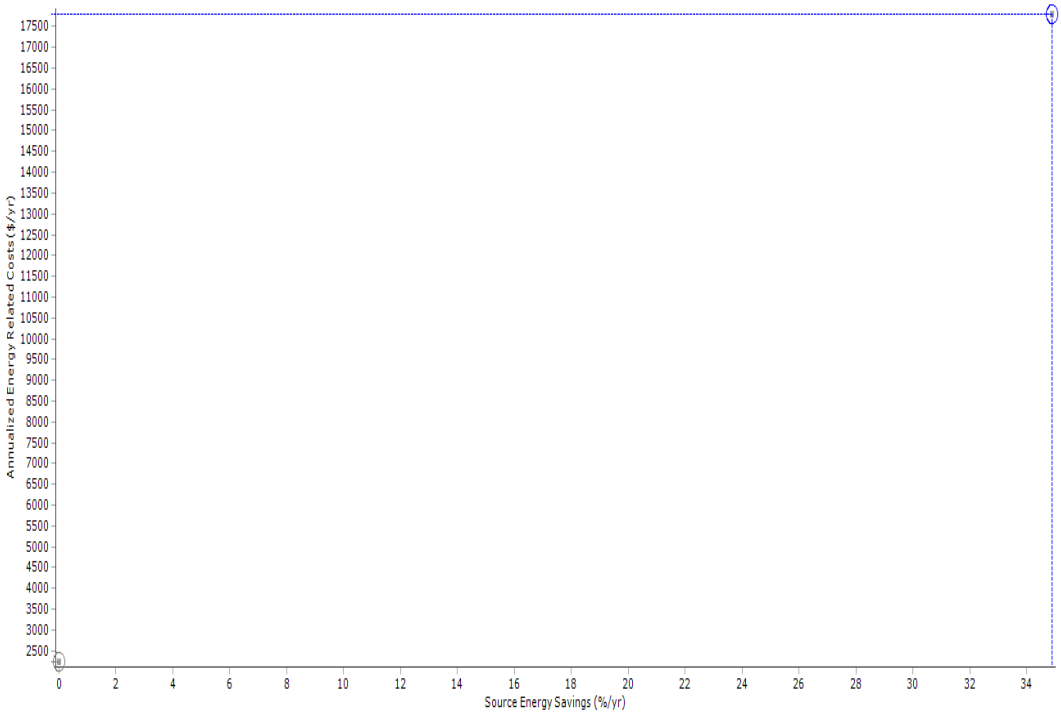

Figure 12. Annualized energy related costs output for the improved building model

Figure 12 shows that the total cost has been reduced from $25000 to $17500 which is a great improvement from the previous design.

Figure 13 shows that the oil consumption has been reduced from 652 MMBTU to 435 MMBTU for one year. The electricity consumption is almost the same. It is not reduced because it is not used for heating. But the oil consumption was very high. If the engineering building can be modified like the improved BEopt model, it can run by a 440 kW fuel cell system. Now,

400*8765=3506000 kWh=3506000/293.1 MMBTU =11961.8 MMBTU

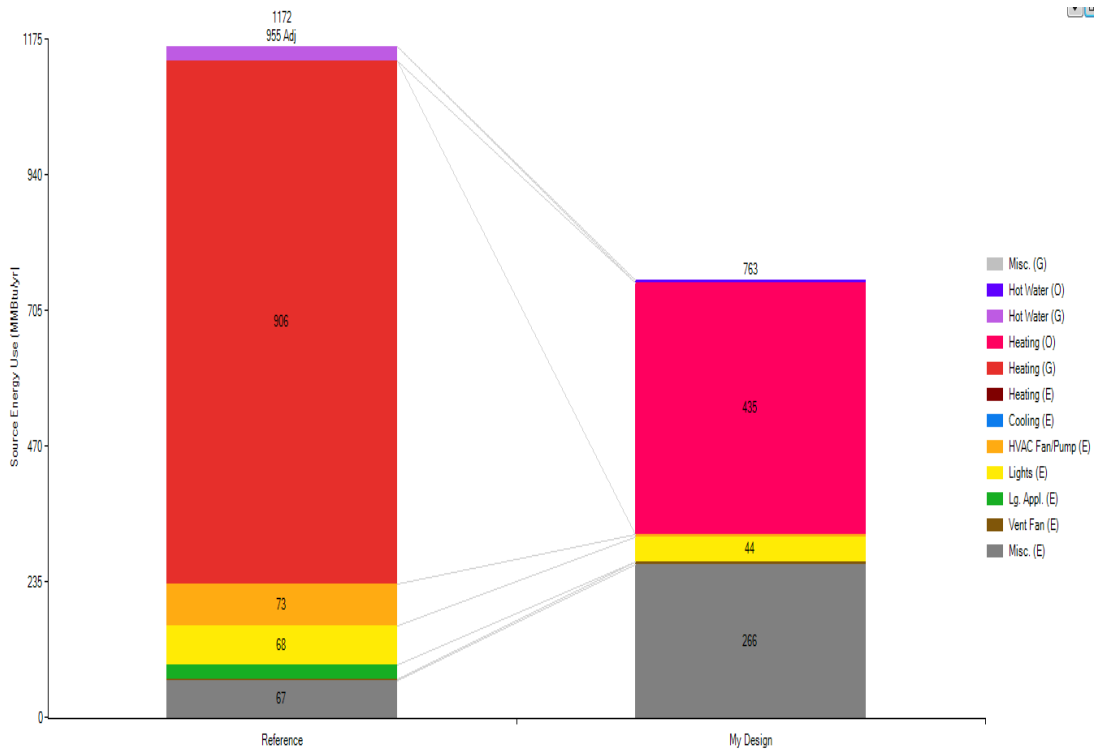

Figure 13. Source Energy Use Output for the second model

From the scaling factors of simulation results, the scaling factor is considered as 30. So fuel cell can supply maximum (11961.8/30=) 398 MMBTU of electricity. But the improved design shows 325 MMBTU. So this is already in range. For heating, fuel cell can supply (0.96+0.59=1.55 MMBTU/hr=1.55/30 MMBTU = 0.0517*8765 MMBTU/yr maximum or 452.86 MMBTU. The improved design shows 435 MMBTU for heating. In this case, this is also in range. So it can be said that this natural gas based fuel cell can provide both required electricity and required heating for the improved BEopt model.

V. CONCLUSION

In this paper, two models of MUN engineering building are built in BEopt software and HOT-2000 software. Then those models were analyzed. They showed almost similar

results and results were close to the provided data. Moreover, an improved version of BEopt model is also developed here which showed less energy consumption than the actual provided data. In this analysis, a 440 kW fuel cell system is also proposed to supply electricity and heat for the engineering building. The impact of scaling factors was also observed. This paper also indicated the limitations of the existing design analysis in both BEopt and HOT-2000 models. Possible improvements to the building are proposed in the section IV.

REFERENCES

[1] Craig Christensen, Ren Anderson, Scott Horowitz, Adam Courtney, and Justin Spencer, "BEopt™ Software for Building Energy Optimization: Features and Capabilities", Technical Report: (National Renewable Energy Laboratory) NREL/TP-550-39929, August 2006.

[2] Provided data of the Engineering Building (S. J. Carew Building) by Facilities Management Department.

[3] ACH Engineering, Microsoft Excel File for mechanical ventilation by Facilities Management Department.

[4] Passive House Requirements, supported by Energy Saving Trust.

CHAPTER 4

Simulink Modeling of a Phosphoric Acid Fuel Cell System

4.1 Fuel Cell Modeling

Modeling has become very important to develop fuel cell technology during the past two decades. The core knowledge of fuel cell development is represented by cell-level models. Here the dimensionality of models is used as the criterion to provide an overview. In this case, from zero-dimensional to fully three-dimensional approaches are considered. Zero-dimensional models consider single equations and one-dimensional models describe processes orthogonal to the electrolyte, simulations in two and more dimensions also describe the mass, heat, and charge transport in the plane of the flow field. Steady state approach is the selected one where all of these models are applicable. But computational effort in the time domain is considerably higher than steady state approaches for the same dimensionality. So it requires adequate computational resources. For this reason, now-a-days transient modeling is becoming popular [21].

Since fuel cell follows non-linear behavior, Matlab/Simulink is used to control its behavior. Matlab/Simulink is very popular to model dynamic and non-linear systems. The following polarization curve of fuel cell can show its non-linear behavior more clearly. Usually this behavior is almost same for all types of fuel cell but the voltage and current level differ.

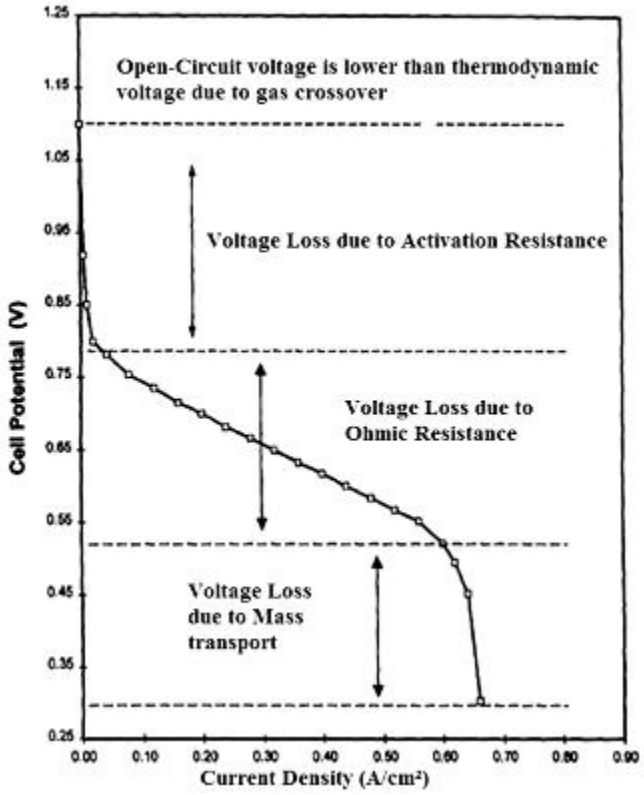

Figure 4.1: Typical polarization curve of fuel cell [22]

Figure 4.1 indicates the characteristic graph of voltage versus current for a set of operating conditions of a fuel cell. It summarizes the three parts of the voltage losses which are activation loss, Ohmic loss and concentration loss [22].

The basics of fuel cell and details of these losses will be explained in the following manuscript. This manuscript will show three models of PAFC type fuel cell in Matlab/Simulink software. Basically the steady state modeling approach will be observed. The first model is based on empirical equations where these three losses can be identified with the system output voltage. The second model is based on a simple curve fitting approach where these losses can't be identified separately. In this model, only the system output voltage can be calculated. The third model is based on the available Simulink

blocks. This model can't calculate the losses separately. But it can calculate the system output voltage. The simulation results of these three models are studied and compared in this paper.

4.2 Preface

A version of this manuscript has been published in the 21st IEEE Newfoundland Electrical and Computer Engineering Conference (NECEC), 2012, St. John's, Newfoundland and Labrador, Canada. This paper has also been presented in the conference by the principal author Mahmuda Ahmed Tanni. The co-author Dr. Tariq Iqbal supervised the principal author Mahmuda to develop the three models in the paper and helped her to conceptualize the theories needed for this research. Mahmuda Tanni wrote this paper, developed these three models in Matlab/Simulink and conducted simulation. Dr. Iqbal reviewed the manuscript, simulations and provided necessary suggestions.

This manuscript will end up with the selection of the best model among the presented three models. The best chosen model will be elaborated and connected with the Power System Blocksets (PSB) in the next chapter. Then the power electronics part of a fuel cell system will be explained. The dynamics of a fuel cell system will also be observed in that chapter.

Simulink Modeling of a Phosphoric Acid Fuel Cell System

[1]Mahmuda Ahmed Tanni, *Student Member IEEE*, [2]Md. Arifujjaman, *Member IEEE,* [1]M. Tariq Iqbal

[1]Faculty of Engineering and Applied Science, Memorial University of Newfoundland, St. John's, Newfoundland, Canada.

[2]EE and Software Engineering, UTC Power, South Windsor, CT, 06074, USA.

***Abstract*-In this paper an approach for the steady state modeling of a Phosphoric Acid Fuel Cell (PAFC) system is presented. The selected PAFC system contains three fuel cell stacks. This paper presents three models. 'Model 1' is based on the empirical equations. Matlab-Simulink software is used to simulate the model. This model mathematically calculates the cell output voltage including Nernst potential, activation loss, ohmic loss and concentration loss. The system characteristics i.e. voltage and current curves with respect to time can be observed through this model. The voltage versus current (V-I) curve is also determined can also be observed including all losses. The effects of output voltage variation can be investigated with respect to different input parameters. 'Model 2' uses a simple curve fitting approach while 'Model 3' is based on available simulink blocs. Details of all three system models and simulation results are included in the paper. The developed models are very simple and require minimal computation time.**

Index Terms-PAFC, Steady State Modeling, System Dynamics, V-I curve.

I. INTRODUCTION

A fuel cell is an electrochemical device which produces electricity from continuously supplied streams of fuel and oxidant to porous anodes and cathodes. A fuel cell is similar to a conventional battery which produces electricity by electrochemical reactions. There are five major types of fuel cells such as Alkaline (AFC), Phosphoric Acid (PAFC), Molten Carbonate (MCFC), Solid Oxide (SOFC) and Proton Exchange Membrane (PEMFC) [1].

Generally PAFC system operates at 150–190^{0}C and the pressure ranges from ambient to 5 atm. Typically Pt is used as a catalyst both for hydrogen and oxygen electrodes in a PAFC system. The PAFC system is attractive because of its various features. The waste heat from the stack can be used in this system which makes co-generation possible. Moreover, a part of the waste heat can be used for process steam generation and can be fed to the upstream reformer. Overall system efficiencies could reach about 80% because of all these features [2].

This paper presents a steady state modeling of a PAFC system containing three fuel cell stacks. Three modeling approaches are presented. The first model is based on empirical equations. It calculates the cell output voltage, stack output voltage and the system (3 fuel stacks) output voltage for each input current density value. The system dynamics can also be observed and the I-V curve can be investigated. Two more models based on simple curve fitting and using Simulink blocks are also presented.

In this paper, section 2 describes the mathematical model, section 3 describes the system simulation, section 4 shows the results and discussions, and section 5 concludes the paper.

II. MATHEMATICAL MODELING

The mathematical modeling is important to understand the steady state modeling. The first modeling of a PAFC is based on empirical equations. This model includes Nernst potential, activation loss, ohmic loss and concentration loss. The overview of an individual fuel cell loss can be observed from the following block diagram,

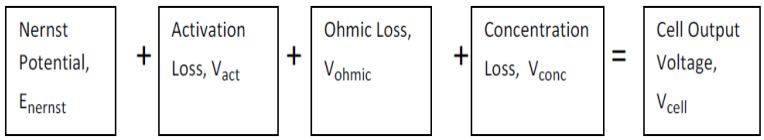

Figure 1. Block diagram of a PAFC

Equation (1) represents the above block diagram [3].

$$V_{Cell} = E_{nernst} + V_{act} + V_{ohmic} + V_{conc} \tag{1}$$

The equation signs of all of the losses are negative, therefore V_{cell} is always less than E_{nernst}.

A. Nernst Potential

The thermodynamic potential is found at thermodynamic balance. Nernst potential expresses this voltage. At standard condition (298.15 K, 1 atm), hydrogen, oxygen and vapor produce a thermodynamic potential [4].

$$E_{nernst} = E^{0} + \frac{RT}{nF}\ln[\frac{p'_{H2}(p'_{O2})^{0.5}}{p'_{H2O}}] \quad (2)$$

Here E^0 represents the reference potential at unity cavity (1.229 V at standard state), p'_{H2}, p'_{O2} and p'_{H2O} are the hydrogen, oxygen and vapor partial pressures (atm), respectively. Moreover, T is the cell temperature (K), R is the universal gas constant (8.31441 J mol^{-1} K^{-1}), F is the Faraday constant (96484.56 C mol^{-1}) and n is the number of electrons participating in the reaction [4].

B. Activation Loss

The activation energy is related to both chemical and electrical reactions. They can be distinguished by the reacting species. The voltage drop due to the activation loss can be minimized by rate parameters and activation energy of one or more rate limiting reaction steps. The equation of activation loss is observed as below [5].

$$V_{act} = -\frac{RT}{\alpha nF}\ln\frac{i}{i_o} \quad (3)$$

where α is the electron transfer coefficient of the reaction at the electrode being addressed, i is the current density and i_0 is the exchange current density.

C. Ohmic Loss

The resistance of flowing ions in the electrolyte and through the electrode causes ohmic loss. This loss can be reduced by decreasing the electrode separation and increasing the ionic conductivity of the electrolyte [5], (P:2-12) . The ohmic loss is given by equation (4) [4].

$$V_{ohmic} = -IR_{\text{int}} \quad (4)$$

Here I is the electrical current and R_{int} is the internal resistance. The equation of R_{int} is developed empirically for the proposed model based on some experimental data keeping the temperature fixed to 451 K (178 ^{0}C). The equation of R_{int} can be expressed as below,

$$R_{\text{int}} = 0.0652 I^{-0.819}$$

D. Concentration Loss

Sometimes reactants may be diluted by the products in electrochemical reactions. Thus concentration loss occurs. The equation of concentration can be written as [5], (P:2-16).

$$V_{conc} = \frac{RT}{nF} \ln\left(1 - \frac{i}{i_L}\right) \tag{5}$$

where i_L is the limiting current density.

The individual stack voltage can be written as follow [4],

$$V_{stack} = NV_{cell} \tag{6}$$

where N is the number of fuel cell in a stack (i.e. 376) and V_{stack} is the stack voltage for a PAFC.

Since the proposed system contains three fuel stacks, the system voltage of the steady state model can be observed by equation (8),

$$V_{system} = 3 \times V_{stack} \tag{7}$$

where V_{system} is the PAFC system output DC voltage.

III. SYSTEM SIMULATION

This paper represents three steady state models and a comparison among them. 'Model 1' is based on empirical equations of fuel cell described in the above section. Figure 9 shows the Matlab/Simulink block diagram of 'Model1'.

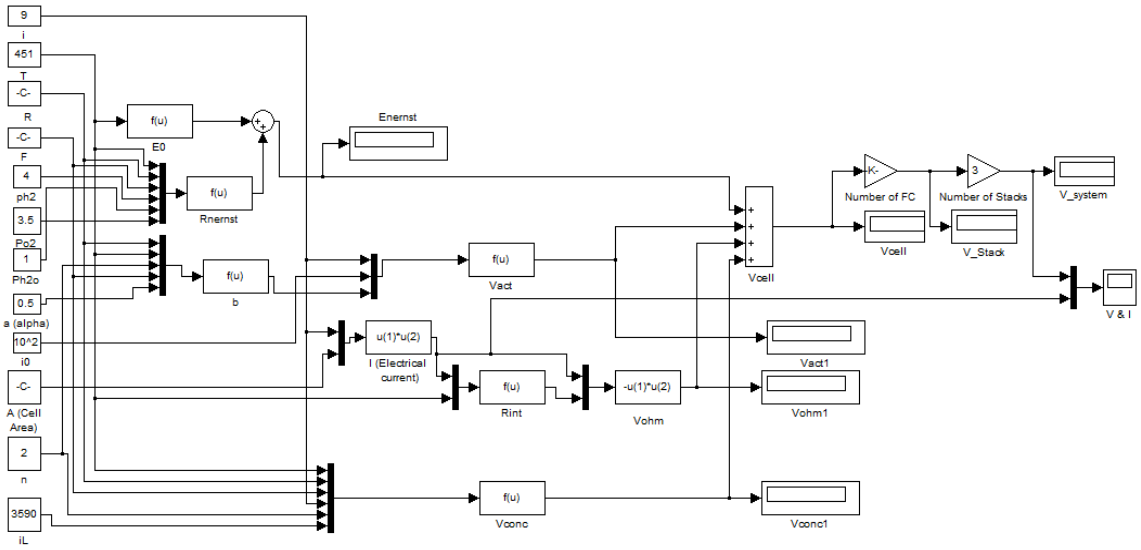

Figure 2. Matlab/Simulink block diagram of 'Model 1'

Figure 2 shows the steady state modeling based on the mathematical equations discussed in section 2. The input parameters which are fixed in 'Model 1' are listed in table I.

TABLE I: INPUT PARAMETER VALUES OF THE PAFC STEADY STATE MODEL

Parameter Name	Parameter Value
Temperature, *T*	451 K
Gas Constant, *R*	8.31441 J mol^{-1} K^{-1}

Faraday Constant, F	96484.56 C mol^{-1}
Partial pressure of hydrogen, p_{H2}	4 atm
Partial pressure of oxygen, p_{O2}	3.5 atm
Partial pressure of vapor, p_{H2O}	1 atm
Electron transfer coefficient, α	0.5
Exchange current density, i_0	10^2 A m^{-2}
Cell area, A	0.1950 m^2
Number of electrons participating in the reaction, n	2
Limiting current density, i_L	3590 A m^{-2}

The variable input parameter of 'Model 1' is the current density (i), indicated at the top of inputs in figure 2. This input parameter is varied to observe different system voltages (V_{system}) at the output. This model also calculates Nernst potential (E_{nernst}), activation loss (V_{act}), ohmic loss (V_{ohm}), concentration loss (V_{conc}), cell output voltage (V_{cell}) and individual stack voltage (V_{stack}) for each input i. The system voltage and current curves with respect to time can be observed through the scope 'V & I' block.

The second model 'Model 2' is based on a simple curve fitting on the manufacturer provided I-V data. Figure 3 shows the steady state modeling based on a I-V curve. This model is named as 'Model 2'. The I-V curve equation is 1398.8*(i^(-0.073)).

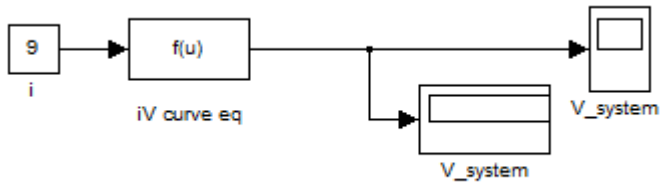

Figure 3. Matlab/Simulink block diagram of 'Model 2'

Here i represents the current density which is the only input to this model. V_{system} is the system output voltage which is the only output of 'Model 2'. This 'Model 2' calculates the system voltages for different input current densities. This model also shows the system voltage curve with respect to time for each selected input.

Simulink has a generic fuel cell stack model as a block in power system block set. This generic block can present any type of fuel cell for a set of input data. We used three such blocks with a set of inputs to represent our fuel cell system. Figure 4 shows the steady state modeling based on the built-in fuel cell stack of Matlab/Simulink software. This 'Model 3' is developed by connecting three built-in fuel cell stack models in series. Only three inputs T, P_{h2}, P_{o2} are allowed in this model. This is the major short coming of this simulink model. This 'Model 3' is a combination of simulink blocks and SimPowerSystem (SPS) blockset. A voltage measurement and mean block are connected to measure the system output voltages. Ground connections are arranged to simulate the model correctly.

A powergui block is kept in the model to run the power system blocks. The scope block shows the system voltage with respect to time.

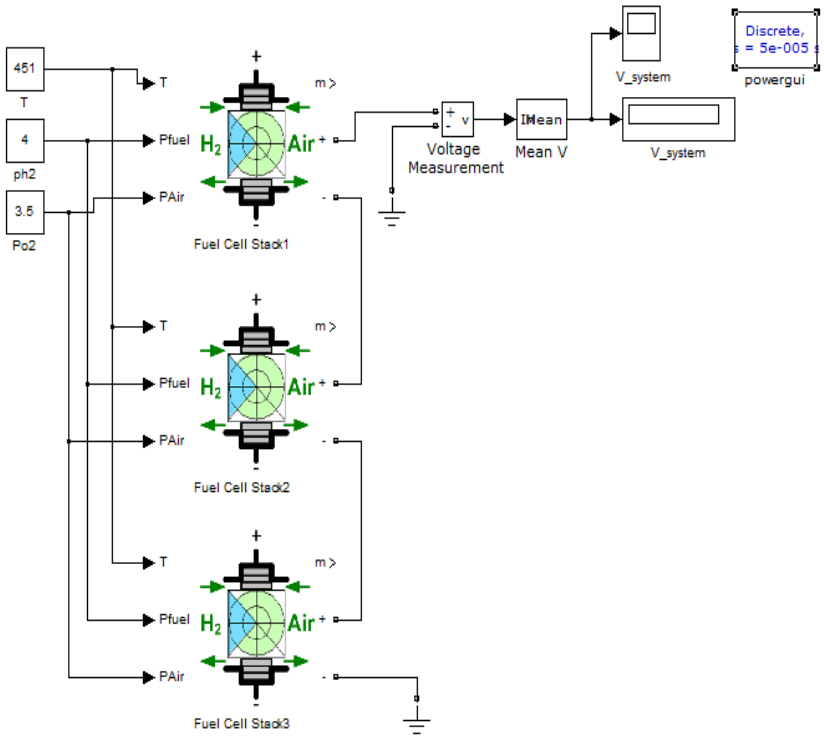

Figure 4. Matlab/Simulink and power system block diagram of 'Model 3'

The values of input T, P_{h2}, P_{o2} are kept same to compare these three models. 'Model 3' is different from 'Model 1' and ' Model 2' since no input I (current density) is possible. In this case, the block parameters of fuel cell stacks can be changed which are different from the other two models. Here the I-V curve and cell parameters can be observed.

IV. RESULTS AND DISCUSSIONS

The comparison of these three models can be investigated by observing the results of each model. Table II shows the results of 'Model 1' and 'Model 2' for different inputs.

TABLE II: RESULTS OF 'MODEL 1' AND 'MODEL 2'

Current Density, i (Am^2)	For 'Model 1':	For 'Model 2':
	System voltage, V_{system} (V)	System voltage, V_{system} (V)
9	1308	1192
500	1042	888.7
1000	984.8	844.8
1512	947	819.7
2012	917.5	802.8
2512	890.5	789.9
3018	861	779.4
3519	801.9	770.7

Table II shows the results of the display blocks of 'Model 1' and 'Model 2'. The scope block observations of these models are given in figure 5 and figure 6. No system transients are shown since all three models are the steady state models.

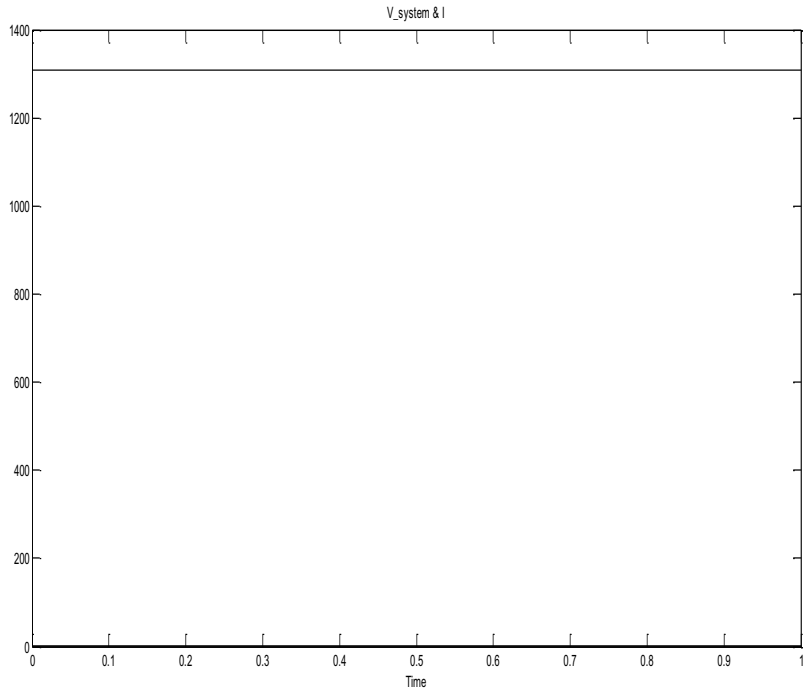

Figure 5. Voltage and Current as a function of time

Figure 5 shows the observation of 'Model 1' for a single input. The topmost straight line is the system voltage line and bottom line is (which almost falls upon x-axis) the system current line. The lines are straight because they are the outputs for only one input. 'Model 1' will show similar figures for all inputs but a different value. The current value is very low which increases with the increase of current density and the voltage value decreases accordingly.

In case of 'Model 2', figure 6 is the result of simulation.

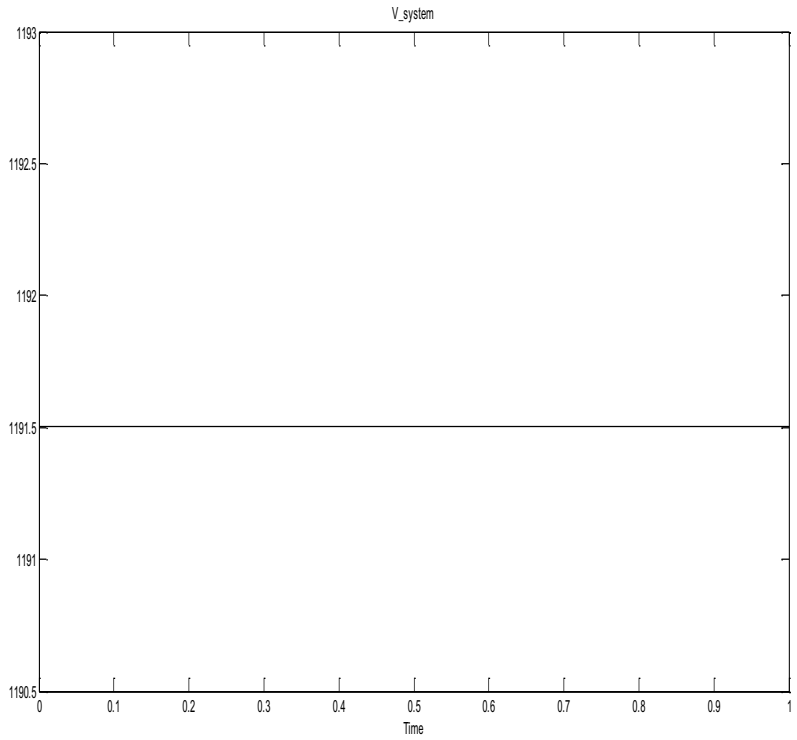

Figure 6. System Voltage as a function of time

Figure 6 shows only the system voltage line for a single input. This value decreases with the increase of current density value.

The display block result of 'Model 3' (Figure 4) is 1314 V which can be controlled by adjusting the three inputs and the block parameters of the three fuel cell stacks. Figure 7 shows the observation of the scope block of 'Model 3'.

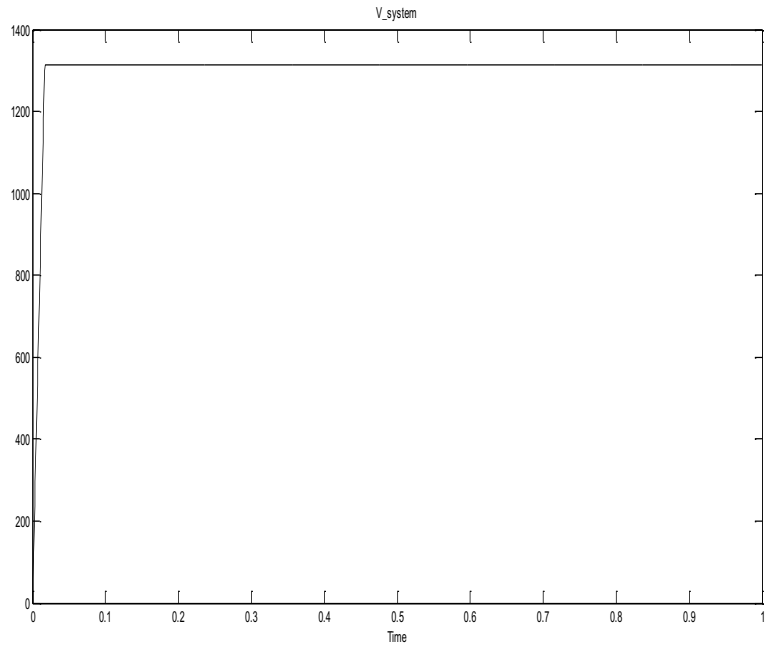

Figure 7. System Voltage as a function of time

Figure 7 shows that the system voltage increases up to 1314 V and then it saturates. This is because 'Model 3' has a mean block which calculates the mean values of each fuel cell stack and then the three values are added.

Figure 8 shows the I-V and I-P curve for fuel cell stack 1 shown in figure 4. The results for fuel cell stack 2 and 3 are same as below. This type of I-V and I-P curves can also be observed by changing block parameters for different inputs of each fuel cell stack. The cell parameters can also be adjusted for 'Model 3'.

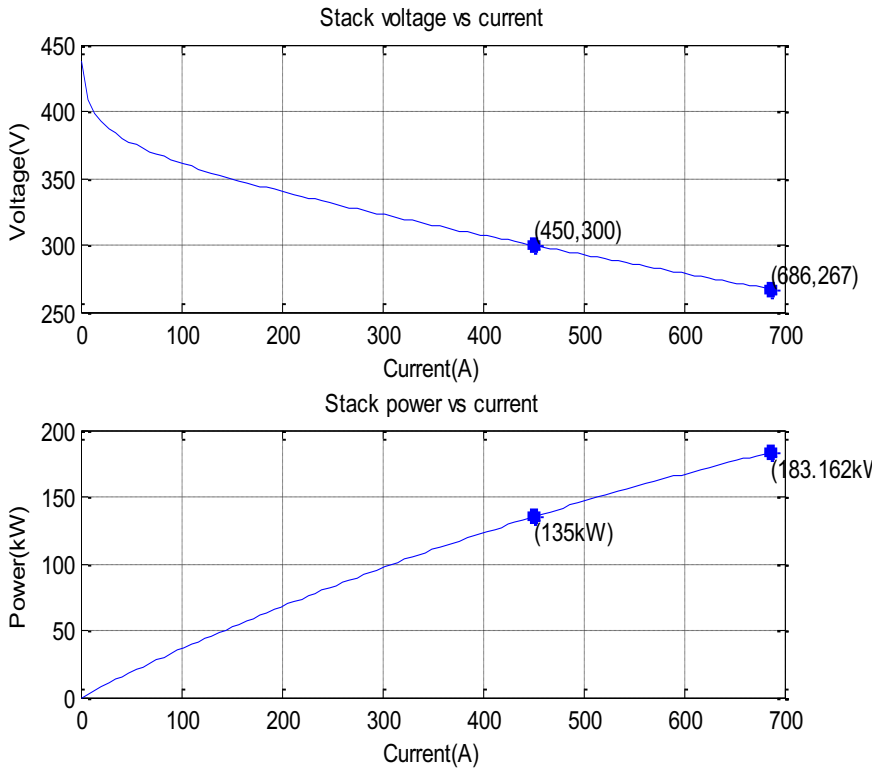

Figure 8. I-V and P-V curves of 'Model 3'

From the results of these three models, it can be observed that 'Model 1' is better than 'Model 2' and 'Model 3' since we have full control on different parameters in 'Model 1'. In 'Model 2', we can only control on parameter i. Table 2 also shows better system voltages for 'Model 1'. In case of 'Model 3', we have limited control on built-in fuel stacks. We can't give our desired inputs to this model. And 'Model 1' can also show similar I-V curves (shown in figure 8) by calculating the outputs or using a X-Y plotter. So 'Model 1' is the best choice among these three models and it has simplicity and all parameters could be adjusted as needed to represent a real fuel cell stack.

V. CONCLUSION

In this paper the steady state modeling of a PAFC system is presented in three ways and simulated. Three models are compared on the basis of results and the best model is chosen. Further analysis could be done as needed and these models can be used to represent a full system by connecting power electronics blocks.

ACKNOWLEDGMENT

M. A. Tanni and Dr. M. T. Iqbal thank the UTC power for financial support of this research.

REFERENCES

[1] M. Ghouse, H. Abaoud, A. Al-Boeiz, M. AbdulHadi, ”Development of a 1 kW Phosphoric Acid Fuel Cell stack", *Applied Energy*, vol. 60, pp. 153-167 (1998).

[2] Suman Roy Choudhury, Raghunathan Rengaswamy, "Characterization and fault diagnosis of PAFC cathode by EIS technique and a novel mathematical model approach", *Journal of Power Sources*, vol. 161, pp. 971–986 (2006).

[3] P.L. Zervas*, M.K. Koukou, N.C. Markatos (March 2006). Predicting the effects of process parameters on the performance of phosphoric acid fuel cells using a 3-D numerical approach. *Energy Conversion and Management* [online]. 47. pp. 2883–2899. Available: http://www.elsevier.com/locate/enconman

[4] M. J. Khan, M. T. Iqbal, "Modelling and analysis of electrochemical, thermal and reactant flow dynamics for a PEM fuel cell system", *Fuel Cells*, November, 2004.

[5] Fuel Cell Handbook, 7th ed., *EG&G Technical Services, Inc*., Morgantown, West Virginia, 2004, pp. 1-7.

CHAPTER 5

Dynamic Modeling a of Phosphoric Acid Fuel Cell (PAFC) and its Power Conditioning System

5.1 Dynamic Modeling of Fuel Cell

Dynamic modeling helps to show the dynamic behavior of a fuel cell. Basically it is the main part for designing the control of a system [23]. The following manuscript will show the dynamic modeling of PAFC type fuel cell under different load conditions. This manuscript will also show the variations of dynamic response of PAFC at different stages of the presented dynamic model.

5.2 Power Conditioning System of Fuel Cell

Since the fuel cell produces dc electricity, this electricity is converted into ac electricity for use. This conversion of dc power into ac power can be observed in the following figure.

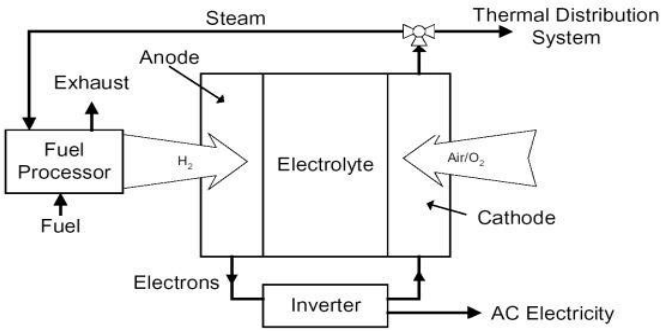

Figure 5.1: Power conditioning system of a fuel cell [24]

The output of the fuel cell can be connected to a dc-dc/dc-ac converter as needed. Sometimes the dc output of the fuel cell is connected to the dc-dc converter to boost the low voltage into high voltage. Besides the dc output is connected to the dc-ac converter and then to the load directly. The load can be resistive, inductive, capacitive, non-linear or combination of these four elements [25].

The following manuscript will describe the power conditioning system more clearly in Matlab/Simulink and its Power System Blocksets (PSB). It will show the dynamic modeling of PAFC type fuel cell with the dynamic responses at different stages of system. It will show the dc-ac conversion directly and the application of pure resistive load in the dynamic model. Simulation results will indicate different dynamic response under different conditions of the resistive load.

5.3 Preface

A version of this manuscript has been published in the 3rd International Conference on Future Environment and Energy (ICFEE), 2013, Rome, Italy. Moreover, this paper has also been published in the *Journal of Clean Energy Technologies (JOCET), vol 1, no. 3, pp. 178-183, ISSN: 1793-821X, July 2013.* This paper has also been presented in the ICFEE conference by the principal author Mahmuda Ahmed Tanni. The co-author Dr. Tariq Iqbal supervised the principal author to develop the dynamic model presented in the paper and helped her to understand the theories and model needed for this research. Mahmuda Tanni wrote this paper, developed the dynamic model in Matlab/Simulink and its Power System Blockset (PSB) and then conducted simulation. Dr. Iqbal reviewed the manuscript, checked and corrected all simulations and provided important suggestions.

This manuscript will end up with the successful conduction of the simulation of a PAFC type dynamic model. The ac power of this dynamic model will be connected to the grid in the next chapter. Moreover, a simple control mechanism will be developed in the next chapter, so that it can deliver required power. Basically, a grid connected PAFC type model will be developed with a simple control mechanism.

Dynamic Modeling a of Phosphoric Acid Fuel Cell (PAFC) and its Power Conditioning System

M. A. Tanni, *Student Member, IEEE*, Md Arifujjaman, *Member, IEEE*, M. T. Iqbal

***Abstract*—This paper presents the dynamics of a phosphoric acid fuel cell (PAFC) and its associated power electronics. The modeling of the power conditioning system for phosphoric acid fuel cell is discussed here. This model is based on empirical equations. The simulation is done using Matlab/Simulink and its Power System Blockset (PSB). This model mathematically calculates cell output voltages and their consequent losses. It also calculates the ac output from the system by simulating an inverter dc input from the fuel stacks. The V-I curves and dynamics can be observed. The effects of variation in outputs for different inputs can also be observed. This model is easy to understand and it requires less computational time.**

***Index Terms*—Distributed Generation, Dynamic Modeling and Simulation, Phosphoric Acid Fuel Cell, Power Conditioning System.**

I. INTRODUCTION

Recently alternative or renewable energy is becoming more popular because of increasing energy consumption. People are also becoming aware of environment impact and declining fossil fuels. Common alternate energy sources are fuel cells, wind turbines, micro-turbines, photovoltaic etc. These are also referred as distributed generation (DG). Fuel cells have drawn more attraction from different distributed generation since it has the potential capability of providing both heat and power [1].

A fuel cell (FC) is an electrochemical device that converts the chemical energy of the fuel directly into electrical energy. Fuel cells have a low environmental impact and operate silently in practical situations with high efficiency and long lifetime. So they can represent a very good option as a DG [2].

A power conditioning stage is essential to produce commercial ac power since the output of a fuel cell is dc electricity [3]. So fuel cell plants can produce this ac power. Generally there are three major subsystems in a fuel cell plant which are a reactant supply subsystem to convert natural gas to a hydrogen-rich gaseous fuel, a power section subsystem including a thermal management assembly to generate dc power and a power conditioning subsystem to convert the dc power generated in the power section subsystem to ac power [4]. Figure 1 shows the process.

According to the type of electrolyte used, the most common fuel cells are: phosphoric acid fuel cells (PAFC), alkaline fuel cells (AFC), molten carbonate fuel cells (MCFC), solid oxide fuel cells (SOFC) and proton exchange membrane fuel cells (PEMFC).

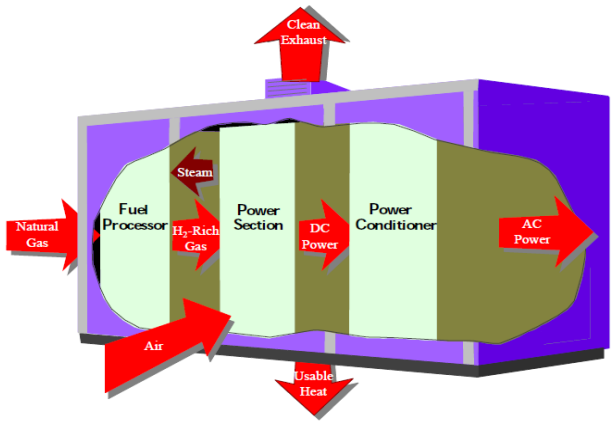

Fig. 1. Fuel Cell Power Plant Major Processes [5], (P: 1-7)

Among them, PAFC has one of the most advanced technologies available commercially. It is possible to improve the performance of a fuel cell by changing the operating variables (e.g. pressure, temperature, gas composition, current density etc.). It is important to select an operating point (cell voltage and related current density) of a fuel cell till the system requirements are satisfied [6].

This paper represents a model of the last two subsystems of fig.1. A dynamic modeling of phosphoric acid fuel cell (PAFC) system including dc to ac power conversion is proposed here. The model is based on empirical equations. This model includes fuel stacks to produce dc power and a dc to ac inverter to produce ac power. The model is validated by SimPowerSystems (SPS) blockset of Matlab/Simulink. Section 2 describes the mathematical model, section 3 describes the dynamic model, section 4 shows the simulation results and discussions, and section 5 concludes the paper.

II. MATHEMATICAL MODELING

Since mathematical modeling gives the idea of valuable insight into the electrochemistry of the fuel cell and the processes that take place in the system, it can be considered as a basic tool in the development of fuel cells [6].

In this paper, the model of PAFC investigates the appropriate load according to the power demand. It also shows the IV curves and values of dc and ac voltage, current and power. The system consists of three PAFC stacks and each stack contains 376 individual cells. The dc output power is converted to ac. The basic block diagram of the proposed model is presented in fig.2.

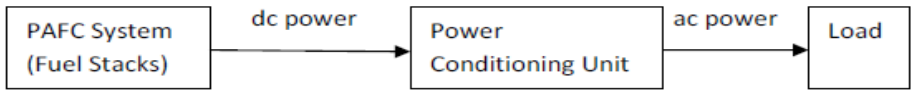

Fig. 2. Basic block diagram of the PAFC model

The mathematical modeling of a PAFC is the foundation for the modeling of the whole PAFC system. The mathematical modeling of an individual PAFC includes Nernst potential, activation loss, ohmic loss and concentration loss. The overview is shown in fig.3 below.

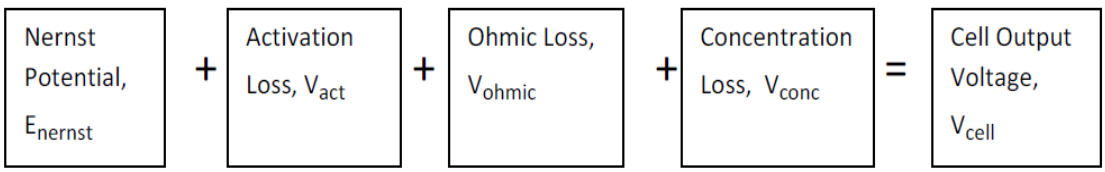

Fig. 3. Block diagram of an individual PAFC

The equation format of fig.3 can be expressed as below [6],

$$V_{Cell} = E_{nernst} + V_{act} + V_{ohmic} + V_{conc} \quad [1]$$

A. Nernst Potential

The thermodynamic potential can be obtained at thermodynamic balance. The Nernst potential is the modified equation to express this voltage. At standard condition (298.15 K, 1atm), the overall reaction includes hydrogen, oxygen and vapor to produce a thermodynamic potential [7].

$$E_{nernst} = E^0 + \frac{RT}{nF} \ln[\frac{p'_{H2}(p'_{O2})^{0.5}}{p'_{H2O}}] \quad [2]$$

Here E^0 represents the reference potential at unity cavity (1.229 V at standard state), p'_{H2}, p'_{O2} and p'_{H2O} are the hydrogen, oxygen and vapor partial pressures (atm), respectively. Moreover, T is the cell temperature (K), R is the universal gas constant (8.31441 J mol^{-1} K^{-1}), F is the Faraday constant (96484.56 C mol^{-1}) and n is the number of electrons participating in the reaction [7].

B. Activation Loss

The activation energy involves both the electrical and chemical reactions. The similarity between them can be overcome by the reacting species. The voltage drop caused by activation losses on a particular electrode under specific conditions can be controlled by the rate parameters and activation energy of one or more rate limiting reaction steps. The equation for activation polarization is described by the following equation [5].

$$V_{act} = -\frac{RT}{\alpha nF} \ln \frac{i}{i_o} \qquad [3]$$

where α is the electron transfer coefficient of the reaction at the electrode being addressed, i is the current density and i_0 is the exchange current density.

C. Ohmic Loss

Ohmic loss occurs because of resistance of flowing ions in the electrolyte and through the electrode. This loss can be reduced by decreasing the electrode separation and enhancing the ionic conductivity of the electrolyte [5], (P:2-12). The ohmic over voltage is given by equation (4) [7].

$$V_{ohmic} = -IR_{\text{int}} \qquad [4]$$

Here I is the electrical current and R_{int} is the internal resistance. The equation of R_{int} is developed empirically for the proposed model based on some experimental data keeping the temperature fixed to 451 K (178 ^{0}C). The equation of R_{int} can be expressed as below,

$$R_{\text{int}} = 0.0652 I^{-0.819} \quad [5]$$

D. Concentration Loss

A reactant is consumed at the electrode by electrochemical reaction where it is often diluted by the products. Concentration loss is the result of this incident. The equation of concentration can be written as [5], (P:2-16).

$$V_{conc} = \frac{RT}{nF} \ln\left(1 - \frac{i}{i_L}\right) \quad [6]$$

where i_L is the limiting current density.

The mathematical modeling of a single PAFC stack follows equation (7) [7],

$$V_{stack} = NV_{cell} \quad [7]$$

where N is the number of fuel cell and V_{stack} is the stack voltage for a PAFC.

III. DYNAMIC MODELING

The mathematical expressions for the fuel-cell system and power conditioning system are modeled in the Matlab-Simulink environment. The dynamic model of PAFC is given in fig.4.

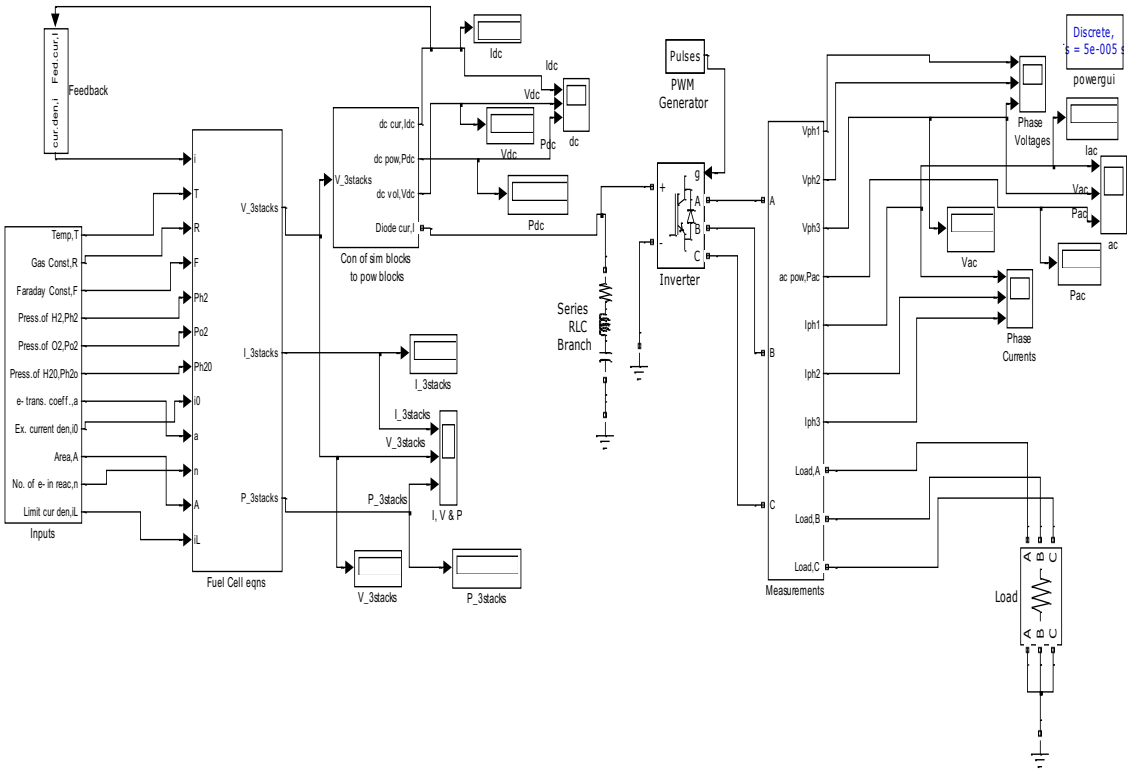

Fig. 4. Dynamic Model of PAFC

From fig.4, the dynamic modeling of the PAFC system including power conditioning system can be simulated. The 'Inputs', 'Feedback', 'Fuel Cell eqns', 'Con of sim blocks to pow blocks' & 'Measurements' block are subsystem blocks. The 'Inputs' block contains all inputs to the model.

Figure 5 shows the inputs of the model which can be observed in table I clearly.

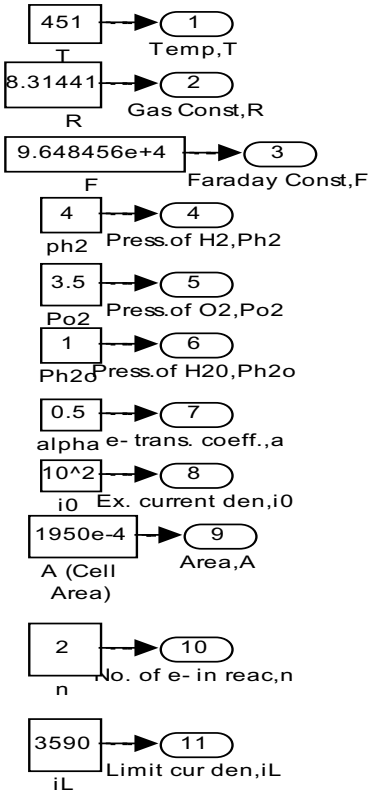

Fig. 5. 'Inputs' subsystem block

TABLE I: Input parameter values of the PAFC dynamic model

Parameter Name	**Parameter Value**
Temperature, *T*	451 K
Gas Constant, *R*	8.31441 J mol^{-1} K^{-1}
Faraday Constant, *F*	96484.56 C mol^{-1}

Partial pressure of hydrogen, p_{H2}	4 atm
Partial pressure of oxygen, p_{O2}	3.5 atm
Partial pressure of vapor, p_{H2O}	1 atm
Electron transfer coefficient, α	0.5
Exchange current density, i_0	10^2 A m^{-2}
Cell area, A	0.1950 m^2
Number of electrons participating in the reaction, n	2
Limiting current density, i_L	3590 A m^{-2}

The 'Fuel Cell eqns' sybsystem block contains all fuel cell equations related to the model. This block simulates equation (1) to equation (7). The PAFC system contains 3 fuel stacks and each stack contains 376 fuel cells. All of the equations are imposed on

each fuel cell of the PAFC system. The final equation of the PAFC system can be expressed as,

$$V\_{stack} = 3 \times Single\_Fuel\_Stack \quad [8]$$

Figure 6 shows the 'Fuel Cell eqns' subsystem block. The outputs (current, voltage & power of three stacks) of this block can be observed through the display blocks and the curves can be investigated through the 'I, V & P' scope block. The output 'V_3stacks' is connected to the 'Con of sim blocks to pow blocks' subsystem block.

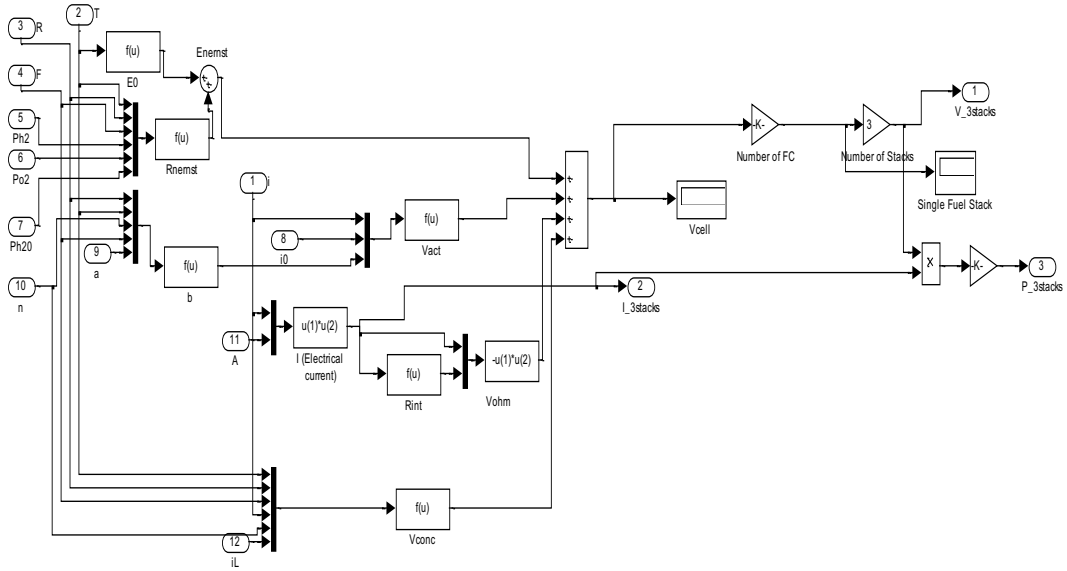

Fig. 6. 'Fuel Cell eqns' subsystem block

In fig.7, the 'Con of sim blocks to pow blocks' subsystem block maintains the connection between the simulink blocks and the power system blocks. It converts the simulink signal ($V\_{3stacks}$, stack voltage for three stacks) into 'simpowersystem' block eligible signal through the controlled voltage source block. There is a rectifier diode after the controlled

voltage source block in this subsystem block to connect to power system blocks. The current measurement and voltage measurement blocks measure the current and voltage, respectively. The mean blocks are connected to calculate the mean value of current and voltage. The dc power is calculated by multiplying the mean value of current and voltage. The power value is converted into kilowatt (kW) unit through a gain block. Thus the subsystem block has four outputs which are dc outputs for current, voltage and power and diode current.

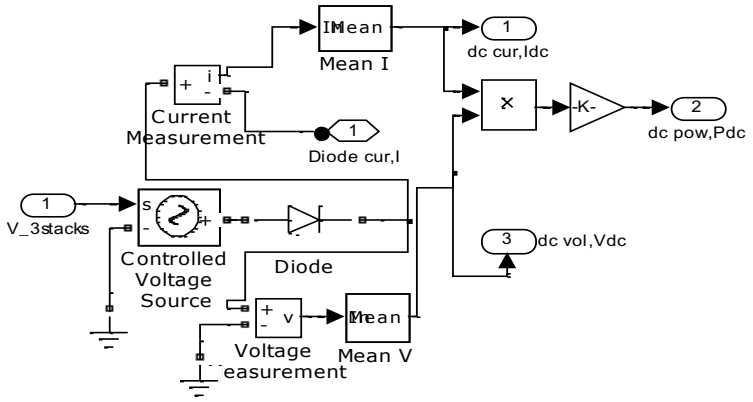

Fig. 7. 'Con of sim blocks to pow blocks' subsystem block

The dc current, voltage and power can be observed through display and scope block in fig.4. A series RLC branch is connected with the diode current from the 'Con of sim blocks to pow blocks' subsystem block and then grounded. The resistance and inductance values are very small compared to the capacitance value in the RLC branch. The value of resistance is taken small to keep the power loss small through this path. A small amount of inductance value helps to block the ac current through this path. A large amount of capacitance value is used to smooth the dc current. After the series RLC branch, the

positive port of an inverter is connected to convert the dc signal into ac signal and the negative port is grounded. The inverter is IGBT type and it has three bridge arms (A, B & C) which are connected to 'Measurements' subsystem block. There is a PWM generator input (g) to the inverter which is a pure ac source. Since the 'internal generating of modulating signal' of the PWM generator block is marked, no reference input current signal is provided. So the wave shapes look like ideal PWM wave shapes.

One feedback of dc current from 'Con of sim blocks to pow blocks' subsystem block is connected to the 'Feedback' subsystem block. Fig.8 shows the 'Feedback' subsystem block. Here the feedback current (I) is converted into current density (i) through a gain block to provide it as an input to the model. The memory block is used to store the initial condition i.e. to specify minimum current density to observe the results.

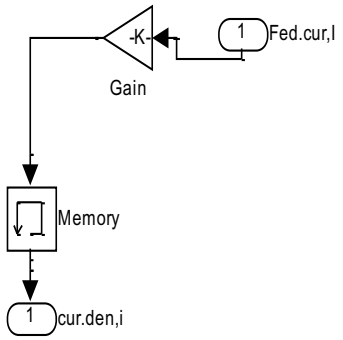

Fig. 8. 'Feedback' subsystem block

In fig.9, the 'Measurements' subsystem block can be observed. The inputs of this block are the outputs of the inverter i.e. A, B & C bridge arms. In this subsystem, these three bridge arms are connected to the three phase V-I measurement (phase-to-phase type)

block. The V_{abc} and I_{abc} port are connected to the RMS blocks to calculate the root mean square (rms) values of voltage and current. Then the rms voltage and current values are demuxed into three so that each phase voltage and each phase current for the three phase setup can be observed. V_{ph1}, V_{ph2} & V_{ph3} are the phase voltages and I_{ph1}, I_{ph2} & I_{ph3} are the phase currents. One phase voltage is multiplied to one phase current which makes the phase power. But this phase power is converted to line power in kilowatt (kW) unit through a gain block. The a, b, & c ports of three phase V-I measurement block are the outputs of this subsystem.

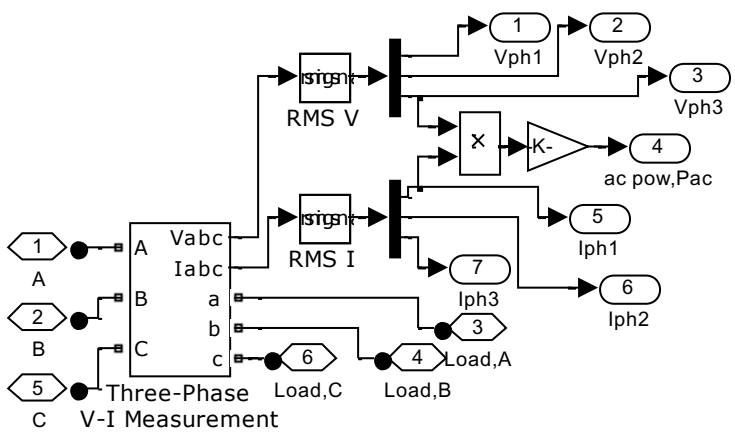

Fig. 9. 'Measurements' subsystem block

In fig.4, the outputs of 'Measurements' block are connected to a three phase parallel RLC branch acting as a resistive load. The outputs of the load is connected together and grounded. The I_{ac}, V_{ac} & P_{ac} display blocks show the ac current, voltage and power, respectively. The scope block shows the phase voltages, phase currents and line power curves in ac with respect to time. A powergui block is used in fig.4 to run the model with simple power system blocks.

IV. SIMULATION RESULTS AND DISCUSSIONS

The dynamic model is simulated for 1 second to observe the results. Table II shows the results for different values of load.

Table II: Results for the PAFC dynamic model

R (Ω)	$I_{\_3stacks}$(A)	$V_{\_3stacks}$(V)	$P_{\_3stacks}$(KW)	I_{dc}(A)	V_{dc}(V)	P_{dc}(KW)	I_{ac}(A)	V_{ac}(V)	P_{ac}(KW)
2.2	587.3	861.4	505.9	586.9	872.1	511.8	276.2	647.3	309.7
4	348.7	930.1	324.4	348.6	933.4	325.4	164	698.7	198.5
9	166.2	998.4	165.9	165.8	1009	167.3	78.24	750.1	101.7

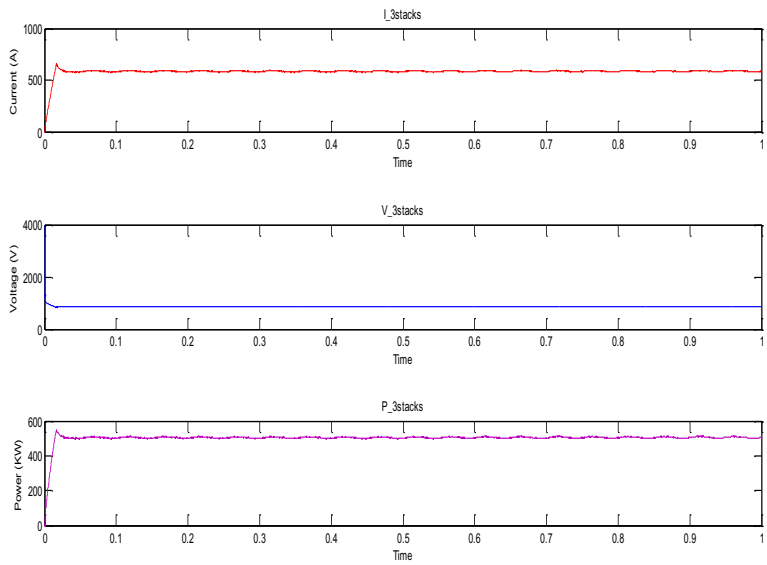

Fig. 10. Stack current, voltage ,and power as a function of time

This table shows that the values of stack current ($I_{\_3stacks}$) and dc current (I_{dc}) are almost similar and the values of ac current (I_{ac}) are less than the half of $I_{\_3stacks}$ or I_{dc} for each value of R. The values of stack voltages ($V_{\_3stacks}$) and dc voltages (V_{dc}) are also similar

but ac voltages (V_{ac}) less than the $V_{\_3stacks}$ or V_{dc}. The same characteristic is observed in case of power. The power loss is observed between the dc power and ac power because of the inverter power loss and absence of filter.

In fig.10, the initial transient of $I_{\_3stacks}$, $V_{\_3stacks}$, and $P_{\_3stacks}$ can be observed through the 'I, V, & P' scope block of the dynamic model with respect to time.

Figure 11 shows the initial transient and steady state values for same parameters with respect to time. These wave shapes can be observed through the 'dc' scope block of the model.

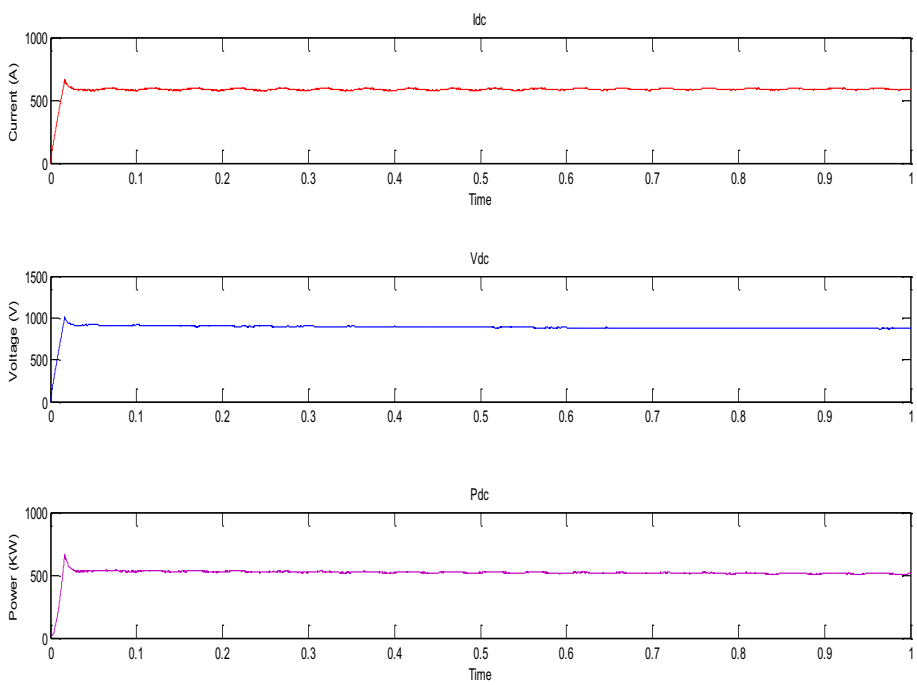

Fig. 11. DC current, voltage, and power as a function of time

Figure 12 shows the wave shapes for ac parameters . The wave shapes for phase currents and phase voltages are not shown here since the ac current & ac voltage wave shapes in fig. 12 are one of the phase currents and voltages, respectively.

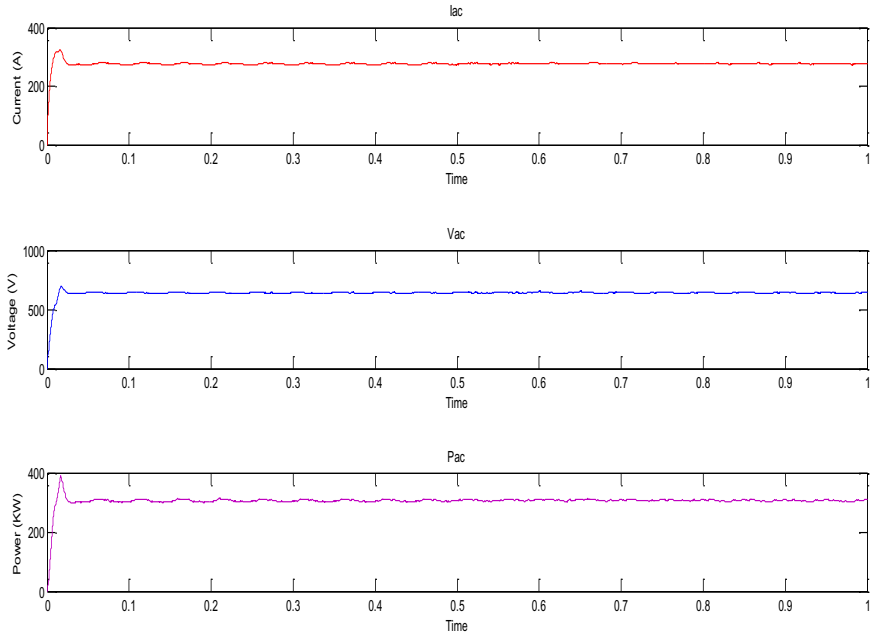

Fig. 12. AC current, voltage, and power values

Figure 10, 11, & 12 are the outputs for the load R=2.2 Ω. Same observations are found for other loads but in different range of values. So only these figures are discussed here. All of the current curves increases initially and then goes almost to a steady state value. Same characteristic is found in case of power. But the stack voltage shows decreasing nature at the beginning and then almost linear. The dc and ac voltages also show the similar characteristic i.e. increasing nature at the beginning and then almost linear nature.

V. CONCLUSION

In this paper the dynamic modeling of a PAFC fuel cell system and its associated power electronics is presented. Simulation results are discussed at different stages of the

model. In future, further analysis can be done by connecting the ac power to the grid and by designing a controller for the whole model to deliver some required power.

ACKNOWLEDGMENT

M. A. Tanni and Dr. M. T. Iqbal thank the UTC power for financial support of this research.

REFERENCES

[1] A. Kirubakaran *, S. Jain, R. K. Nema. (April 2009). A review on fuel cell technologies and power electronic interface. *Renewable and Sustainable Energy Reviews.* [Online]. 13. pp. 2430-2440. Available: http://www.elsevier.com/locate/rser

[2] F. A. O. Berenguer *, M. G. Molina. (December 2009). Design of improved fuel cell controller for distributed generation systems. *International Journal of Hydrogen Energy.* [Online]. 35. pp. 5974- 5980. Available: http://www.elsevier.com/locate/he

[3] W. Choi, P. N. Enjeti, J. W. Howze, "Development of an equivalent circuit model of a fuel cell to evaluate the effects of inverter ripple current", *IEEE*, 2004.

[4] T. Asaeda, T. Yutani, T. Kawabata, Y. Hamasaki, "Dc-to-ac power converter for fuel cell system", *IEEE*, 1983.

[5] *Fuel Cell Handbook*, 7th ed., EG&G Technical Services, Inc., Morgantown, West Virginia, 2004, pp. 1-7.

[6] P.L. Zervas*, M.K. Koukou, N.C. Markatos (March 2006). Predicting the effects of process parameters on the performance of phosphoric acid fuel cells using a 3-D numerical approach. *Energy Conversion and Management* [online]. 47. pp. 2883–2899. Available: http://www.elsevier.com/locate/enconman

[7] M. J. Khan, M. T. Iqbal, "Modelling and analysis of electrochemical, thermal and reactant flow dynamics for a PEM fuel cell system", *Fuel Cells*, November, 2004.

M. A. Tanni was born in Dhaka, Bangladesh. She is currently a full time graduate student at Memorial University of Newfoundland, Canada. She is doing her masters in the Department of Engineering and Applied Science. Her major is electrical and she is studying on thesis based program under the supervision of Dr. Tariq Iqbal. Her research topics is related to fuel cell. She is a student member of IEEE. She has obtained her bachelor degree in Electrical and Electronic Engineering (EEE) from Khulna University of Engineering & Technology (KUET), Bangladesh.

She worked on renewable energy field on her undergraduate program. Her thesis topic was related to solar cell. At that time, she worked on a journal paper and three conference papers which are already published. Her current research interest is fuel cell related.

She achieved the second prize in a paper competition from KUET Excellence Foundation (KFS) at the time of undergraduate.

Md Arifujjaman was born in Khulna, Bangladesh on January 12, 1979. He received the B.Sc. Eng. degree in electrical and electronic engineering from the Khulna University of Engineering and Technology (KUET), Khulna, Bangladesh, in 2002, and the M.Eng. and Ph.D. degrees in electrical engineering from the Memorial University of Newfoundland, St. John's, NL, Canada, in 2006 and 2010, respectively.

During 2010–2011, he was a Post Doctoral Fellow with the Faculty of Engineering, University of New Brunswick. He is currently a Senior Research Engineer - Power Electronics with UTC Power, South Windsor, CT, USA. His industrial experience in power conversion includes research and development at the Khulna University of Engineering and Technology, Nalcor Energy, The Partnership Group for Science and Engineering (PAGSE), and UTC Power, where he developed high-density dc–dc power converters, grid tied wind and solar inverters, and digital controllers using DSPs. His research interests include power electronics reliability, maximum power point tracking algorithm, wind turbine, fuel cell, and high-performance power converters topologies. His current research activities are supported by the UTC Power. He is the technical point of contact on power electronics research between UTC Power and Massachusetts Institute of Technology (MIT), Texas A & M University, Rensselaer Polytechnic Institute (RPI) in USA and Memorial University of Newfoundland (MUN), Canada.

M. Tariq Iqbal received the B.Sc.(EE) degree from the University of Engineering and Technology, Lahore in 1986, the M. Sc. Nuclear Engineering degree from the Quaid-e-Azam University, Islamabad in 1988 and the Ph.D. degree in Electrical Engineering from the Imperial College London in 1994. From 1988 to 1991 and again from 1995 to 1999 he worked at the Pakistan Institute of Engineering and Applied Science, Islamabad, Pakistan. From 1999 to 2000 he worked as an Associate Professor at IIEC, Riphah International University. Since 2001 he is working at Faculty of Engineering and Applied Science, Memorial University of Newfoundland. Presently he is a full Professor. His teaching activities cover a range of electrical engineering topics including electronics devices, control systems, renewable energy systems and power electronics. Currently, his research focuses on modeling and control of renewable energy systems with interests in the areas of design of control systems and comparison of control strategies of hybrid energy systems.

CHAPTER 6

Modeling and Control of a Grid Connected PAFC System

6.1 Control of a Grid Connection System

The main goal of a power conditioning system is to convert the dc power of fuel cell into ac power so that it can be delivered to the grid at maximum efficiency. Moreover, the quality function of the power conditioning system depends on the control of the system [26]. So, control of a grid connected system is very important.

The following figure shows the fuel cell power system topology.

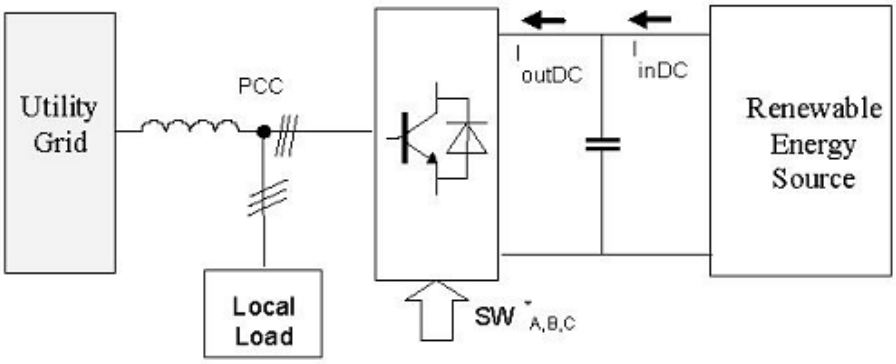

Figure 6.1: Block diagram of grid connected fuel cell power system [26]

Figure 6.1 shows the grid connected power system which consists of Renewable Energy Source (RES), grid inverter, local load and grid interconnection. Here, the grid inverter indicates a three-phase power converter with IGBT where active and reactive power control is achieved using an adequate control of the DC-AC power inverter [26].

The following manuscript describes the modeling and control of a grid connected PAFC system. It will show the modeling with Matlab/Simulink and Power System Blocksets. It will use the built-in IGBT type inverter to convert the dc output of the PAFC system from the previous chapter. Moreover, this manuscript will develop a simple control mechanism for the grid connected system so that required power can be achieved with negligible losses. In this case, required power indicates the power to meet the energy demand of engineering building of MUN. This produced power of the grid connected system will be enough to meet the energy demand of MUN engineering building mentioned in chapter three.

6.2 Preface

A version of this manuscript has been accepted for publication in the *International Journal of Energy Science (IJES), Paper ID: IJES10380.* The principal author Mahmuda Tanni wrote the paper, developed the grid connected model in Matlab/Simulink and its Power System Blockset (PSB) and then conducted simulation. She also developed the control mechanism needed for this model. The co-author Dr. Tariq Iqbal supervised and helped her to develop the model and the control mechanism in the paper. He also provided her necessary concepts for this model. Finally. Dr. Iqbal reviewed the manuscript, checked and corrected all Simulink models and suggested necessary corrections to the manuscript.

This manuscript will end up with the completion of main objective of this thesis. Finally, a grid connected PAFC system will be developed for MUN engineering building.

Modeling and Control of a Grid Connected PAFC System

M. A. Tanni[1], M. T. Iqbal[2]

[1,2] Faculty of Engineering and Applied Science

Memorial University of Newfoundland, St. John's, Canada, A1B3X5

[1]mat078@mun.ca, [2]tariq @mun.ca

***Abstract*-This paper presents a closed-loop control of a 440kW fuel cell system including power electronics and grid side filters. Simulation results show the dynamics of a phosphoric acid fuel cell (PAFC) and its associated power electronics including grid connection. The proposed model is based on empirical equations and Simulink blocks. The modeling and simulation is done in Matlab/Simulink software with its Power System Blockset (PSB). This model mathematically calculates cell output voltages and their consequent losses. Moreover, this model includes dc power conversion of fuel cell output into ac and grid interface. Presented model is simple and easy to understand.**

Keywords-Phosphoric Acid Fuel Cell; Modeling and Simulation; Power Conditioning System; LCL Filters; Distributed Generation

I. INTRODUCTION

Energy is one of the major requirements to develop the economy of a country [1]. The energy demand is increasing and due to a limited resource within few generations affordable fossil fuel reserves will be finished. Non-renewable energy sources have been utilized worldwide for several years [3]. Moreover, energy transition from the

conventional fossil fuels to sustainable energy is very important for the existence of future generations and to sustain our economy. This transition can cure the environment and offers a secure future for the generations to come. Among alternative energy solutions, hydrogen based fuel cell energy is one option to address and alleviate the imminent and critical problems [1].

Fuel Cells (FC) are electrochemical devices, which use chemical energy within a fuel. This energy is directly converted into electrical energy via an electrochemical reaction. The main components of an FC based power system are fuel processing unit (reformer), FC stack and Power Conditioning Unit [1].

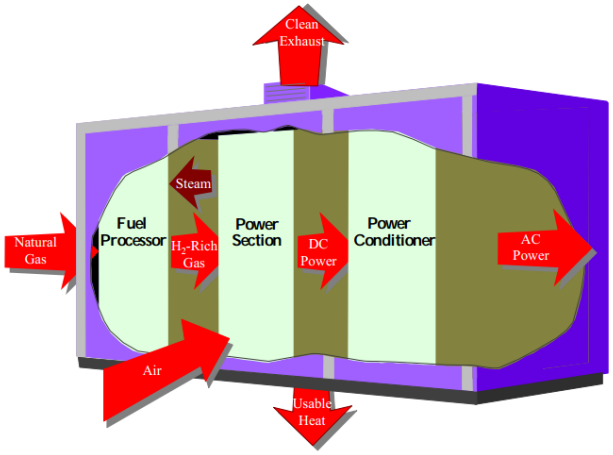

Figure. 1. Fuel Cell Power Plant Major Processes [4]

FCs are broadly classified into five categories based on the type of electrolytic material and the type of chemical operation. They are Alkaline FCs, Proton Electrolyte Membrane FCs, Phosphoric Acid FCs, Molten Carbonate FCs and Solid Oxide FCs [1]. Phosphoric Acid Fuel Cell (PAFC) is one of the most advanced and commercially available technology among all other fuel cells [2].

FC based system requires power conditioning circuits to condition its output DC voltage and convert the DC output into AC voltage. For a grid-connected system, an inverter is used with a FC. This must be synchronized with the grid in terms of voltage and frequency [1].

This paper represents a model and a control mechanism of a 440kW PAFC system including power electronics and grid filters. A modeling of PAFC system including dc to ac power conversion and grid connection is proposed. The FC model is based on empirical equations. Power electronics and grid interface is modelled in Simulink. This model includes fuel stacks to produce dc power, a dc to ac inverter to produce ac power, filters to eliminate fluctuation, grid connection and a closed loop control mechanism to maintain a constant output power. The closed loop control mechanism basically compares the inverter output with the reference and controls the PWM inverter. The error signal is used by the PID controller and PWM generator. Section 2 describes the mathematical model, section 3 describes the proposed model, section 4 shows the simulation results and discussions, and section 5 concludes the paper.

II. MATHEMATICAL MODELING

A valuable insight into the electrochemistry of the fuel cell can be gained by mathematical modeling. It also shows the processes that take place in the system. In this model, the main approach is to keep the ac output fixed so that it can be injected to the grid. It is known that grid requires three phase balanced output and no fluctuation. Another approach is to minimize the losses at different stages of the whole model and to

produce 440 kW power at the final stage. The block diagram of the proposed model is given below in figure 2.

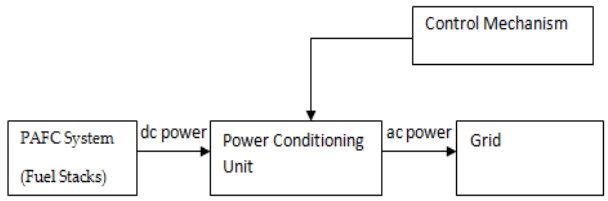

Figure. 2. Basic block diagram of the PAFC grid connected model

In this model, the PAFC system consists of 3 fuel stacks and each stack contains 376 fuel cells. The dc power of this PAFC system is converted into ac power through the power conditioning unit. A simple control mechanism controls the whole system through power conditioning unit (PCU). Since the PAFC system of the proposed model is built empirically, only the mathematical modeling of the FC part will be explained. The other three parts of figure 2 i.e. power conditioning unit, control mechanism and grid are built using available blocks available in Matlab/Simulink Power System Blockset (PSB).

The output voltage of an individual PAFC includes Nernst potential, activation loss, ohmic loss and concentration loss. The overview can be observed in figure 3 below [2].

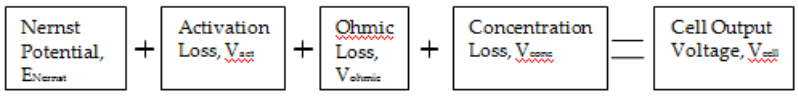

Figure. 3. Block diagram of the output of an individual PAFC [2]

Figure 3 can be expressed in an equation form as explained below [2].

$$V_{Cell} = E_{nernst} + V_{act} + V_{ohmic} + V_{conc} \quad [1]$$

A. Nernst Potential

At thermodynamic balance, the thermodynamic potential can be obtained. The equation of Nernst potential explains this voltage. At standard condition (298.15 K, 1atm), the overall reaction result in hydrogen, oxygen and vapor, and produce a thermodynamic potential [2].

$$E_{nernst} = E^{0} + \frac{RT}{nF} \ln[\frac{p'_{H2}(p'_{O2})^{0.5}}{p'_{H2O}}] \quad [2]$$

In equation 2, E^0 is the reference potential at unity cavity (1.229 V at standard state). Here p'_{H2}, p'_{O2} and p'_{H2O} represents the hydrogen, oxygen and vapor partial pressures (atm), respectively. Additionally, T represents the cell temperature (K), R represents the universal gas constant (8.31441 J mol^{-1} K^{-1}), F represents the Faraday constant (96484.56 C mol^{-1}) and n represents the number of electrons participating in the reaction.

B. Activation Loss

Both electrical and chemical reactions result in activation energy. Reacting species can differentiate between them. Rate parameters and activation energy of one or more rate limiting reaction steps can control the voltage drop during activation loss. The following equation can explain the activation polarization [2].

$$V_{act} = -\frac{RT}{\alpha nF} \ln \frac{i}{i_o} \quad [3]$$

Here α represents the electron transfer coefficient, i represents the current density and i_0 represents the exchange current density.

C. Ohmic Loss

Flowing ions incur resistance in the electrolyte and through the electrode. And ohmic loss occurs due to this resistance. The ohmic over voltage can be expressed by the following equation [2].

$$V_{ohmic} = -IR_{\text{int}} \quad [4]$$

Here I represents the electrical current and R_{int} represents the internal resistance. The developed equation of R_{int} at the temperature of 451 K (178 ^{0}C) can be written as below [2].

$$R_{\text{int}} = 0.0652 I^{-0.819} \quad [5]$$

D. Concentration Loss

Sometimes a reactant is consumed at the electrode by electrochemical reaction. The products often dilute that reactant and thus concentration loss occurs. The following equation explains the concentration loss [2].

$$V_{conc} = \frac{RT}{nF} \ln\left(1 - \frac{i}{i_L}\right) \quad [6]$$

Here i_L represents the limiting current density.

The following equation will explain the mathematical modeling of a single PAFC stack since 376 fuel cells are connected in series in a single fuel stack [2].

$$V_{stack} = NV_{cell} \quad [7]$$

Here N represents the number of fuel cells and V_{stack} represents the stack voltage for a PAFC.

Since three fuel stacks are connected in series in the system, the output voltage of the PAFC system can be expressed with the following equation.

$$V_{3stacks} = N_s V_{stack} \qquad [8]$$

Here N_s represents the number of fuel stacks, $V_{3stacks}$ represents the output voltage of the PAFC system and V_{stack} represents the individual stack voltage.

III. PROPOSED MODEL

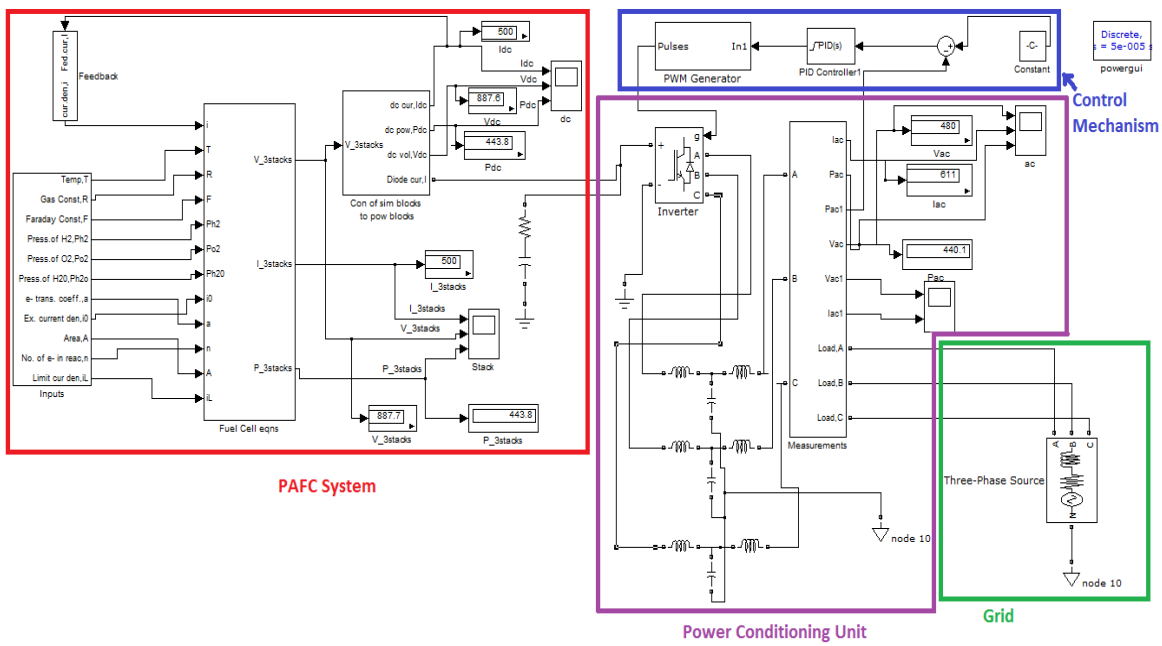

Figure. 4. Proposed Model of PAFC type power plant with grid connection

Figure 4 shows the proposed model in Matlab/ Simulink environment. This figure also shows the control mechanism of a 440 kW PAFC type power plant with grid connection. Here a three phase sink is used as grid. Figure 4 is the Matlab/Simulink representation of system shown in figure 2. In figure 4, the PAFC system can be identified by red color block, the PCU by purple color, grid by green color and control mechanism by blue color.

The powergui block helps to provide system initial conditions and run the model with simple power system blocks. The subsystem blocks of the proposed model are 'Inputs', 'Feedback', 'Fuel Cell equations', 'Con of simulink blocks to power blocks' & 'Measurements'. The proposed model will be explained in the following four sections named as PAFC system, PCU, grid and control mechanism.

A. PAFC System

The first block of the PAFC system is 'Inputs' subsystem block. It contains all of the inputs of the model. This subsystem block consists of constants and in-port blocks.

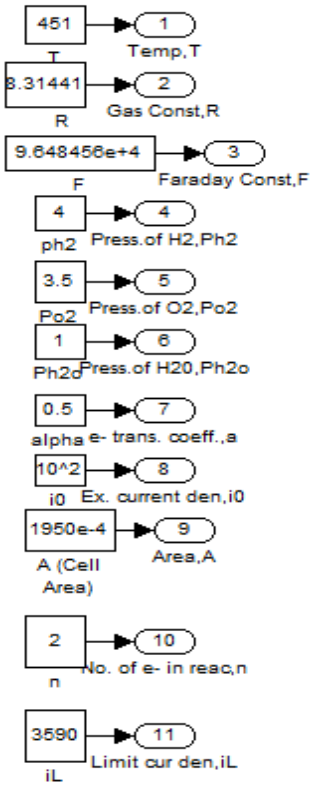

Figure. 5. 'Inputs' subsystem block

Figure 5 shows the inputs of the model. All values used in simulation are listed in table 1.

TABLE 1 INPUT PARAMETER VALUES OF THE PROPOSED MODEL

Parameter Name	**Parameter Value**
Temperature, T	451 K
Gas Constant, R	8.31441 J mol^{-1} K^{-1}
Faraday Constant, F	96484.56 C mol^{-1}
Partial pressure of hydrogen, p_{H2}	4 atm
Partial pressure of oxygen, p_{O2}	3.5 atm
Partial pressure of vapor, p_{H2O}	1 atm
Electron transfer coefficient, α	0.5
Exchange current density, i_0	10^2 A m^{-2}
Cell area, A	0.1950 m^2
Number of electrons participating in the reaction, n	2
Limiting current density, i_L	3590 A m^{-2}

The second subsystem block is 'Fuel Cell equations' subsystem block. It contains all fuel cell equations of the mathematical modeling section. This block simulates from equation (1) to equation (8). All of the equations are used for each fuel cell of the 376 cells of the PAFC system.

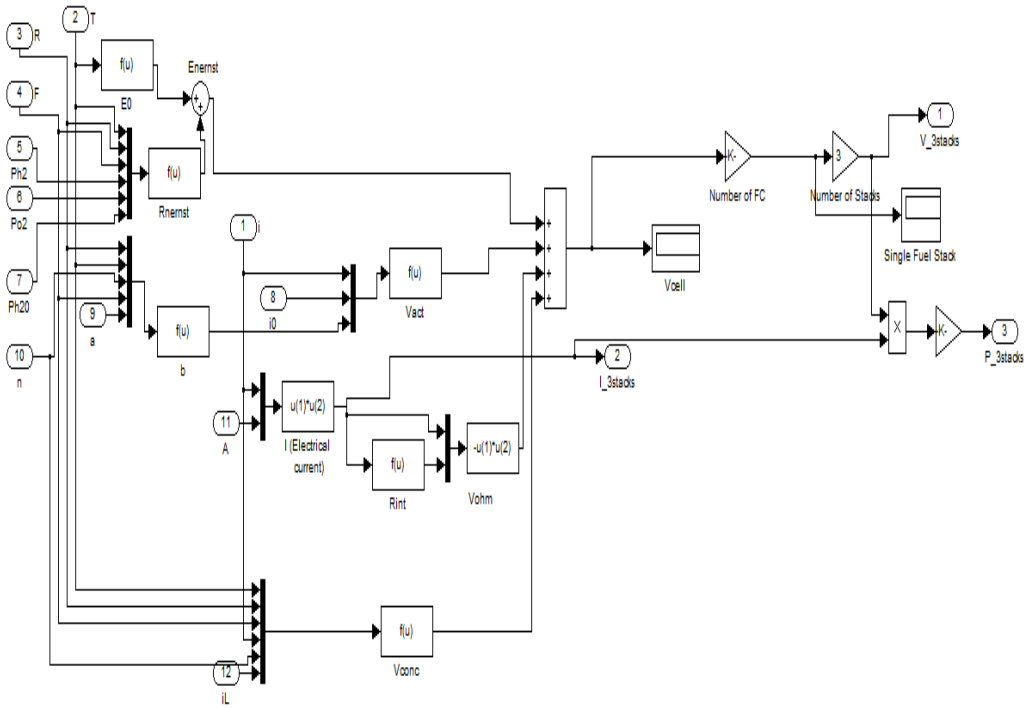

Figure. 6. 'Fuel Cell equations' subsystem

Figure 6 shows the 'Fuel Cell equations' subsystem block. The outputs (current, voltage & power of three stacks) of this subsystem block can be observed through the display blocks of figure 4. The system outputs can be investigated through one single window i.e. the 'Stack' scope block of figure 4. The output 'V_3stacks' of figure 6 is connected to the 'Connection of simulink blocks to power blocks' subsystem block of figure 4.

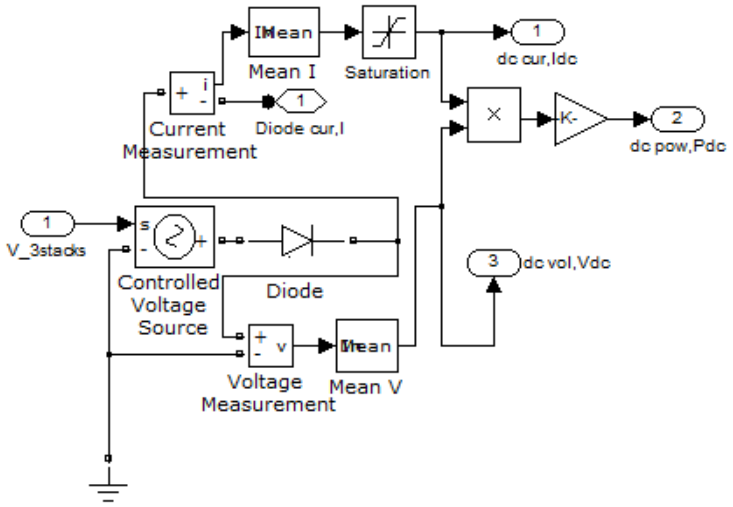

Figure. 7. Connection of simulink blocks to power blocks' subsystem block

Basically the 'Connection of simulink blocks to power blocks' subsystem block is the connection between two sections i.e. red colored 'PAFC System' and purple colored 'Power Conditioning Unit'. This subsystem block also connects simulink blocks with power system blocks. From figure 7, it can be seen that the simulink signal ($V\_{3stacks}$, stack voltage for three stacks) is input into 'simpowersystem' block i.e. controlled voltage source block. The rectifier diode after the controlled voltage source block makes the current to flow in one direction. Moreover, the current measurement and voltage measurement blocks can be observed. They measure the current and voltage. The mean blocks calculate the mean value of current and voltage. The saturation block keeps the signal in the range from 500 A to 700 A. This range helps to remove fluctuation from grid. Then the dc power is calculated by multiplying the output of the saturation block with the mean voltage. A gain block is used to convert the watt (power) value into

kilowatt (kW) value. In this way, the outputs of the subsystem block are dc outputs current, voltage and power and diode current.

From figure 4, the dc current, voltage and power can be observed through display and scope block. A series RC branch is connected with the diode current. Then the diode current is connected to the power conditioning unit which is another section (purple colored). This RC branch is a DC filter representing a large capacitor and its internal resistance. The value of resistance is taken small to keep the power loss small through this path.

One current feedback can be observed in the red colored 'PAFC System' of figure 4. This is basically the dc current from 'Connection of simulink blocks to power blocks' subsystem block to the 'Feedback' subsystem block.

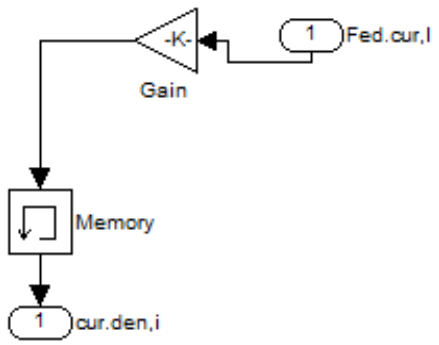

Figure. 8. 'Feedback' subsystem block

From figure 8, it can be seen that the feedback current (*I*) is converted into current density (*i*) through a gain block. Then it is sent as an input to the model. The memory

block stores the initial condition i.e. specifies minimum current density observed in the results.

B. Power Conditioning Unit (PCU)

The purple colored power conditioning unit of figure 4 mainly contains an inverter, three LCL filters and a measurement subsystem block. The positive port of the inverter is connected to the dc signal and the negative port is grounded. It converts the dc signal into ac signal. The inverter is Insulated Gate Bipolar Transistor (IGBT) type. It has three bridge arms (A, B & C) which contain three phase current. Each of these phases (A, B & C) is connected to an LCL filter. These filters are used to reduce harmonics going to the grid. This is an important requirement of the grid. Each filter contains two inductors and a capacitor. The shape of each filter is similar to 'T'. The value of left arm inductance of each filter is same but different from the right arm inductance. Similarly the values of right arm inductance and capacitance are same for each filter. One port of all capacitors is connected to a common point. This common point is connected to the same node which can be observed with the grid in figure 4. The right arm inductances are connected to the 'Measurements' subsystem block.

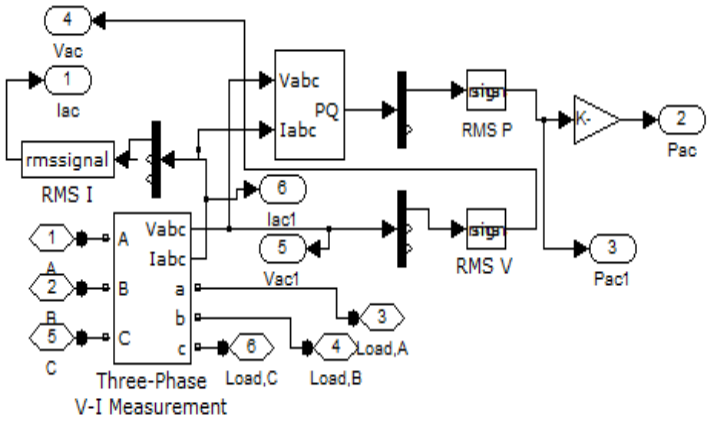

Figure. 9. 'Measurements' subsystem block

Figure 9 shows the 'Measurements' subsystem block. In this subsystem, the three input arms are connected to the three phase V-I measurement (phase-to-phase type) block. The V_{abc} and I_{abc} port are demuxed into three outputs. Then each phase voltage and each phase current for the three phase setup can be observed. One phase voltage and one phase current are connected to RMS blocks to calculate the root mean square (rms) values of voltage and current. This rms voltage and rms current are the ac voltage and ac current, respectively in figure 4. Moreover, the V_{abc} and I_{abc} of figure 9 are also entered into the '3 phase instantaneous active and reactive power' block. The output of this block is demuxed from where active and reactive power can be obtained. The active power is connected to an RMS block to calculate the rms power and then to a gain block to calculate the power in kilowatt (kW). The output of the 'RMS P' block is also sent to the blue colored 'Control Mechanism' section. Additionally, the V_{abc} and I_{abc} are also connected to a scope block in figure 4 to observe the instantaneous voltages and instantaneous currents. Thus the

outputs of this PCU section are I_{ac}, V_{ac} & P_{ac}. These values can be measured through display blocks and curves can be observed through the 'ac' scope block.

C. Grid

The green colored 'Grid' section contains a three phase sink and a neutral block. The three phase sink represents the grid in figure 4 and 'node 10' neutral indicates the same neutral of PCU section. This type of neutral is a floating type neutral without drawing the connection line between two points. The three phase sink i.e. grid window looks like below.

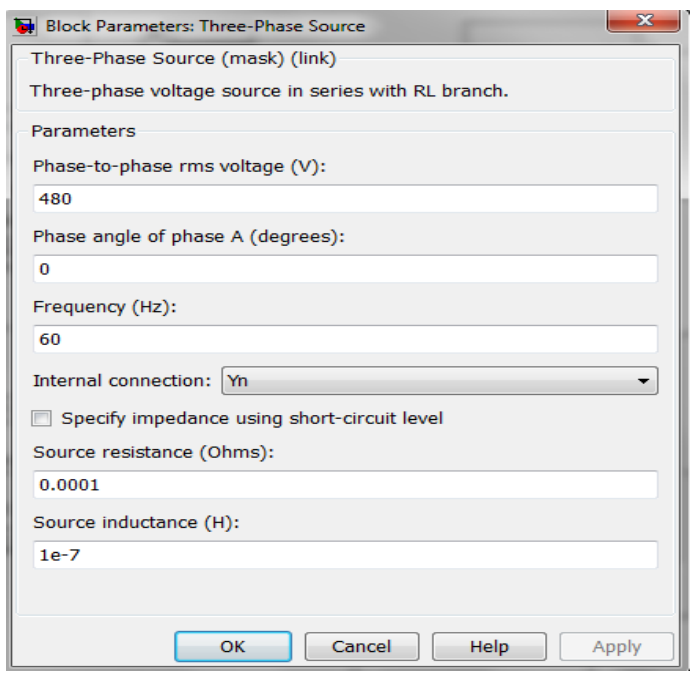

From this window, it can be seen that the phase to phase rms voltage is considered as 480 V (240+240) and the frequency as 60 Hz. Since the grid block is connected to a neutral block, internal connection is chosen as Y_n. Moreover, an ideal grid has no resistance and inductance. So the resistance and inductance values are considered as very small.

D. Control Mechanism

The control mechanism basically consists of a PWM generator, a PID controller, a constant and a sum block. The PWM generator gives an input (g) to the inverter which is a pure ac source. This PWM generator block looks like below.

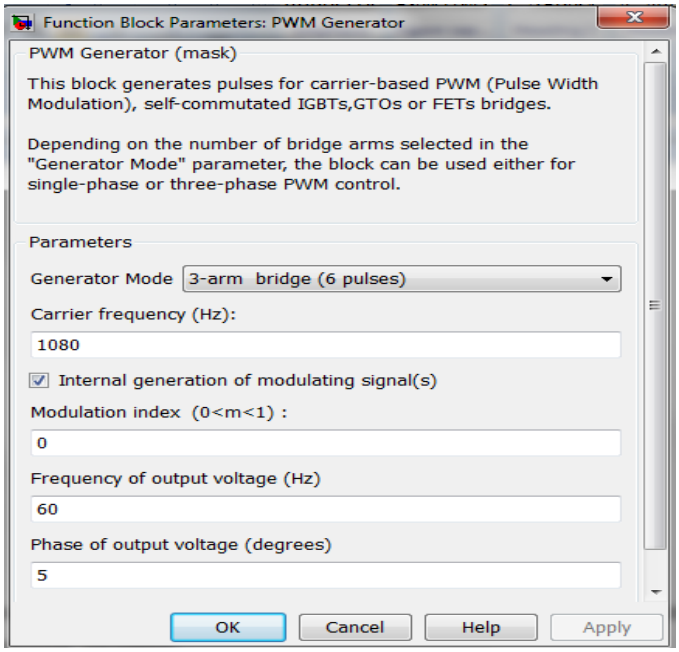

This window shows that the generator mode is chosen as 3-arm bridge (6 pulses). Because this is a grid connected model. The carrier frequency is considered as 1080 Hz and phase of output voltage as 5 degree. The frequency of output voltage is chosen as 60 Hz, since the frequency of ac current was 60 Hz. The modulation index is controlled by a PID controller. The main window of PID controller looks as below.

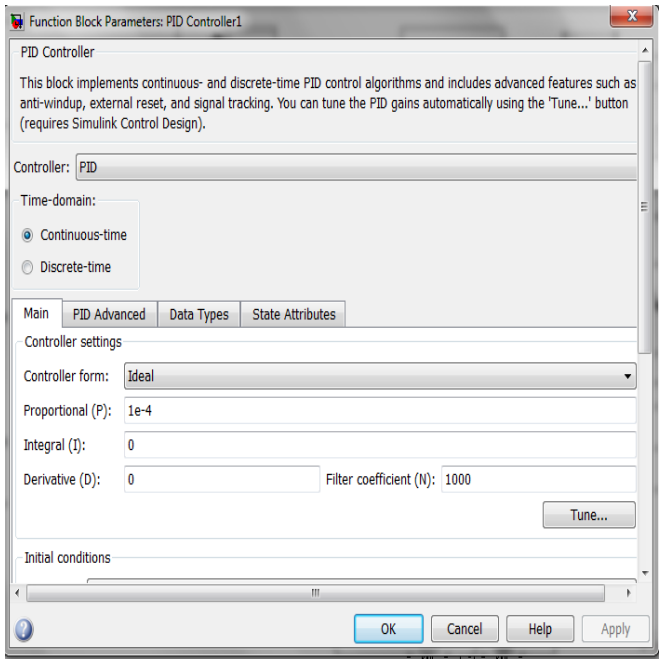

Only a small proportional value is taken here. The PID advanced window looks as below.

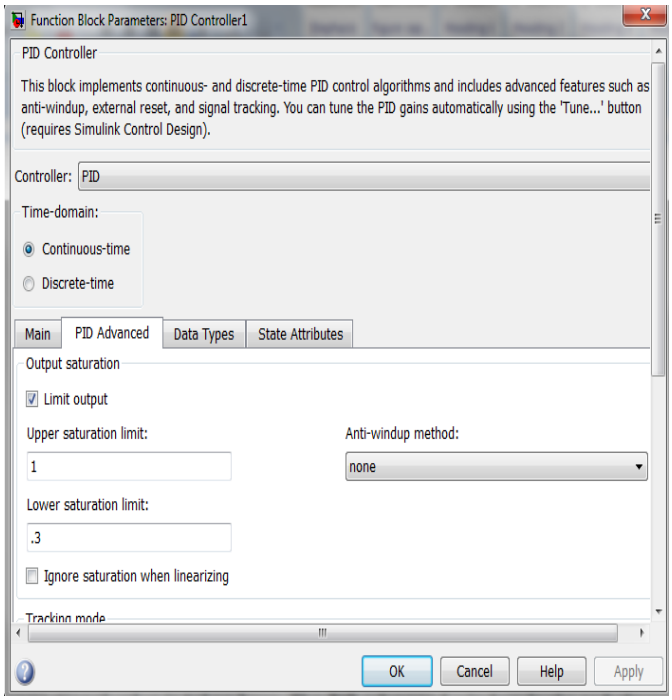

The upper and lower limits basically indicate the range of the modulation index. The modulation index can vary within this range. The other two windows of this PID controller are kept as such. The input to this PID controller block is an error signal. From figure 4, it can be seen that this error signal is the difference between the reference signal and the power signal from PCU section. The reference signal is indicated by a constant block. The value in the constant block is taken as 440000 which is in watt. This is basically 440 kW which is expected to obtain as output. This reference is compared with the actual output (P_{ac1}) of the model.

IV. SIMULATION RESULTS AND DISCUSSIONS

The proposed model is run for 2 seconds in Matlab/Simulink R2010a to observe the results. Our main objective is fulfilled in this proposed model. The ac output is around 440 kW and it is fixed during the simulation. There is almost no fluctuation. And so, it is safe to inject this power into the grid. Another main objective is to reduce losses at each stage. Measurements are done at three stages of the proposed model to meet this objective. Firstly, the measurement is done after the fuel stacks, secondly after the connection of power block i.e. diode (dc measurement) and thirdly after converting the dc power into ac (ac measurement). The display blocks show that the fuel stacks can produce 443.8 kW power and the dc power is also 443.8 kW. So there is no power loss between these two stages. Finally the ac power is measured as 440.1 kW. Here a few kW power loss is observed. This loss occurs due to inverter and filters which is reasonable. The output of 'stack' scope i.e. wave shapes of current, voltage and power after the fuel stacks look like below.

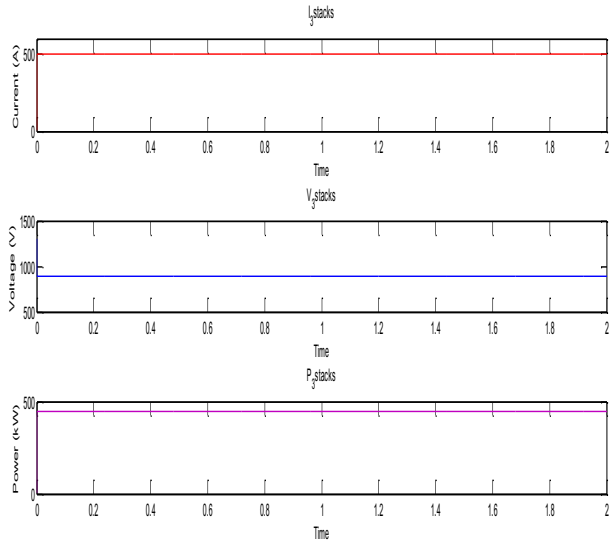

Figure. 10. Stack current, voltage and power as a function of time

Figure 10 shows the steady state condition of current, voltage and power. There is no transient condition for stack parameters.

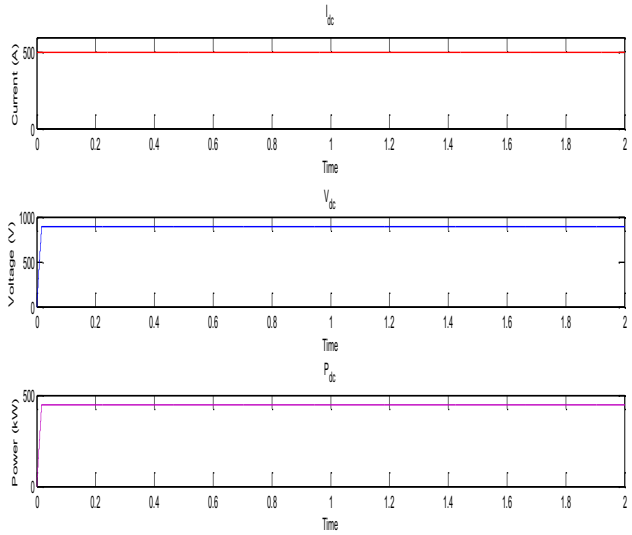

Figure. 11. DC current, voltage, and power as a function of time

Figure 11 shows the output of 'dc' scope. No transient condition can be observed for dc current but initial transients can be observed for dc voltage and dc power. After that they reach a steady value.

Figure 12 shows the output of 'ac' scope. The initial transients and after that steady state values can be observed for ac parameters. This simulation is run for 0.3 seconds to observe the dynamics more clearly. From the above figure, the dynamics of ac power can be observed from t=0.05 seconds to t=0.15 seconds.

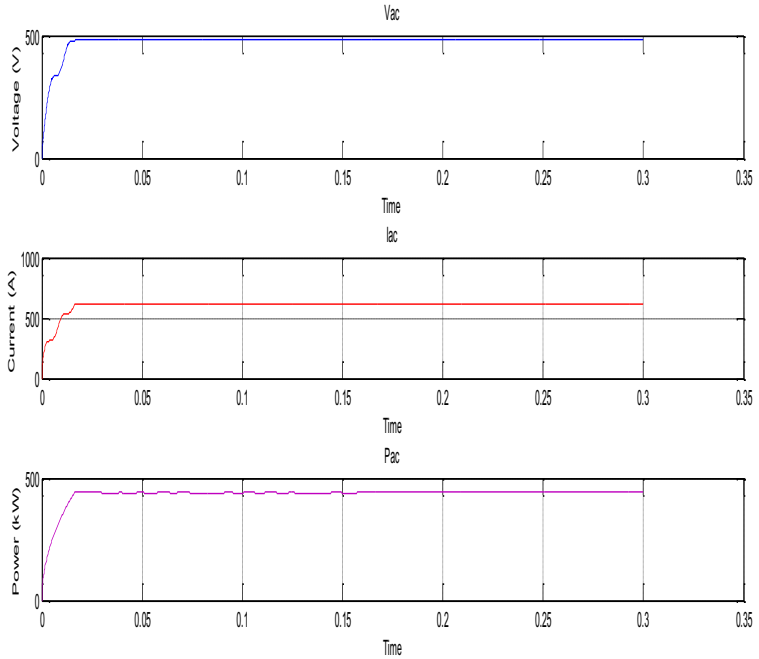

Figure. 12. AC current, voltage, and power values

Figure 13 shows the three phase voltages and currents. It can be seen that both voltages and currents are balanced. Since no fluctuation is observed, they are safe to inject into the grid.

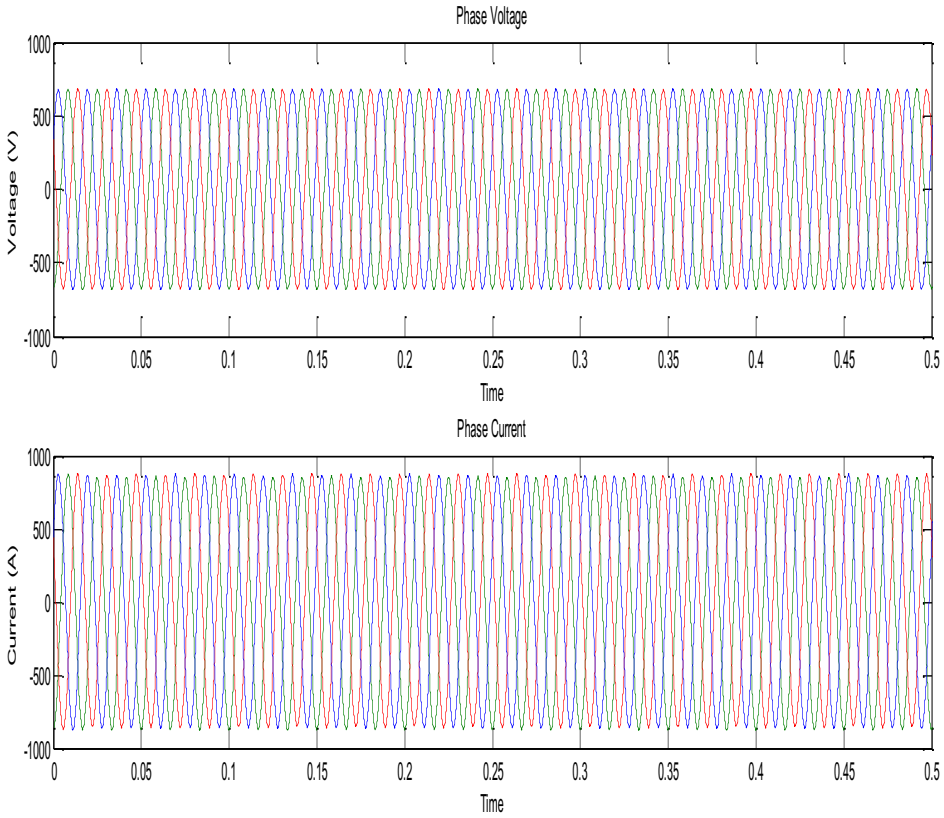

Figure. 13. Three phase voltages and currents

V. CONCLUSION

This paper represents a steady state and dynamic model of a 440 kW power plant operated by a PAFC type fuel cell system with grid connection. Moreover, a simple control mechanism is used to control the PWM inverter. Model details and simulation results are discussed in the paper. The proposed model has a simple control mechanism, grid connection and negligible losses and it is simulated in Simulink. Simulation on a Sony i5 based laptop takes few minutes to simulate the system for 2 seconds.

REFERENCES

[1] Mehta, Gitanjali, and Singh, S. P. "Grid-interfacing Fuel Cell System with active and Reactive Power Flow Control." International Conference on Sustainable Energy and Intelligent System, India, (SEISCON 2011).

[2]Tanni, M. A., Arifujjaman, Md, and Iqbal, M. T."Dynamic Modeling a of Phosphoric Acid Fuel Cell (PAFC) and Its Power Conditioning System." Journal of Clean Energy Technologies, Vol. 1, No. 3, July 2013.

[3] Berenguer, Olsen F.A., and Molina, M.G. "Design of improved fuel cell controller for distributed generation systems." International Journal of Hydrogen Energy 35 (2010): 5974–5980. Accessed January 20, 2010. http://www.elsevier.com/locate/he.

[4] Fuel Cell Handbook, 7th ed., EG&G Technical Services, Inc., Morgantown, West Virginia, 2004, pp. 1-7.

M. A. Tanni was born in Dhaka, Bangladesh. She is currently a full time graduate student at Memorial University of Newfoundland, Canada. She is doing her masters in the Faculty of Engineering and Applied Science. Her major is electrical and she is studying in thesis based program. Her research topics are related to fuel cells. She is a student member of IEEE. She has obtained her bachelor degree in Electrical and Electronic Engineering (EEE) from Khulna University of Engineering & Technology (KUET), Bangladesh. She also worked on renewable energy in her undergraduate program. Her

thesis topic was related to solar cell. She was awarded the second prize in a paper competition from KUET Excellence Foundation (KFS).

M. Tariq Iqbal received the B.Sc.(EE) degree from the University of Engineering and Technology, Lahore in 1986, the M. Sc. Nuclear Engineering degree from the Quaid-e-Azam University, Islamabad in 1988 and the Ph.D. degree in Electrical Engineering from the Imperial College London in 1994. Since 2001 he is working at the Faculty of Engineering and Applied Science, Memorial University of Newfoundland. Presently he is a full Professor. His teaching activities cover a range of electrical engineering topics. Currently, his research focuses on modeling and control of renewable energy systems with interests in the areas of design of control systems and comparison of control strategies of hybrid energy systems.

CHAPTER 7

Conclusions, Contributions and Future Works

7.1 Conclusions

The summary of this research is explained briefly as below:

The main objective of this research was to develop a fuel cell based power system for MUN engineering building. To analyze MUN engineering building, literature review was done based on energy consumption of Canadian buildings specially commercial buildings. Moreover, to develop the fuel cell based power system, literatures were also reviewed based on fuel cell system. Besides, models of the MUN engineering building were developed in BEopt (Building Energy Optimization) and HOT-2000 software. Those BEopt and HOT models were validated by provided data by the Facilities Management Department. Those models showed the actual energy consumption. After that, an improved model of the building was developed in BEopt software with a list of recommendations which showed less energy consumption than the actual model. It also suggested a list of recommendations to explain how to reduce the energy consumption. Moreover, a 440 kW natural gas fuel cell based power system was proposed for the improved model. That 440 kW natural gas fuel cell based power system was developed in Matlab/Simulink software with its Power System Blockset (PSB). The development of the power system was done step by step through three manuscripts. Firstly, three models of a PAFC system were developed in Matlab/Simulink software. Since, one of them model had many controllable parameters, it was chosen as the best model. Then the best

chosen model was extended with the power electronics part in Matlab/Simulink software with its Power System Blockset (PSB). The dynamics of that model were studied. Basically, the dc power of the fuel cell system was converted into ac power to observe different dynamics at different stages of that dynamic model. Then the model was extended to connect with the grid. The model was also simulated in Matlab/Simulink software with its Power System Blockset (PSB). Actually, the ac power of the model was filtered and entered into the grid with negligible losses. Moreover, a simple closed-loop control mechanism was developed to handle this 440 kW grid connected power system. Finally, the main objective of this thesis was fulfilled by the development of natural gas fuel cell based power system for MUN engineering building.

The main conclusions of this research are:

a) Improved building model: An improved MUN Engineering building model was presented in the third chapter which showed less energy consumption. So that model can be a role model for Canadian commercial buildings. That model shows that with the suggested improvements energy consumption in the engineering building can be significantly reduced.

b) Dynamic modelling of a fuel cell system: This study showed simple and easy simulation in each manuscript. Every model from chapter four to five had detailed simulations results which have been published. These models had no serious complexity. Since those models showed simulation results that match with the manufacture specification, researchers can be benefit from those models.

c) Fuel cell control mechanism: The chapter six showed an effective control mechanism for a natural gas fuel cell system. Proposed closed-loop control mechanism can help the future researchers how to implement control on a 440 kW power plant operated by fuel cell.

d) Negligible losses: The grid connected model of chapter six showed negligible losses in every stage. The proposed model could be used for loss calculations.

7.2 Contributions

Some major contributions of this research to the field of fuel cells and building energy analysis are:

a) Building energy analysis: This study does an energy analysis of a commercial building. This commercial building is the engineering building of MUN. In the third chapter, this building energy analysis is done. The engineering building is modeled in BEopt and HOT-2000 software. These models show actual energy consumption of the building. Then an improved model is developed in BEopt software which shows less energy consumption. So this study is very useful for energy analysis of commercial buildings in Canada and how buildings could be improved.

b) **Dynamic model of 440 kW power plant operated by natural gas**: This study develops a dynamic model of 440 kW power plant operated by natural gas based fuel cell in Matlab/Simulink software and its Power System Blockset (PSB). This model shows a simple closed-loop control mechanism. The usefulness of natural gas based fuel cell is already highlighted. So the reliability of such power plant can be understood. The

usefulness of this power plant is explained in this thesis. This power system can meet the electrical and heating demand of MUN engineering building providing a reliable and sustainable option. Moreover, the proposed system have some extra energy for small future building extension.

7.3 Future Works

a) Since it was not possible to validate these models experimentally, experimental set up can be developed in future. An experimental data can explain the reliability of these models more clearly.

b) Energy analysis of other commercial buildings can be done to study how a 440 kW power system can supply energy for those buildings.

Bibliography

[1] R. Parameshwaran, S. Kalaiselvam, S. Harikrishnan and A. Elayaperumal, “Sustainable thermal energy storage technologies for buildings: A review,” *Renewable and Sustainable Energy Reviews,* pp. 2394-2433, 2012.

[2] A. A. Bazmi and G. Zahedi, “Sustainable energy systems: Role of optimization modeling techniques in power generation and supply-A review,” *Renewable and Sustainable Energy Reviews,* pp. 3480-3500, 2011.

[3] S. Wang, C. Yan and F. Xiao, "Quantitative energy performance assessment methods for existing buildings," *Energy and Buildings,* pp. 873-888, 2012.

[4] L. Perez-Lombard, J. Ortiz and C. Pout, “A review on buildings energy consumption information,” *Energy and Buildings,* pp. 394-398, 2007.

[5] V. I. Ugursal and A. S. Fung, “Impact of appliance efficiency and fuel substitution on residential end-use energy consumption in Canada,” *Energy and Buildings,* pp. 137-146, 1996.

[6] M. F. Touchie, C. Binkley and K. D. Pressnail, “Correlating energy consumption with multi-unit residential building characteristics in the city of Toronto,” *Energy and Buildings,* pp. 648-656, 2013.

[7] L. G. Swan, V. I. Ugursal and I. Beausoleil-Morrison, "Occupant related household energy consumption in Canada: Estimation using a bottom-up neural-network technique," *Energy and Buildings,* pp. 326-337, 2010.

[8] S. E. Chidiac, E. J. C. Catania, E. Morofsky and S. Foo, "A screening methodology for implementing cost effective energy retrofit measures in Canadian office buildings," *Energy and Buildings,* pp. 614-620, 2010.

[9] B. Rezaie, E. Esmailzadeh and I. Dincer, "Renewable energy options for buildings: Case studies," *Energy and Buildings,* pp. 56-65, 2010.

[10] S. R. Choudhury, M. B. Deshmukh and R. Rengaswamy, "A Two-Dimensional Steady-State Model for Phosphoric Acid Fuel Cells (PAFC)," *Journal of Power Sources,* pp. 137-152, 2002.

[11] P. L. Zervas, A. Tatsis, H. Sarimveis and N. C. G. Markatos, "Development of a novel computational tool for optimizing the operation of fuel cells systems: Application for phosphoric acid fuel cells," *Journal of Power Sources,* pp. 345-355, 2008.

[12] P. L. Zervas, M. K. Koukou and N. C. Markatos, "Predicting the effects of process parameters on the performance of phosphoric acid fuel cells using a 3-D numerical approach," *Energy Conversion and Management,* pp. 2883-2899, 2006.

[13] S. R. Choudhury and R. Rengaswamy, "Characterization and fault diagnosis of

PAFC cathode by EIS technique and a novel mathematical model approach," *Journal of Power Sources,* pp. 971-986, 2006.

[14] S. R. Choudhury, S. R. Choudhury, J. Rangarajan and R. Rengaswamy, "Step response analysis of phosphoric acid fuel cell (PAFC) cathode through a transient model," *Journal of Power Sources,* pp. 274-279, 2004.

[15] "Energy Efficiency Trends in Canada," Office of Energy Efficiency, 1990 to 2009. [Online]. Available: http://oee.nrcan.gc.ca/publications/statistics/trends11/pdf/trends.pdf. [Accessed December 2011].

[16] "Natural Gas and Technology," 2004-2011. [Online]. Available: http://www.naturalgas.org/environment/technology.asp.

[17] " Renewable Energy: An Overview," March 2001. [Online]. Available: http://www.nrel.gov.

[18] " Focusing Our Energy," Newfoundland and Labrador, Provincial Energy Plan, St. John's.

[19] Fuel Cell Handbook, Morgantown, West Virginia: EG & G Technical Services, Inc., 2004.

[20] *Facility Energy Summary of S.J. Carew (Engineering) Building,* St. John's, NL:

Facilities Management Department, 2012.

[21] V. S. Bagotsky, Fuel Cells-Problems and Solutions, Wiley, 2012.

[22] B. Abderezzak, B. Khelidj and M. T. Abbes, "Modeling charge transfer in a PEM fuel cell using solar hydrogen," *International Journal of Hydrogen Energy,* vol. 39, pp. 1593-1603, 2013.

[23] Y. Zhao and E. Pistikopoulos, "Dynamic modelling and parametric control for the polymer electrolyte," *Journal of Power Sources,* vol. 232, pp. 270-278, 2013.

[24] "Fuel Cells CHP," [Online]. Available: http://www.understandingchp.com/appguide/Chapters/Chap4/4-4_Fuel_Cells.htm#Introduction.

[25] M. E. Schenck, J. S. Lai and K. Stanton, "Fuel cell and power conditioning system interactions," in *Applied Power Electronics Conference and Exposition*, Austin, TX , 2005.

[26] M. Gaiceanu, "Inverter Control for Three Phase Grid Connected Fuel Cell Power System," in *Compatibility in Power Electronics*, Gdansk, German, 2007.

[27] "Bing Maps," [Online]. Available: http://www.bing.com/maps/#Y3A9NDcuNTY0OTk5fi01Mi43MDk5OTkmbHZsPTE0JnN0eT1y.

[28] W. Tian and R. Choudhary, "Energy Use of Buildings at Urban Scale: A Case Study of London School Buildings," in *12th Conference of International Building Performance Simulation Association* , Sydney, 2011.

Appendix

a) Simulation results in HOT-2000 software for zone 1 of MUN engineering building

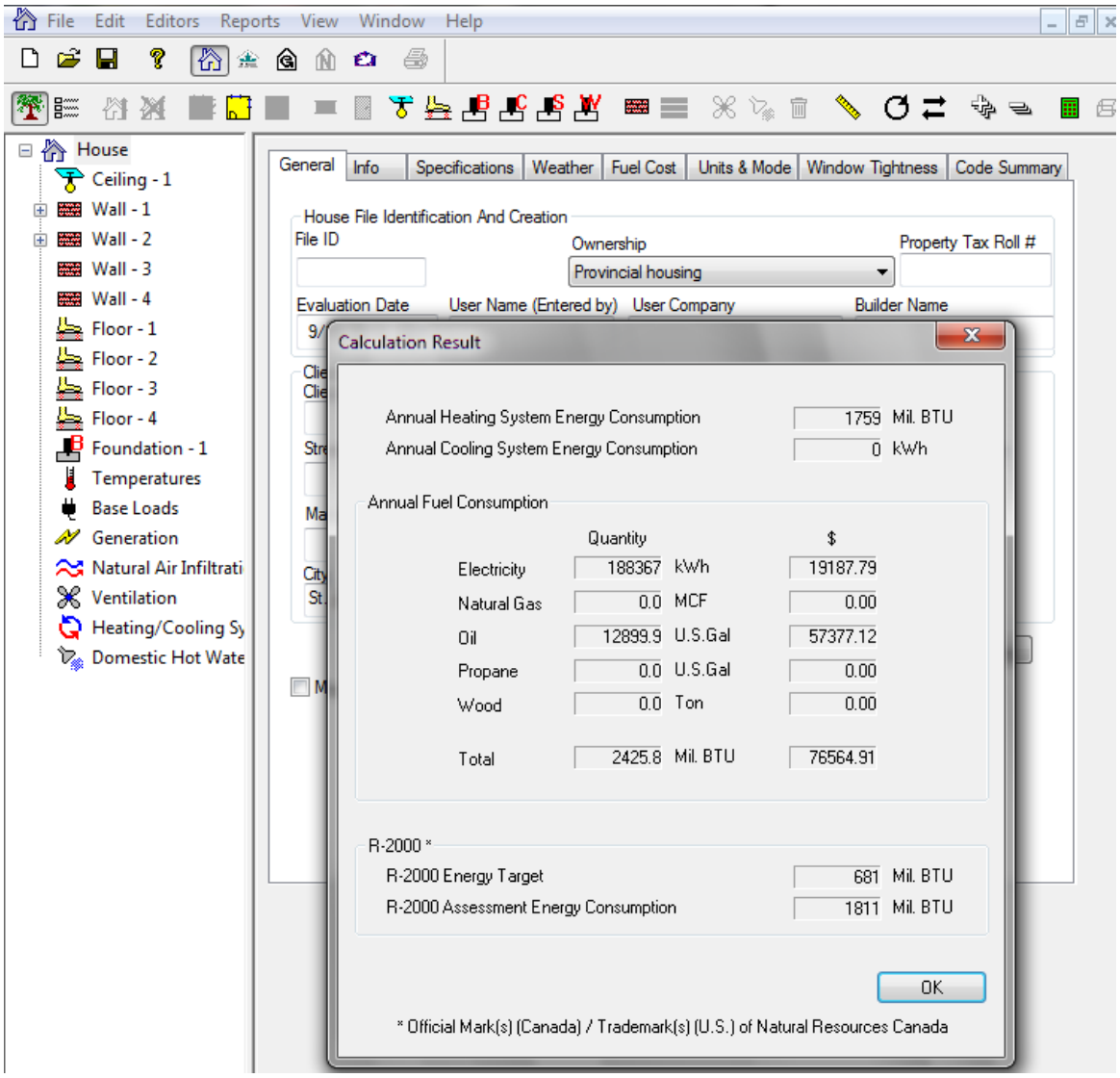

b) Datasheet of the fuel cell used for building 440 kW power system

MODEL 400
PureCell® System

Introducing a new generation of fuel cell technology:

The PureCell® Model 400 Energy Solution.

UTC Power
A United Technologies Company

UTC Power is a world leader in developing and producing fuel cells for on-site power, transportation, space and defense applications. UTC Power, a United Technologies Corp. company, is the only fuel cell manufacturer with experience in all five major fuel cell technologies – alkaline, proton exchange membrane, solid oxide, molten carbonate and phosphoric acid. With more than 300 stationary fuel cell units installed, we are committed to providing customers with distributed energy solutions that increase energy productivity and reliability and reduce operational costs.

The PureCell® Model 400 system is the stationary fuel cell energy solution for the commercial marketplace. The ultra clean and quiet Model 400 uses proven phosphoric acid technology, which offers the optimum blend of system performance and durability. The Model 400 can provide up to 400 kW of assured electrical power, plus approximately 1.5 million Btu/hour (450 kW) of heat, for combined heat and power applications. With an unmatched 10-year stack life and total energy efficiencies more than double those of traditional power sources, the Model 400 is an energy solution that will help save money, shield operations from interruption and secure environmentally sustainable business practices.

Performance Characteristics*

Power

Electric power	400 kW/471 kVA
Voltage/frequency	480VAC/60 Hz/3 phase

Efficiency

Electrical (LHV)	42%
Overall (LHV)	90% with full heat recovery

Fuel

Supply	Natural gas
Consumption (HHV)	3.61 MMBtu/hr (1,058 kW)
Inlet pressure	10 to 14 in. water (2.5 to 3.5 kPa)

Heat Recovery

Low grade up to (140°F supply)†	0.96 MMBtu/hr (281 kW)
High grade up to (250°F supply)†	0.59 MMBtu/hr (174 kW)

Emissions**

NO_x	0.02 lb/MWh (0.009 kg/MWh)
CO	0.02 lb/MWh (0.009 kg/MWh)
CO_2	1,050 lb/MWh (477 kg/MWh) with no heat recovery 487 lb/MWh (221 kg/MWh) with full heat recovery
SO_x	Negligible
Particulate matter	Negligible
VOCs	0.02 lb/MWh (0.009 kg/MWh)

This document contains no technical information subject to U.S. Export Regulations.

Water

Consumption	None (up to 85°F (30°C) ambient)
Discharge	None (normal operating conditions)

Other

Noise	<65 dBA at 33 ft (10m) with no heat recovery <60 dBA at 33 ft (10m) with full heat recovery
Operating life	20 yr
Overhaul interval	10 yr
Ambient operating temperature	-20°F to 113°F (-29°C to 45°C)

PureCell®
energy
Reinvented

*Average performance during 1st year of operation. Refer to the Product Data and Applications Guide for additional performance characteristics. **Certified to 2007 California Air Resources Board standards. †Low-grade heat assumes a return temperature of 80°F (27°C) or lower; high-grade heat assumes a return temperature of 200°F (93°C) or lower.

MODEL 400
PureCell® System

c) Provided data by MUN Facilities Management Department

Facility Energy Summary, S.J. Carew 25,474.3 m²

197.9412 kWh/m² oil 190.7 kWh/m² elec 388.6 kWh/m² total

MONTH	Y2008 MMBTU	Y2009 MMBTU	Y2010 MMBTU	Y2011 MMBTU	Y2012 MMBTU	Y2013 MMBTU
APR	2,734	3,219	1,395	902	1,646	0
MAY	2,151	1,182	1,208	1,286	1,318	0
JUN	1,710	938	886	1,328	1,164	0
JUL	290	741	850	806	774	0
AUG	440	720	731	793	525	0
SEP	616	853	881	939	391	0
OCT	1,060	1,321	1,332	1,192	1,438	0
NOV	1,719	1,387	1,567	2,029	1,659	0
DEC	2,293	1,670	1,737	2,028	1,915	0
JAN	2,758	1,940	1,962	2,166	2,389	0
FEB	2,024	1,741	1,811	2,146	2,051	0
MAR	1,936	1,746	2,040	2,166	1,939	0
TOT	19,730	17,459	16,400	17,782	17,210	0

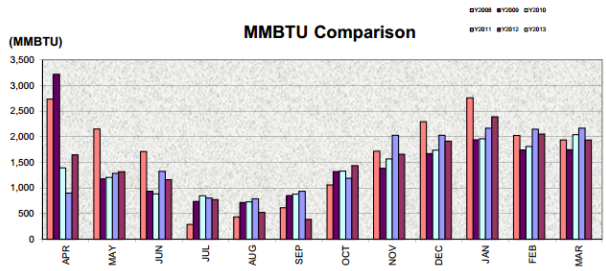

MONTH	Y2008 kWh	Y2009 kWh	Y2010 kWh	Y2011 kWh	Y2012 kWh	Y2013 kWh
APR	398,352	347,985	440,666	466,133	366,300	0
MAY	279,304	412,088	422,337	442,903	393,773	0
JUN	412,088	421,245	272,393	436,985	434,982	0
JUL	476,190	366,300	486,483	398,867	407,509	0
AUG	412,088	366,300	440,845	411,545	366,300	0
SEP	347,985	361,722	446,263	393,773	402,930	0
OCT	380,037	421,245	456,412	402,930	439,560	0
NOV	380,037	334,249	466,561	508,242	412,088	0
DEC	370,879	416,667	438,280	421,245	393,773	0
JAN	407,509	384,615	468,315	434,982	439,560	0
FEB	414,194	370,879	411,520	434,982	398,352	0
MAR	405,403	389,194	379,716	425,824	402,930	0
TOT	4,684,066	4,592,491	5,129,790	5,178,411	4,858,059	0

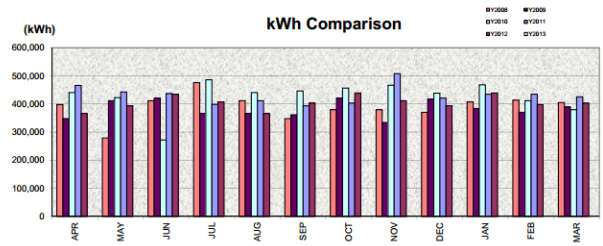

MONTH	Y2008 DEMAND	Y2009 DEMAND	Y2010 DEMAND	Y2011 DEMAND	Y2012 DEMAND	Y2013 DEMAND
APR	960	984	1,134	1,104	803	0
MAY	898	1,003	1,005	1,078	957	0
JUN	1,238	1,200	1,252	1,197	950	0
JUL	1,406	1,262	1,242	1,227	990	0
AUG	1,186	1,176	1,261	1,187	933	0
SEP	1,368	1,282	1,352	1,287	967	0
OCT	1,147	1,032	1,240	1,204	907	0
NOV	1,094	1,128	1,129	1,140	740	0
DEC	1,094	1,037	1,173	1,133	773	0
JAN	1,128	1,142	1,193	1,073	780	0
FEB	1,267	1,090	950	840	793	0
MAR	1,186	1,162	1,206	800	843	0
TOT	13,972	13,498	14,138	13,270	10,437	0

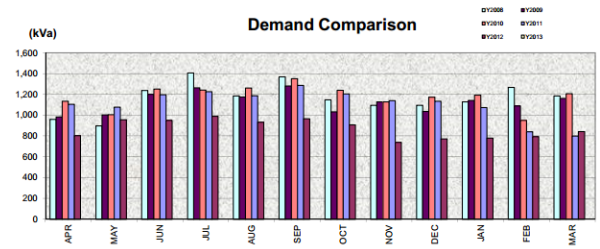

Facility Energy Summary, S.J. Carew

MONTH	Y2008 FUEL$	Y2009 FUEL$	Y2010 FUEL$	Y2011 FUEL$	Y2012 FUEL$	Y2013 FUEL$
APR	94,340.32	66,164.14	37,384.34	29,622.66	56,243.36	0.00
MAY	84,685.01	27,867.43	33,033.93	42,117.47	51,980.16	0.00
JUN	71,910.52	25,075.08	27,548.30	60,756.47	41,878.37	0.00
JUL	18,132.07	28,344.60	39,744.52	35,621.71	38,001.31	0.00
AUG	20,432.17	26,578.54	27,627.80	29,841.82	35,038.83	0.00
SEP	27,329.22	22,701.42	30,382.23	39,794.27	17,794.51	0.00
OCT	33,525.67	33,257.21	38,716.73	42,903.03	57,251.61	0.00
NOV	52,418.26	34,076.34	44,762.95	52,042.57	70,060.54	0.00
DEC	54,928.20	44,337.99	52,574.78	70,745.77	63,990.67	0.00
JAN	67,022.85	51,015.88	60,046.50	74,067.50	74,272.01	0.00
FEB	51,279.74	43,422.26	57,234.43	73,599.27	76,992.41	0.00
MAR	40,261.95	46,422.30	73,452.61	78,184.70	76,431.28	0.00
TOT	616,265.98	449,263.19	522,509.12	629,297.24	659,935.06	0.00

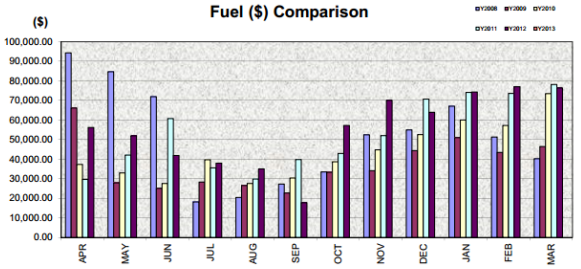

MONTH	Y2008 ELEC $	Y2009 ELEC $	Y2010 ELEC $	Y2011 ELEC $	Y2012 ELEC $	Y2013 ELEC $
APR	31,585.23	30,727.45	36,026.85	38,746.45	33,381.34	0.00
MAY	23,415.92	35,476.53	34,066.62	36,978.13	36,414.60	0.00
JUN	34,065.82	37,248.93	25,379.59	37,251.14	39,621.18	0.00
JUL	42,381.62	30,742.18	40,632.69	38,236.59	40,919.94	0.00
AUG	36,502.27	30,256.19	37,582.67	39,125.07	37,222.01	0.00
SEP	32,891.29	30,558.31	38,471.44	38,298.21	40,604.67	0.00
OCT	34,218.28	32,987.54	38,543.09	38,546.69	43,450.79	0.00
NOV	33,669.24	27,916.85	38,615.50	46,456.85	40,110.36	0.00
DEC	34,804.16	34,421.18	38,840.91	41,440.45	39,969.11	0.00
JAN	37,694.83	34,177.37	41,363.78	42,078.27	44,010.84	0.00
FEB	39,192.42	32,872.94	35,626.70	40,367.94	40,515.41	0.00
MAR	37,962.63	34,624.82	35,290.45	39,355.61	41,285.40	0.00
TOT	418,383.72	392,010.29	440,440.28	476,881.40	477,505.65	0.00

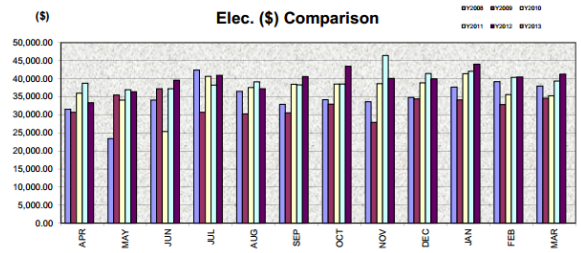

MONTH	Y2008 TOTAL $	Y2009 TOTAL $	Y2010 TOTAL $	Y2011 TOTAL $	Y2012 TOTAL $	Y2013 TOTAL $
APR	125,925.55	96,891.59	73,411.19	68,369.11	89,624.70	0.00
MAY	108,100.93	63,343.96	67,100.55	79,095.60	88,394.76	0.00
JUN	105,976.34	62,324.01	52,927.89	98,007.61	81,499.55	0.00
JUL	60,513.69	59,086.78	80,377.21	73,858.30	78,921.25	0.00
AUG	56,934.44	56,834.73	65,210.47	68,966.89	72,260.84	0.00
SEP	60,220.51	53,259.73	68,853.67	78,092.48	58,399.18	0.00
OCT	67,743.95	66,244.75	77,259.82	81,449.72	100,702.40	0.00
NOV	86,087.50	61,993.19	83,378.45	98,499.42	110,170.90	0.00
DEC	89,732.36	78,759.17	91,415.69	112,186.22	103,959.78	0.00
JAN	104,717.68	85,193.25	101,410.28	116,145.77	118,282.85	0.00
FEB	90,472.16	76,295.20	92,861.13	113,967.21	117,507.82	0.00
MAR	78,224.58	81,047.12	108,743.06	117,540.31	117,716.68	0.00
TOT	1,034,649.70	841,273.48	962,949.40	1,106,178.64	1,137,440.71	0.00